

UNIVERSITÀ
DI PAVIA

UNIVERSITY OF PAVIA
FACULTY OF ENGINEERING
DEPARTMENT OF ELECTRICAL, COMPUTER AND BIOMEDICAL ENGINEERING

MASTER'S DEGREE IN ELECTRICAL ENGINEERING

MASTER THESIS

FEASIBILITY STUDY AND SIZING OF A STATCOM SYSTEM (STATIC SYNCHRONOUS COMPENSATOR-RPCS) FOR STEEL FURNACES APPLICATIONS (EAF TYPE)

Analisi di fattibilità e dimensionamento di un sistema STATCOM (compensatore statico di potenza reattiva - RPCS) in applicazioni steel furnaces (EAF type)

Supervisor:
Prof.ssa Lucia Frosini

Co-supervisor:
Ing. Giovanni Gallotta

Candidate:
Marco Basellini

Academic year 2025/2026

Abstract

This thesis investigates the electrical behaviour, power quality performance and regulatory compliance of an Electric Arc Furnace (EAF) installation, focusing on the disturbances generated during the steelmaking process and on the effectiveness of modern compensation technologies. A comprehensive assessment was carried out through field measurements, analytical evaluations and detailed DigSILENT simulations, allowing the characterization of the furnace's dynamic impact on the network in terms of reactive power oscillations, harmonic distortion, flicker and voltage stability. The study also examines the modelling of the EAF through its operational phases, particularly the boring and melting stages, on the electrical response of the system.

The results highlight several critical issues in the existing installation, including non-compliance with power quality limits and significant stress on upstream equipment. To address these challenges, the thesis evaluates the integration of a STATCOM based Reactive Power Compensation System, demonstrating its capability to stabilize voltage, mitigate flicker, improve power factor, and reduce harmonic content under highly variable load conditions. The adoption of advanced power electronics based compensation emerges as a decisive technological enabler for ensuring robust power quality, enhancing furnace operation and supporting the long term efficiency and competitiveness of energy intensive industrial processes.

Abstract

La presente tesi analizza il comportamento elettrico, le prestazioni di power quality e la conformità normativa di un impianto dotato di Forno ad Arco Elettrico (EAF), concentrandosi sui disturbi generati durante il processo siderurgico e sull'efficacia delle moderne tecnologie di compensazione. L'attività di studio è stata condotta attraverso misure in campo, valutazioni analitiche e simulazioni dettagliate in DigSILENT, consentendo di caratterizzare l'impatto dinamico del forno sulla rete in termini di oscillazioni della potenza reattiva, distorsione armonica, flicker e stabilità della tensione. La tesi esamina inoltre la modellazione del forno nelle sue diverse fasi operative, in particolare fase di penetrazione e fase di fusione, sulla risposta elettrica del sistema.

I risultati evidenziano diverse criticità nell'impianto esistente, tra cui la non conformità ai limiti di "power quality" e un significativo stress sulle apparecchiature a monte. Per affrontare tali problematiche, viene valutata l'integrazione di un sistema STATCOM per la compensazione della potenza reattiva, dimostrando la sua capacità di stabilizzare la tensione, mitigare il flicker, migliorare il fattore di potenza e ridurre il contenuto armonico in presenza di carichi altamente variabili. L'adozione di soluzioni avanzate basate sull'elettronica di potenza emerge come un fattore tecnologico decisivo per garantire i livelli di power quality prestabiliti, migliorare l'operatività del forno e sostenere l'efficienza e la competitività a lungo termine dei processi industriali ad alta intensità energetica.

CONTENTS

1. INTRODUCTION 1

1.1. PREAMBLE 1

1.2. COMPANY DESCRIPTION 2

1.2.1. NIDEC GROUP 2

1.2.2. NIDEC CONVERSION PLATFORM 4

1.2.3. NIDEC ASI – Milan site 5

1.2.4. NIDEC: POWER QUALITY 6

1.2.5. NIDEC POWER QUALITY PRODUCT PORTFOLIO 7

2. DESCRIPTION OF FURNACE APPLICATIONS 8

2.1. STEEL MAKE FURNACES TYPE 8

2.1.1. TRANSITION FORM BOF TO EAF 9

2.2. EAF FURNACES 11

2.2.1. REACTOR CHAMBER AND EXTERNAL WALLS 13

2.2.2. REFRACTORY LINING AND COOLING SYSTEM 14

2.3. FURNACE PROCESS 16

2.3.1. FETTLING 17

2.3.2. CHARGE COMPOSITION 18

2.3.3. CHARGE LOADING 20

2.3.4. MELTDOWN PERIOD 21

2.3.5. TAPPING 23

3. GRID STANDARDS AND FURNACE CHALLENGES 25

3.1. POWER QUALITY 25

3.2. POWER FACTOR 25

3.3. HARMONIC CONTENT 28
3.4. FLICKER PHENOMENOM 30
3.5. FURNACE OPERATIONAL CHALLENGES 34
4. DESCRIPTION OF THE EXAMINATED PLANT 37
4.1. INTRODUCTION 37
4.2. SINGLE-LINE DIAGRAM OF THE PLANT 38
4.3. HIGH VOLTAGE NETWORK 40
4.4. MAIN COMPONENTS OF THE PLANT 44
4.4.1. HV/MV STEP-DOWN TRANSFORMER 44
4.4.2. SERIES IMPEDANCE 47
4.4.3. FURNACE TRANSFORMER 48
4.4.4. EXISTING FILTERS 52
4.4.5. FURNACE EQUIVALENT IMPEDANCE 55
5. AS-IT-IS PLANT ANALYSIS 57
5.1. MEASUREMENTS: POSITION, MEASUREMENTS ANALYSIS AT PCC, DIRTY BUS AND CLEAN BUS 57
5.2. LOADFLOW 60
5.2.1. ANALYTIC CALCULATION 68
5.2.2. DIGSILENT CALCULATION 73
5.3. HARMONIC ANALYSIS 80
5.4. FLICKER ANALYSIS 85
6. STATCOM CONVERTER 90
6.1. INTRODUCTION 90
6.1.1. RPCS DEFINITON 91
6.1.2. STATCOM TECHNOLOGY OVERVIEW 92
6.2. NIDEC STATCOM: SILCOVAR-H 94
6.2.1. SILCOVAR-H ARCHITECTURE 96
6.2.2. CASCADED H-BRIDGE TOPOLOGY 96

6.2.3. STAR AND DELTA CONFIGURATION 98
6.3. MAIN COMPONENTS 99
6.3.1. DECOUPLING REACTOR 99
6.3.2. CONTROL 107
7. PLANT ANALYSIS WITH RPCS 111
7.1. ANALYTIC LOADFLOW CALCULATION 111
7.2. LOADFLOW ANALYSIS DIGSILENT 114
7.3. HARMONIC ANALYSIS 122
7.4. FLICKER ANALYSIS 129
8. CONCLUSION 135
8.1. AS-IT-IS SITUATION 135
8.2. STANDARD LIMITS 136
8.3. REVAMPED SITUATION 136
9. REFERENCES 138

1. INTRODUCTION

1.1. PREAMBLE

Modern industrial processes require increasing amounts of electrical energy, while grid connection requirements are becoming progressively more stringent in terms of Power Quality, efficiency, and reliability. In this context, Power Quality is not merely a technical constraint: it directly affects process performance, operating costs, equipment utilization, and compliance at the point of common coupling (PCC).

Steel production based on alternating-current Electric Arc Furnaces (EAFs) is widely adopted because of its operational flexibility and its compatibility with advanced technologies for arc regulation, process efficiency, and plant control.

Despite their considerable advantages over conventional steelmaking technologies, EAFs behave as highly nonlinear, unbalanced, and rapidly varying loads. Changes in arc length, arc extinction and reignition, scrap movement, and the different phases of the melting cycle produce substantial fluctuations in active and reactive power demand. These fluctuations cause rapid variations in the RMS voltage at the point of common coupling and, more markedly, at the EAF busbar.

These operating characteristics may lead to several power quality disturbances, including voltage fluctuations, flicker, phase unbalance, harmonic distortion, and reduced power factor. If not properly mitigated, such disturbances can propagate through the supplying network, affect neighboring consumers, increase system losses, reduce the amount of useful electrical energy transferred to the furnace, and potentially lead to penalties related to poor power factor or non-compliance with grid requirements.

For these reasons, reactive power compensation is essential in electrical networks supplying EAF installations. Conventional fixed or mechanically switched systems can compensate slowly varying reactive power components, whereas dynamic systems are required to follow the rapid fluctuations produced by the furnace. Depending on its rating, control strategy, and interaction with the supplying network, a dynamic compensator can improve bus-voltage regulation, flicker performance, power factor, and overall electrical-system efficiency.

A STATCOM controls reactive current through a voltage-source converter and provides continuous, bidirectional, and rapidly adjustable reactive power compensation. This operating principle makes it particularly suitable for EAF installations, where the compensator must follow large and rapid changes in reactive power demand.

The high-speed response of a STATCOM enables rapid tracking of reactive power fluctuations. The resulting improvement in voltage regulation and flicker performance depends on the compensator rating, control strategy, network short-circuit level, furnace operating cycle, and applicable limits at the point of common coupling.

The sizing is based on the furnace operating profiles, the electrical characteristics of the plant and supplying network, the existing compensation equipment, and the applicable Power Quality requirements. These inputs are used to establish the required operating range and dynamic reserve of the STATCOM under the relevant furnace operating conditions.

This thesis addresses the preliminary sizing of a STATCOM for an alternating-current Electric Arc Furnace installation. It first describes the EAF process and the associated grid disturbances, then identifies the applicable grid requirements and characterizes the electrical system under investigation. Plant measurements and operating data are subsequently used to assess the existing installation, determine the required dynamic reactive power compensation, define a suitable STATCOM configuration, and evaluate the expected post-compensation performance and the main installation constraints.

The whole process of this thesis along with the necessary know-how to properly understand the EAF and correctly design the proposed converter, has been supervised by Nidec Conversion. During my internship at Nidec company, located in Milan, from November 2025 to October 2026, I had the opportunity to learn and observe the whole process of dimension and construction of a real STATCOM converter.

1.2. COMPANY DESCRIPTION

Nidec Conversion develops power conversion, automation, and Power Quality systems for industrial and utility applications. The following sections briefly introduce the Nidec Group (Nidec Corporation), the Nidec Conversion platform, and the Milan site where the thesis activity was carried out, before focusing on the Power Quality expertise relevant to the STATCOM case study.

1.2.1. NIDEC GROUP

Nidec Conversion is part of Nidec Corporation, a Japanese multinational and global leader in the production of electric motors. Founded in Kyoto in 1973 by Shigenobu Nagamori, Nidec Corporation achieved global leadership in components for hard disk drives and has progressively expanded its scope through a targeted international acquisition strategy.

Over time, the Group has expanded internationally and extended its activities across a broad range of industrial and infrastructure applications.

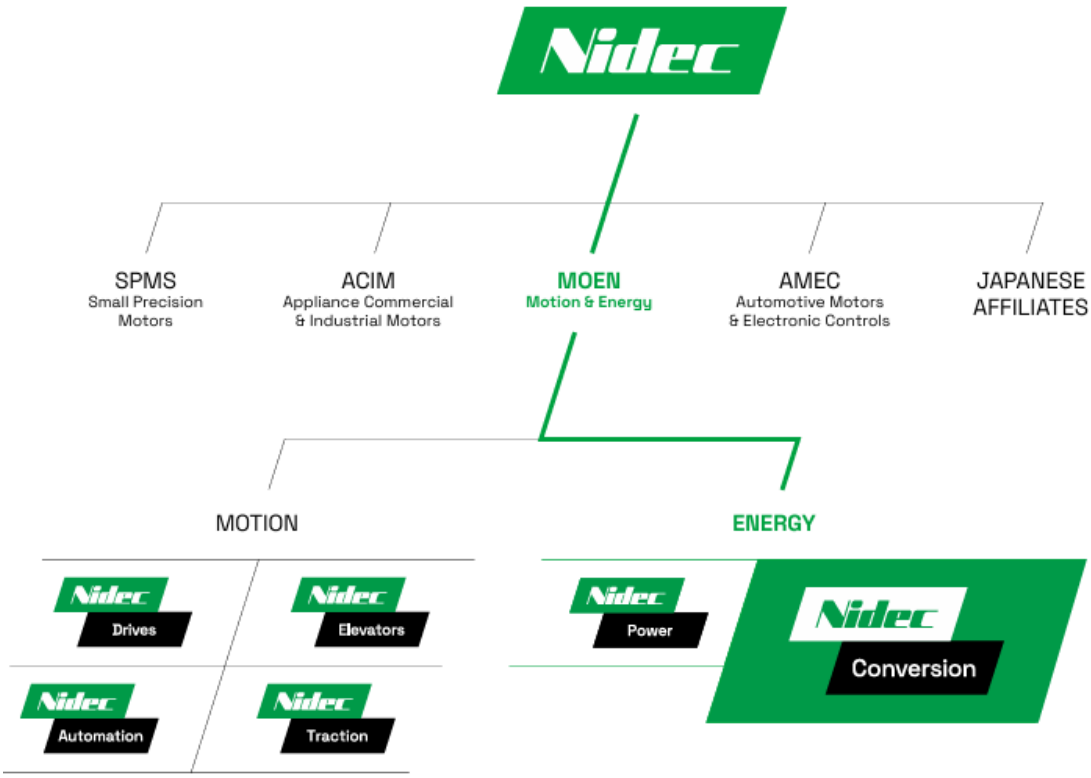


Figure 1-1Nidec Group organizational structure. Source: www.nidec-conversion.com

1.2.2. NIDEC CONVERSION PLATFORM

Nidec Conversion is a Business Segment of Nidec Group, which combines the products and services of Nidec ASI, Avtron Industrial Automation, Nidec Industrial Automation and Motortecnica to supply comprehensive electric systems globally.

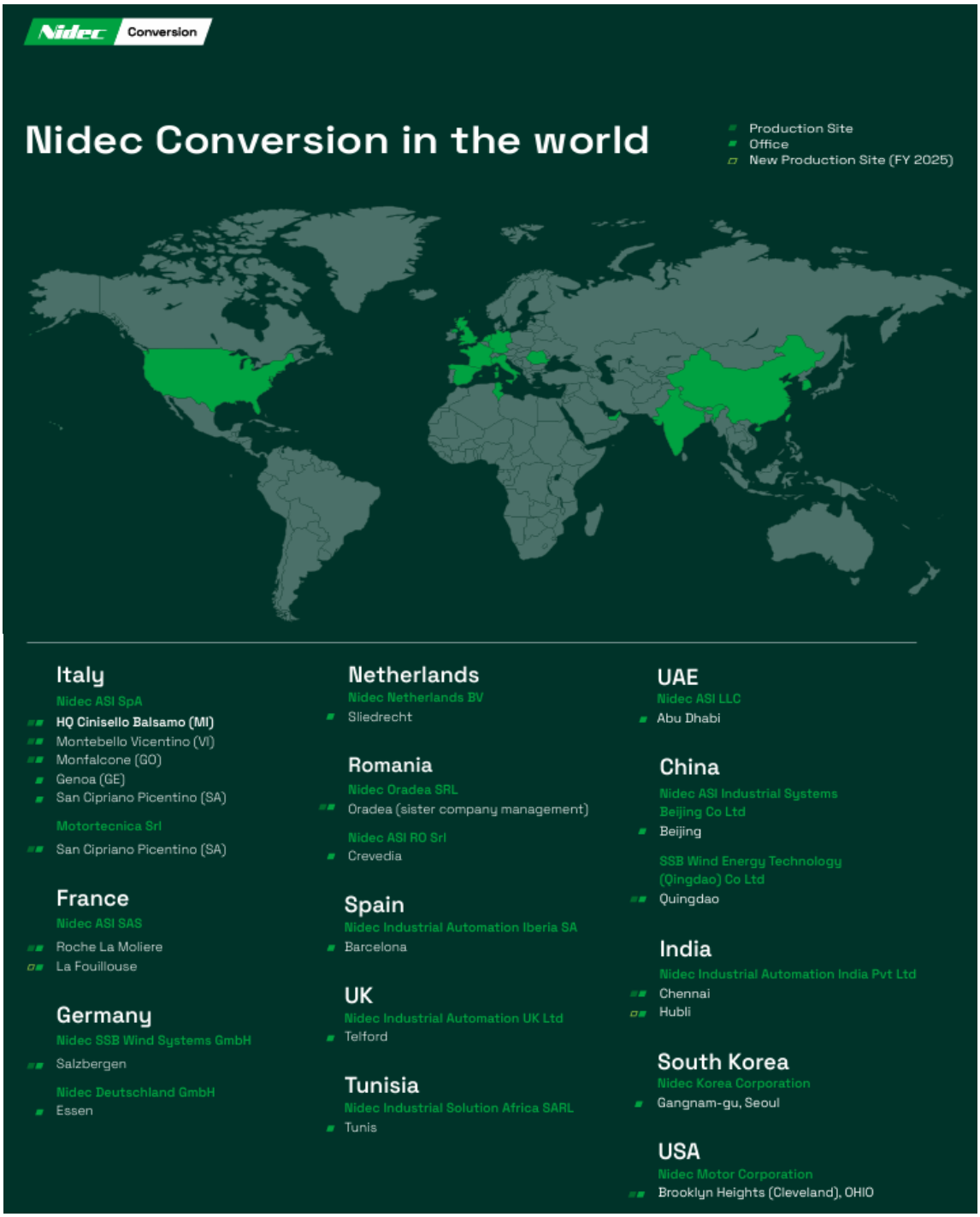


Figure 1-2: Global presence of Nidec Conversion. Source: www.nidec-conversion.com

Nidec Conversion supports the energy transition through power conversion and storage systems, high-efficiency motors, drives, and technologies designed to improve the stability and efficiency of

electrical networks. Within this framework, Power Quality solutions contribute to the reliable connection of energy-intensive industrial loads and to the efficient use of electrical energy.

1.2.3. NIDEC ASI – Milan site

The thesis activity was carried out at the Nidec ASI site in Cinisello Balsamo, Milan, Italy. The site develops medium-voltage power-electronic equipment and electrical engineering solutions for industrial applications. Its activities include electric motors and generators, power converters, and control and automation systems.

The Milan site serves industrial sectors including Oil and Gas, steelmaking, renewable and conventional power generation, marine applications, material handling, mining, cement production, rubber processing, and ropeway systems. Its experience in medium-voltage power conversion and Power Quality provides the industrial context for the EAF STATCOM application examined in this thesis.

1.2.4. NIDEC: POWER QUALITY

Power Quality is one of Nidec's key areas of expertise. Nidec works with EAF operators, grid operators, and utilities to identify suitable compensation solutions for industrial plants connected to transmission and distribution networks. For EAF applications, the assessment combines network characteristics, furnace operating data, applicable grid requirements, and the expected performance of the compensation system.



Figure 1-3: Power Quality main applications. Source: www.nidec-conversion.com

Nidec can deliver complete Power Quality projects, including engineering, equipment supply, civil works, permitting support, installation, commissioning, and long-term service. Its reactive power compensation portfolio includes SVC and STATCOM solutions for low- and medium-voltage applications. The appropriate architecture is selected according to the required dynamic performance, connection voltage, network characteristics, installation constraints, and applicable grid requirements.

1.2.5. NIDEC POWER QUALITY PRODUCT PORTFOLIO



Figure 1-4: Nidec Power Quality product portfolio. Source: Nidec Conversion, Power Quality brochure, www.nidec-conversion.com

- SILCOVAR C is an SVC based on thyristor-controlled and thyristor-switched branches. It provides dynamic reactive power compensation and voltage support in industrial and utility electrical networks.

- SILCOVAR D and SILCOVAR T are low-voltage IGBT-based STATCOM solutions using a three-phase neutral-point-clamped voltage-source converter. Their configuration enables rapid and continuous control of reactive current for dynamic compensation applications.

- SILCOVAR H is a medium-voltage IGBT-based STATCOM using a multilevel cascaded H-bridge converter. Depending on the required operating range and system design, the converter cells can be arranged in star or delta configuration.

2. DESCRIPTION OF FURNACE APPLICATIONS

2.1.STEEL MAKE FURNACES TYPE

If we consider the so called “primary steelmaking” meaning the production of steel from raw materials, there are two technologies that stand above the others, both implies the using of furnaces. In particular, they are: Basic Oxygen Furnace (BOF) and Electric Arc Furnace (EAF). In the BOF process, molten iron produced in a blast furnace is converted into steel by blowing oxygen into the furnace to reduce its carbon content and remove impurities. In an EAF, steel is produced mainly by melting steel scrap, and sometimes direct reduced iron, using the heat generated by electric arcs between graphite electrodes and the metallic charge. Due to the highly variable and non-linear behavior of the electric arcs, EAFs may cause significant reactive power variations, voltage fluctuations, flicker, current unbalance and harmonic distortion in the connected electrical network. Therefore, depending on the furnace rating, network strength and applicable grid-code limits, reactive power compensation and power-quality systems—such as STATCOMs and harmonic filters—may be required to mitigate these disturbances and ensure compliance at the point of connection.

We are interested in the last one (EAF) because it uses electricity as energy carrier and it will be part of our case study.

Together with a furnace for primary steelmaking, another type of furnace is always present for the secondary metallurgical works: that type of technology is called Ladle Furnace (LF).

At least 25% of primary steelmaking furnaces are EAF type, the basic working principle implies the use of high currents to obtain an electric arc strong enough to melt discarded steel scrap: in this way liquid steel is assessed.

Like any other technology, an electric arc furnace has its pros and cons: it allows better thermal control rather than a basic oxygen furnace, but the dissolved gasses (oxygen and nitrogen) are greater.

The quality of the scrap is an important aspect of EAF operation. Scrap may contain residual elements, such as copper, tin or nickel, which are difficult to remove during melting and may affect the quality of the final steel. The physical characteristics of the charge are also important. If the scrap is not distributed uniformly, the melting process may become irregular, causing unstable arcs and unbalanced currents

It should be noted that producing a perfectly chemically balanced steel is not the objective of a primary steelmaking furnace, this task is instead carried out by the secondary steelmaking furnace: because it is more economically efficient to operate a primary furnace as a high-speed melter, the chemical composition of the steel is adjusted with the Ladle furnace.

Before entering the Ladle furnace, the liquid steel is transferred in the ladle: this operation is called “tapping”, it can be assessed by tilting the electric arc furnace. During the tapping phase some of the main operations involved in the secondary steelmaking are made: adding deoxidizing agents, slag-forming constituents and minor additions of alloying elements. These operations can be performed before tapping or while the tapping stream is flowing in the ladle.

The principal function of the ladle furnace is the temperature control. This is necessary to ensure that the tapping stage, from the ladle to the tundish, can be carried out under optimal conditions; to restore the temperature to its nominal values after the heat losses caused by the exposure of the ladle’s upper surface, containing liquid metal, to the environment; to compensate for the thermal drop occurring during tapping from the EAF to the ladle; and, finally, to maintain a stable temperature so as to prevent certain condensed slag materials from entering again the liquid steel composition.

2.1.1. TRANSITION FORM BOF TO EAF

Steel plays a central role in economic growth. It is widely used to manufacture consumer products, build transport infrastructure such as roads and bridges, and develop the utility systems required by both established and emerging economies. Since steelmaking is strategically important for many world countries, reducing emissions simply by limiting production or replacing steel with other materials would not be a practical solution. The industry therefore needs technically feasible and economically sustainable decarbonisation measures that can be implemented without restricting current manufacturing capacity. However, reducing emissions from steel production remains particularly challenging because many of them arise directly from the chemical reactions and physical requirements of the steelmaking process.

The steel sector is one of the main sources of greenhouse gas (GHG) emissions. For this reason, the industry is undertaking a difficult transition aimed at lowering its environmental impact through the development of low-carbon technologies and improvements in process efficiency.

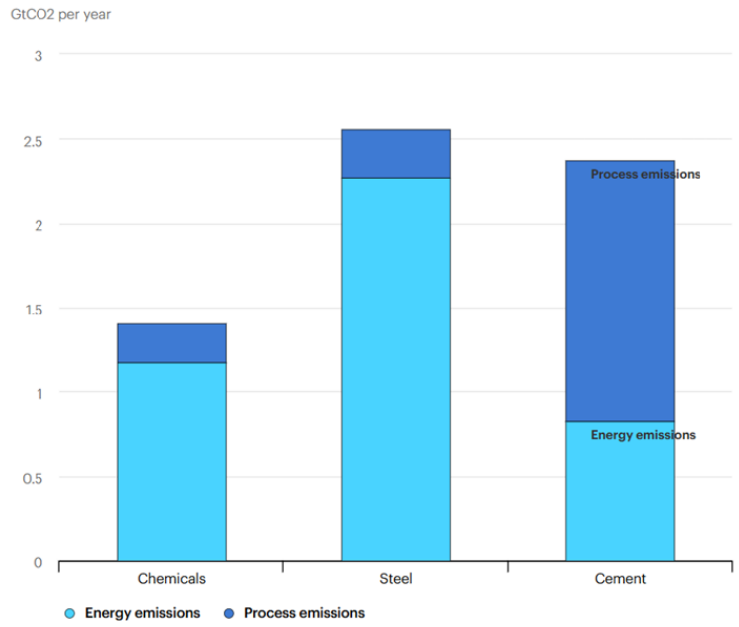


Figure 2-1Direct CO2 emissions from selected heavy industry sectors. Source:www.iea.org

Moreover global demand for steel is projected to increase by more than a third through to 2050.

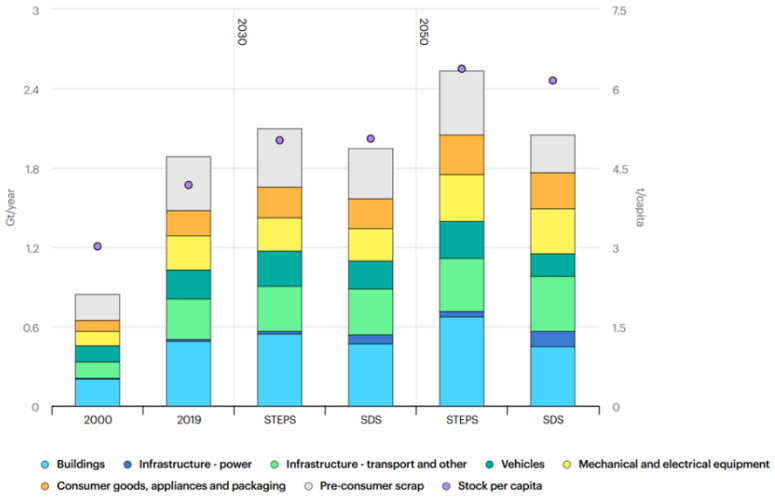


Figure 2-2: Global end-use steel demand and in-use steel stock by scenario, 2000-2050. Source:www.iea.org

The BOF furnaces make up about 70% of global steel production today, but the trend is going down: this mainly because they relies on coal-derived energy. The EAF furnaces are emerging and increasing year by year because of their lower-carbon pathways compared to BOF furnaces types. This is also in line with net zero emissions strategies that countries in the worlds are more and more implemented. The ongoing decarbonization of the steel sector can be viewed as a progressive electrification of steelmaking: more EAF furnaces means

also a new electrical impact into the network transmission and distribution grid creating a growing need for advanced Power Quality and reactive power compensation systems.

2.2. EAF FURNACES

Electric arc furnaces are composed of three main equipments:

- The furnace vessel with its roof,
- The mechanical equipment,
- The electrical equipment.

The metallurgical process of steel production takes place inside the vessel which therefore represents the main structural element of the plant. It is composed of steel shell, internally lined with refractory materials. The reactor chamber, closed at the top by a roof, is so defined. The roof is equipped with opening for inserting the electrodes and for gas evacuation.

The main mechanical equipment of an EAF includes tilting system, the mechanism for lifting/lowering the roof, the electrodes and the main door latch, as well as the systems for gas extraction and dust removal.

The last equipment, the electrical one, includes the furnace substation with the transformer and the secondary circuit, the system power input, and the accessories for control cabin. This topic will be further explored in the next chapters.

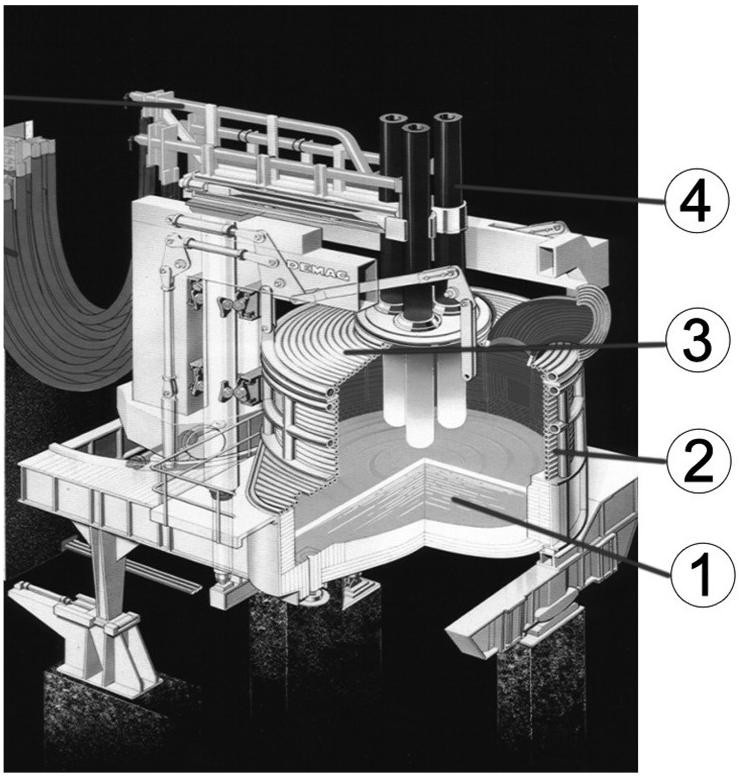


Figure 2-3 – vessel of an Electric Arc Furnace. Source: Electric Arc Furnace Steelmaking, Miroslaw Karbowniczek

In the figure above we can appreciate the vessel, composed as already mentioned by the hearth (1) where the melted steel is collected during the melting phase, the water-cooled walls (2), the roof (3), the electrodes (4).

The entire furnace is installed on foundation made of concrete, where it is placed using a steel structure shaped like two rockers: in this way, the tilting is possible.

The graphite electrodes are inserted into the furnace from above, through the opening in the roof. They represent the last elements of the electrical power supply system, de facto, thanks to these elements, during the operation is possible to assess the electric arc. The electrodes are supported by carrying arms connected with a vertical mast, together, they can perform movements on a vertical plane and a partial rotation in the horizontal one. This range of movements is essential to enabling the removing of the roof and the electrodes during the tapping and to adjust the electrodes position during the melting of the slag.

In order to supply the power at the electrodes, the so-called tabular conductors are fixed to the upper part of the support arms. The cables connected with these conductors and the transformer should guarantee some degree of flexibility to allow the proper functioning between a stationary item (the transformer) and a movable item (the electrodes).

The graphite electrodes are manufactured with high standards by specialized producers, assembled from individual sections joined by graphite nipples. Shorter sections are preferred because they facilitate manufacturing, transport, and handling. Electrode diameter scales with furnace size; for example, a 100-ton AC-EAF typically employs 600 millimetres electrodes. AC electric arc furnaces consist in a set of three electrodes while DC one only need one conducting electrode and another embedded in the furnace bottom: this one is needed to close the current path, and it is in contact with the molten steel.

The transformer is usually located near the furnace but in a separated room, for safety reasons.

2.2.1. REACTOR CHAMBER AND EXTERNAL WALLS

Focusing on the vessel, it is possible to identify three main components: the reactor chamber, the shell, the refractory lining and the cooling system of the external walls.

The reactor chamber of an electric arc furnace generally has a horizontal circular shaped cross section, its dimension depends on the following main criteria: the furnace capacity, its construction configuration, on the installed equipment, on the type of production process adopted as well as the range of steel produced. The bottom has a geometry reassembly a conical-spherical shape and its volume is sized according to the mass of the slag it will handle in a single charge. When defining the fundamental dimension of the bottom of the furnace, the diameter-to-depth ratio should be fixed: usually around 4.0 and 7.0. Lower values are typical of EAF with smaller capacity because a minimum depth of the metal bath should be guaranteed to protect the bottom shell from overheating due to the electric arc. In larger furnaces, lower value of this ratio can be adopted, remembering that the maximum depth of the bath must not exceed 1.2 m.

The angle between the conical bottom part and the horizontal one must space from 30° (for larger furnaces) and 45° (for smaller and medium furnaces), this choice ensures the complete flow of metal during the tapping. The height of the conical portion of the bottom corresponds to 4/5 of the total depth, while the remaining 1/5 is the spherical part.

Regarding the height of the chamber, a greater camber height results in a greater distance between the roof and the electric arc, thus increasing its operating life. However, an excessive height leads to greater heat losses causing an increasing in the specific consumption of the electrical energy. For small and medium furnace, the height of the reactor chamber should be increased more as the capacity increases respected to larger furnace, this

is due to the fact that a minimum distance between the roof and the electric arc must be guaranteed to avoid any electrical interaction. This phenomenon does not influence larger furnaces because the minimum distance is always fulfilled, the increase in height of the chamber is determined mainly by the power of the electric arcs.

A few words will be spent on the shell, de facto, it constitutes the outer part of the vessel. The shell is designed to withstand the whole weight of the reactor chamber, the cooling system and the refractory lining; for this purpose, its construction is made using welded steel plates, with thickness ranging from 20 to 40 mm, depending on the furnace capacity. The most stressed part of the shell is, as might be expected, the bottom part, for this reason an increment of 2-5 mm of its thickness is applied. The structure is further stiffened by vertical and horizontal ribs welded to the external surface.

In addition to the stresses due to the static and dynamic loads, the shell must also absorb the traction stresses generated by the thermal expansion of the refractory lining, also the stresses related to the non-uniformity of temperature filed must be consider.

In the upper part of the shell, two opening are always present: one for the main door and one for the tapping spout. The main door, equipped with a proper water-cooling device, allows operators to perform the routine procedures, such as temperature measurement, sample taking, insertion of oxygen and carbon lances and the use of a gas burner. The tapping spout is made of steel plate and it is gradually tapered, it conveys the liquid steel in the ladle during the tapping.

Previously, the shell was used to be built as a single structure composed of an upper cylindrical (or conical) part with a spherical bottom, resembling a dome. Instead, in the most modern one, the lower part of the shell is a separate component, the vessel walls are still water-cooled but the metal shell disappear. The two sections are joined by a flange, allowing the replacing of a single component in case of fault.

Typical shell diameters are approximately 2.5 meters for 10-ton furnaces, 6 meters for 100-ton furnaces and 9 meters for 300-ton furnaces.

2.2.2. REFRACTORY LINING AND COOLING SYSTEM

During steel production in electric arc furnaces, the refractory lining is exposed to the corrosive action of the molten bath and, in particular, to the intense radiation of the electric

arcs. The arcs produced in an EAF act as a point-type radiations sources, whose distance from the various element of the lining changes continuously.

Over the course of time, significant progress has been made in reducing arc power asymmetry and in controlling the delivered power. However, the cycling repetition of fettling, charging and tapping expose the refractory lining to abrupt high temperature variations. At the same time, the quality of the steel produced, the furnace productivity and the production cost depend directly on the life of the lining. For this reason, the refractory lining composition must be properly selected and adapted to the conditions of every EAF (they can vary based on steel grade produced). Two main factors must be considered: minimize the share of the refractory materials in steel production costs, ensure high furnace performance and good product quality.

The characteristics of a well selected material for the lining of the furnace hearth must exhibit: highest possible chemical resistance to the action of the liquid metal and slag, high mechanical strength, minimal volume changes due to temperature variations and the lowest possible thermal conductivity. Within all the alternatives materials such as magnesia, magnesia-chromite, chromite-magnesia and spinel materials, the preferred one of the refractory materials are the magnesia-carbon materials. These alternatives present poor wettability, low linear expansion compared to other solutions, low sliding friction coefficient, easy deformation at strain and anisotropic flaky structure. All features that are desired for a material used as refractory lining in an electric arc furnace.

It is possible to distinguish two types of design for the refractory lining, one for the bottom part of the vessel and the other for the walls. Regarding the bottom lining, it can be divided in three layers, from the inner one to the outer:

1. Working layer: in direct contact with the liquid bath, it is made with rammed magnesia. After been rammed, dried and burnt, a monolithic working layer with a thickness spacing from 400 to 600 mm is formed,
2. Protective layer: made of multiple lines of refractory magnesia bricks, its thickness space from 250 to 300 mm. The main purpose is to protect the possible leaked metal from the working layer,
3. Insulating layer: provide the basic thermal insulation in order to not exceed 150°C on the shell, its thickness vary from 10 to 30 mm.

The life of a well-designed bottom refractory lining along with a corrected operation of the meltdown process, can last more than thousands of heats. However, the bottleneck of a continuous operating cycle is due to the life of the refractory lining of the taphole. It can range from a few decades of heats (for an old designed taphole) to 150-200 heats (for a new designed taphole placed on the bottom of the furnace). Considering the wall refractory lining, the working layers composition change if it is considered the part covered by the metal bath and the part above the slag zone. For the first part, the condition are not so different from the bottom lining, de facto, the materials used are the same (magnesia-carbon materials). If it is considered the upper part instead, magnesia-chromite materials are adopted. This latter lining experience much harsher conditions, it is directly expose to the intense radiation of the electric arcs and their unbalanced power. The main problem is due to the fact that the graphite electrodes are not equally distant from every part of the perimeter (composed by the walls), for this reason, overheated spots appear in the zone closer to the arc plasma radiation.

The cooling system is necessary when the power supply increase, in this scenario, the only presence of refractory lining is not sufficient anymore. Furnace wall water-cooling has become a common solution in EAF design. The first approach was to apply the water-cooled panels only in the hot spots of the wall lining to extend its life. In present days, coolers were deployed along the whole wall length, here are listed some of the main design adopted:

- steel plate water-cooling panels,
- layered cooling system,
- cast iron blocks with embedded water-cooling steel pipes, sometimes with embedded refractory bricks on the internal surface,
- cast steel blocks with embedded water-cooling pipes,
- water-cooling panels made of thick copper plate,
- panel cooling with steel pipes,
- system of coaxial pipes covering the furnace volume.

It is not within the scope of this thesis to explore in greater depth the explanation of these solutions.

2.3.FURNACE PROCESS

The process of steel production in electric arc furnaces uses as main charge material the scrap. It is also possible to directly use crude iron, or materials produce from iron ore but the

percentage of the world steel production due to these latter solutions is exceedingly small. However, the type of material implied does not alter the course of melting in an EAF, on the contrary it is the chemical composition of the scrap being processed that really impact on the melting practice.

In the processing of scrap in electric arc furnaces, three main groups of operating practice can be identified:

- Melting of non-alloy charges,
- Melting of alloyed charges,
- Melting of high-chromium charges.

The first group of methods are typical of steelmaking plants with high production volumes, equipped with large capacity furnaces and high-power transformers. Inside the vessel, a metal bath is produced which, once tapped into the ladle, is subject to secondary metallurgical procedures. The second group of practices are typical of steel plants with limited production volumes, equipped with furnaces of small capacity and lower-power transformers. Also in this case, the secondary metallurgical procedures are carried in the ladle furnace whereas in the EAF a semi-product is only obtained.

Regardless of the type of steelmaking practice adopted, the production process in an electric arc furnace always include the following periods:

- Fettling,
- Charge composition,
- Charge loading,
- Meltdown period,
- Tapping.

These operations stages are present in every case and for every type of practice and they comprise the entire melting process of the furnace.

2.3.1. FETTLING

The so-called fettling is the first stage of the production process; it occurs every time after the previous metal bath and before the new one. Essentially, it is the furnace maintenance and the purpose of this stage is to prepare all furnace equipment so that the production of the new heat can proceed safely and efficiently. The operation includes assessing the technical condition of all structural components of the furnace as the lining (bottom, walls, roof) and

the graphite electrodes. Every damage found is consider and the components restored. It is common that, after every heat, it is necessary to intervene on the refractory lining of the wall at slag level and in the zone where the arc is created as well as to restoring the taphole.

The furnace walls wear down due to the erosive action of the slag or the high intensity of arc radiation when the scrap cover is insufficient. While, if we consider the monolithic bottom section, the damage may result from the indentation caused by the impact of heavy scrap pieces during the charge, especially when the protective layer of light scrap at the bottom of the basket has not been properly prepared. Another classic damage is linked to the electrodes arcs, if the depth of the liquid metal and arc is not sufficient during the initial melting phase, the monolithic bottom layer may undergo excessive wear due to the overheating. This condition usually occurs also when scrap with inadequate density is used.

The refractory lining is restored after each tapping to extend its service life. Immediately after the tapping is completed, any residual metal and slag are removed from the damaged areas of the bottom of the chamber, this latter step is essential to guarantee a proper repair. The actual restoration then follows, using finely ground, calcined magnesite or dolomite. In order to apply these materials, two approaches can be identified:

- In small furnaces they are manually applied with shovels,
- In medium and large furnaces they are applied by means of machinery as centrifugal spreader or belt-type spreading machine.

The part that requires more attention is the taphole, in this part, the lining is eroded directly by the stream of flowing metal.

In every zone, the repairing must be carried out as quickly as possible, minimizing cooling, since only under these conditions a good bond between the repair material and the existing lining can be achieved.

Depending on the furnace capacity, the extent of the interventions and the method of execution, the fettling stage generally takes from 5 to 20 minutes.

2.3.2. CHARGE COMPOSITION

In electric arc furnaces, various type of steels are produced, ranging from common carbon steels to the special high-alloy ones, such as stainless steel and acid-resistant grades. However, in most of the cases, EAF are employed to produce carbon steels.

In the production of common carbon steels, the charge consists of unalloyed scrap and only a small part of alloyed additions are allowed. Usually for this type of product, the production takes place in large capacity furnaces equipped with high power transformer. From the chemical standpoint, the charge composition is not particularly critical, the main concern resides in selecting the appropriate scrap type and arranging it correctly inside the charging basket. This is crucial both to reduce the risk of mechanical damage to the refractory bottom lining during the charging phase and to ensure that the melting phase proceeds homogeneously.

On the other hand, the chemical composition of the material in the charge becomes essential if the production of high-alloy steels is considered. In fact, if this step is correctly managed, it allows to recover alloying elements contained in the scrap, which are often very expensive; in such cases, recovery technologies are employed.

Another aspect to consider in the charge composition is related to the presence of carbon and the related carburizing materials (materials that contain carbon), which usually are: pig iron, coke, coal, graphite electrode scrap, etc. The proportion of carburizing agents present in the mix of scrap composing the charge is defined to achieve a sufficiently intense “boiling” of the metal bath already during the melting phase. Furthermore, maintaining the correct carbon content in the molten bath during the tapping in the ladle is essential to unsure that the secondary metallurgical processes proceed under the proper conditions. Summarizing, the carbon content in the charge should be close to the value required for the steel grade being produced. An excessive carbon content in the metal bath after melting would oxidation steps that could lead to the unwanted oxidation of the bath constituents. In this scenario, low carbon steel scrap is added to the charge. If, on the other hand, the carbon content in the alloyed scrap is insufficient, it can be supplemented with carbonizing materials.

Also, there are other undesired materials as silicon, manganese, chromium that should be finely calibrated. In all grades of manufactured steel significant restrictions are imposed to guarantee an acceptable percentage of these elements. The reason is their influence in the deterioration of the mechanical properties of the steel.

The charge, in addition to the metallic and carburizing materials described earlier, must also include slag-forming materials. The main component responsible for the formation of the slag is the metallurgical lime, commonly referred to as quicklime. Either for alloyed charges or non-alloy charges, an amount of quicklime ranging from 1% to 3% of the total weight is

added. When alloy steels are produced, recovery practices are generally employed as the remelting of the alloy-steel scrap with the aim of maximizing the recovery of the alloying elements, which are often very expensive.

Apart from the chemical composition, the bulk density of the scrap and the way it is arranged inside the vessel play a fundamental role in ensuring the proper progress of the charge meltdown process. Operational experience shows that the most favourable conditions are achieved by using a charge composed of 20% to 30% light scrap, positioned in the basket in a way that, during the loading, it settles on the bottom of the furnace shell. The desired effect is the attenuation of the damage caused on the refractory lining by the fall of heavy scrap. Another 40% should consist of heavy scrap, positioned directly beneath the electrodes. The remaining portion, amounting to 30% or 40%, should comprise scrap of medium size, placed near the furnace walls.

2.3.3. CHARGE LOADING

The charge, prepared in accordance with the criteria described above, is introduced into the furnace by special self-discharging baskets. For medium and large capacity furnaces, the baskets used for the loading are equipped with bottom closures formed by two semi-domes. In contrast, the baskets used for loading furnaces of small and medium capacity are usually closed at the bottom by a dome made of articulated segments.

The scrap is loaded into the basket by taking it from storage piles using bins suspended from cranes. Electromagnetic lifting device are typically used, where the scrap is hold together due to the magnetic field generated around the device by the current flowing through the internal coils.

The arrangement of the charge inside the basket must reproduce the configuration intended for the furnace, since no significant changes occur in the structure of the pile during the loading. For this purpose, light scrap is placed at the bottom of the basket followed by a layer of pig iron or other carbonizing agents, then by a layer of quicklime. Near the arcing zone the heavy scrap is loaded while, at the furnace periphery, medium size scrap and scrap containing easily volatilized components are positioned. Finally, another layer of light scrap is placed on top, in order to fill the gaps between medium and heavy pieces. The loading of the charge into the furnace proceeds as follows: first, the roof is removed, lifted and swung aside. Then, using a crane, the basket is positioned above the furnace shell at approximately half a meter above the upper edge of the vessel. At this point, the basket is opened and the

materials fall to the bottom due to the gravity. Once the charge is completed, the basket is moved away and the roof is immediately repositioned.

2.3.4. MELTDOWN PERIOD

Immediately after loading the charge and closing the vessel with the roof, the voltage supply is switched on and the automatic electrode-positioning control system is activated. The electrodes begin to descend and, as soon as they encounter the charge, the electric arc is ignited, starting the melting process of the scrap. The electric arcs form at the tips of the electrodes, between their face and the upper light scrap previously positioned. This produces the so-called “craters in the scrap”, whose diameter is approximately 50% larger than the electrodes.

This marks the beginning of the boring phase, during which the electrodes must bore their way through the upper layer of lighter scrap until they reach the denser material inside the charge. During this period, the arcs are highly unstable due to the low reactance of the cold scrap and the rapid variations in the arc resistance caused by the unavoidable non homogeneity of the charge, the fast melting of small pieces or the sudden movement of large pieces which may lead to short circuits. Also the presence of an efficient automatic electrode-control system cannot avoid the large fluctuations in arc voltage and current, which compromise the power quality of the external network. To limit these effects and protect the furnace, the arc power is reduced during the boring phase up 60% to 80% of the transformer maximum power. Usually, the boring phase is carried out in a preset time (e.g. 2 minutes) or after a specified amount of energy has been introduced into the furnace (e.g. 1,500 kWh). After this phase, the transformer is switched to maximum power, producing longer electric arcs with increased power.

After the first minutes, the arc burning condition become more stable: the boring phase ends and the melting phase begins. The graphite electrodes have bored their way down till the inner part of the vessel, in addition to melting downward, thermal energy radiates from the arcs onto the surrounding charge initiating intense lateral melting. Since the arcs are surrounded by solid scrap, they cannot radiate directly toward the furnace walls, eliminating the risk of overheating the refractory lining or damaging the cooling system. From the moment the arcs ignite, molten metal flows toward the bottom, initiating the formation of the metal bath, whose level rises as the scrap melts. Even in this phase, that usually takes from 8 to 12 minutes, the electric arcs experiences interruption and short circuit in the network are possible due to the suddenly sink of large pieces of scrap. Once the metal bath

is formed, the arcs burn between the electrode tips and the liquid metal. At this stage, the burning condition stabilizes significantly and, as the bath level rises, the electrodes are lifted gradually. From this point onward, the melting process involves only the lateral scrap. Maximum arc power is maintained until a specified amount of energy has been introduced into the furnace (around 250 kWh per ton of charge), after this, the power may be reduced to about 60% of maximum. Melting at reduced power continues until most of the scrap has melted, the arcs are exposed and only a few pieces remain along the walls above the metal bath. The total duration of the melting phase, depending on the transformer power, ranges from 30 to 100 minutes.

After the melting phase, the power supply is disconnected and all the operations in order to allow the correct loading of the next basket are performed.

Summarizing, all the meltdown process can be divided in these following four phases:

- 1st phase: from the power-on of the transformer until the craters in the scrap are melted,
- 2nd phase: from the complete melting of the craters to the formation of the metal bath, including the lateral melting,
- 3rd phase: melting the residual scrap with reduced power,
- 4th phase: performed after all the baskets have been melted, it consists in melting the solid scrap pieces located near the vessel walls and the re-heating of the metal bath to the correct temperature for tapping.

In order to optimize the technical, thermal and business condition of the meltdown phase, the so-called power programs are established. These programs consist in a set of rules and operations all furnaces impose in the selection of the electrical parameters of the power supply system, obtaining the most suitable operating state. The selection of the right power program is obtained in an empirical way, verifying the following rules:

1. The amount of energy required to melt a single basket is divided in three parts: 5%-10% of the total for the boring phase, 75%-80% for the full power part of the meltdown phase, 10%-15% for the last part,
2. Design of furnace transformer (voltage and numbers of taps) based on each point of work the charge meltdown assumes,
3. Numbers of times of change in the tap-changer,
4. Chemical energy stored in the burners and in the components of the metal bath,

5. Other considerations based in advanced techniques that can be adopted in the meltdown phase.

Considering the electrical power control system of the furnace, it can be divided in two parts:

- Electric arc power control: executed by selecting different taps of the furnace transformer and changing the current intensity,
- Arc length control: achieved by changing the electrodes support arms.

Another process that can be distinguished is called “refining period”, where secondary metallurgical processes are persecuted. This period is placed temporally after the meltdown period but, in most modern furnaces, the secondary metallurgical processes are done in the ladle furnace.

2.3.5. TAPPING

The last stage of the steelmaking process in the electric arc furnace is the tapping of the metal bath. The steel is poured into the ladle, positioned beneath the furnace. Two tapping methods are usually adopted: through a pouring spout or through a taphole.

If we consider the pouring spout, the operation begins by positioning the ladle under the furnace, suspended from an overhead crane. The ladle must be placed so that the end of the spout results above a point that allows the steel stream to reach the central area of the ladle. A particular attention must be paid in avoiding the direct contact between the stream and the sidewall or the refractory lining would erode. In addition to this latter aspect, the chemical composition of the metal would be compromised. The next step is to open the taphole, which had been sealed with refractory mass during the melting phase. Before starting the tapping operation, it is necessary to ensure that the entire runner is completely clean and free of debris. After this preparation, the furnace is tilted toward the runner until the stream of liquid appears. In this period it is crucial to maintain the correct tilt angle in order to ensure a metal stream compact and continuous. It is also crucial to finish this transient as soon as possible because, while the metal stream flows in the ladle, it is exposed to the atmospheric oxygen. This exposure deteriorates the metallurgical cleanliness of the steel produced so, the more compact the stream and shorter its trajectory, the lower the likelihood of damaging the chemical composition. The time required for tapping depends on the weight of the charge and the size of the taphole, on average it ranges from 5 to 7 minutes. In the case of the bottom taphole, the ladle is placed on a transport platform that moves along rails installed beneath the furnace. The ladle must be centered with respect to the taphole, with this configuration

no positioning movements of the ladle is required: the liquid metal flows vertically from the taphole directly into the ladle vessel. The diameter of the taphole is sized according to the furnace capacity to guarantee a tapping phase not exceeding three minutes.

Regardless of the method, a particular attention must be paid in preventing the furnace slag entering the ladle during the tapping. Also in this case to avoid this problem, two types of method can be distinguished:

- Tapping to the ladle is ended before all the liquid metal has been poured. In this way, the slag (and part of the steel) remain in the furnace. This practice takes the name of “hot heel”, about 5%-10% is left in the furnace.
- The metal is deliberately tapped with the slag.

In any case, after tapping ends, the ladle with the liquid bath is transported to the secondary metallurgy stations.

3. GRID STANDARDS AND FURNACE CHALLENGES

3.1. POWER QUALITY

In an ideal power system, at every node of supply would be observe a constant voltage, a constant frequency, no harmonics present and a power factor equal to one. These requirements, independently from the characteristics of each load supplied, should be granted. In particular, in an ideal world, the loads connected to the systems shall not interfere with the parameters of the latter.

Another parameter characterizing the grid is the so-called flicker effect, the name come from the visible effect produced in the past years on the incandesced lightbulbs, this effect in mainly due to the abrupt variation in frequency. Only few loads can produce flicker on the external network and one of these is an electric arc furnace. A deepened exploration of this phenomenon, how it is formed and how to mitigate it, will be reported in the following paragraphs and chapters.

It is useful to elaborate a notion of the quality of supply, in order to standardize the variations of the main electrical parameters that defined the grid. The topic concerning the quality of voltage, frequency, harmonics, power factor and flicker is referred as *Power Quality.*

In the following sections, the most common standard (IEC, IEE, CEI, ARERA) regarding power factor, harmonic content and flicker effect are presented. The objective is to establish the guidelines and the thresholds needed to properly design the RPCS (Reactive Power Compensating System) for the electric arc furnace, to be compliant with the power quality limits.

3.2. POWER FACTOR

The documentation adopted for power factor limit is provided by the Italian nation authority ARERA (Autorità di Regolazione per Energia Reti e Ambiente). In particular, the paper of interest is “DELIBERAZIONE 20 DICEMBRE 2022 712/2022/R/EEL: DISPOSIZIONI IN MATERIA DI REGOLAZIONE TARIFFARIA DELL’ENERGIA REATTIVA SULLE RETI ELETTRICHE IN ALTISSIMA E ALTA TENSIONE”. The reported standard is referred to all the connections (end-users or MV interconnections) connected to HV-EHV network, as study case of the electric arc furnace considered.

The power factor is strictly related to the reactive power. Although common misinterpretation, power factor PF can be considered equal to cosine of the angle between

voltage and current only if the waveforms are perfectly sinusoidal. A general definition of power factor can be the following:

$$PF = \frac{P}{S} \tag{3.1}$$

Where:

- P : Active Power $[W]$
- S : Apparent Power $[VA]$

If the waveforms are strictly sinusoidal, the following relationship is valid:

$$P = S \cdot \cos\varphi \tag{3.2}$$

Obtaining:

$$PF = \frac{P}{S} = \frac{S \cdot \cos\varphi}{S} = \cos\varphi \tag{3.3}$$

The regulation on PF is due to the fact that a sudden injection or withdrawn of reactive power from the grid produces an increase or decrease of the voltage. These interactions yield in a deterioration of the voltage stability.

It can be proven that the relationship between the reactive power and the voltage of the busbar is as follows: if the line receives reactive power, its voltage tends to decrease (inductive behaviour). Meanwhile if the line injects reactive power or receives capacitive reactive power, its voltage tends to increase (capacitive behaviour).

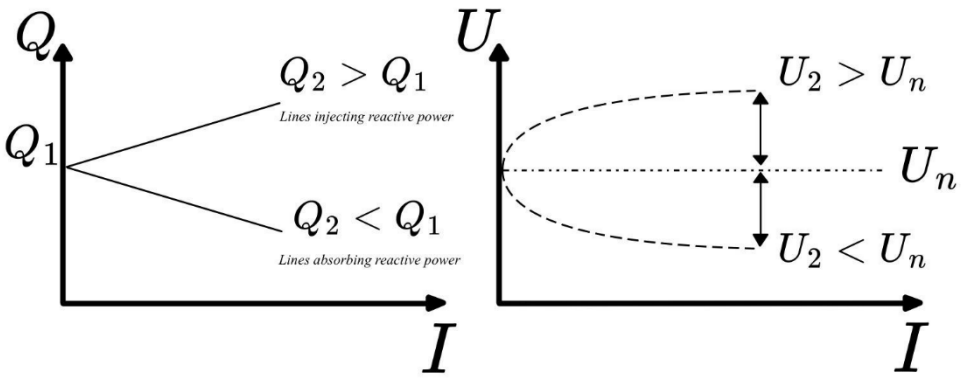


Figure 3-1 relationship between voltage and reactive power

For these reasons, the standard provides for an increase in the electricity price only if reactive power withdrawing exceeds 33% of active power, if this occurs in the time band F1 or F2. For instance, in the Italian electrical system for every Mvarh exceeding the 33% cap, a fee of 1.44 €/Mvarh is applied. Regarding the F3 band, the same fee is applied on the injection of reactive power in the grid. That difference is due to the common method of compensation of reactive power adopted in the past years, when customers used to install capacitor banks to compensate reactive power imbalance during the operation hours (usually F1 and F2 bands). This way of operation leads in an injection of reactive power in the grid during F3 band. A schematizing table can be represented in the following way:

Table 3-1 penalties for each bands

band	*Reactive Power Absorption (Q inductive)*	*Reactive Power Injection (Q capacitive)*
	Penalty [€/Mvarh]	
F1	*1,44* (if Q/P > 33%)	NO
F2	*1,44* (if Q/P > 33%)	NO
F3	NO	*1.44*

If a customer absorbs the maximum amount of reactive power allowed in proportion to the active power absorbed (33% of it), before incurring penalties and considering the waveforms purely sinusoidal, then:

$$Q = P \cdot \tan\varphi \rightarrow 0.33 \cdot P = P \cdot \tan\varphi \rightarrow \tan\varphi = 0.33$$

The power factor, equal to $\cos\varphi$ with sinusoidal waveforms, is the following:

$$PF = \cos(\tan^{-1} 0.33) = 0.9496 \approx 0.95$$

As reported in TIT (Testo Integrato Transissione), the thresholds on reactive and active energy must be respected at the end of every billing period (one month in Italy).

3.3.HARMONIC CONTENT

For harmonic content evaluation and its limitations, the technical standard adopted is the IEC/TR 61000-3-6. This standard "refers to electromagnetic compatibility, in particular to the assessment of emission limits for the connection of distorting installations to MV, HV and EHV power systems."

Referring to the IEC 61000, problems related to harmonics fall basically into two categories:

- Harmonics currents injected into the supply system by converters and harmonic sources, resulting in harmonic voltages in the system. These two phenomena cause problems in the conduction of current.
- Harmonic currents that induce interference into the communication systems. More related to higher orders of harmonics (higher frequencies).

The standard suggested the following planning level, harmonic content that every system operator accept its circulation in the network. It is a choice of the TSO (transmission system operator) to decide the limits of the planning levels, in any case, they must be more strict than the compatibility levels (values of harmonics that every device connected to the grid must be able to withstand).

Table 3-2 planning levels for every harmonic order

	Harmonic order h	*Harmonic voltage %*	
		MV	*EHV*
Odd harmonics non multiple of three	*5*	*5*	*3*
	7	*4*	*9*
	11	*3*	*15*
	13	*2.5*	*21*
	$17 \leq h \leq 49$	$1.9 \cdot \frac{17}{h} - 0.22$	$1.2 \cdot \frac{17}{h}$
Odd harmonics multiple of three	*3*	*4*	*2*
	9	*1.2*	*1*
	15	*0.3*	*0.3*
	21	*0.2*	*0.2*
	$21 \leq h \leq 45$	*0.2*	*0.2*
Even harmonics	*2*	*1.8*	*1.4*
	4	*1*	*0.8*
	6	*0.5*	*0.4*
	8	*0.5*	*0.4*
	$10 \leq h \leq 50$	$0.25 \cdot \frac{10}{h} + 0.22$	$0.19 \cdot \frac{10}{h} + 0.16$

In the standard, the indicative planning levels for the total harmonic distortion are reported:

- $THD_{MV} = 6.5\%$
- $THD_{HV-EHV} = 3\%$

Defined as:

$$THD = \sqrt{\sum_{h=2}^{H} \left(\frac{Q_h}{Q_1}\right)^2} \tag{3.4}$$

Harmonics limitation for short-terms phenomena (less than 3 seconds), planning levels are scaled by the following factor:

$$k_{HVS} = 1.3 + \frac{0.7}{45} \cdot (h - 5) \tag{3.5}$$

In order to establish the correct harmonics injection of a load, one week of normal business operation must be the minimum period the measurement campaign must cover. In this period, periods of expected maximum harmonics injection should be included.

It is important to note that harmonic content is usually considered up to the fiftieth multiple of the fundamental frequency, because this level of approximation is sufficient to correctly evaluate the distorting effect of power disturbances. However, in some cases such as power electronics equipment commanded by PWM interfaced with the power system, considering harmonic order up to 100th is necessary to avoid the induced noise interference with nearby sensitive appliances. This phenomenon can be accentuated if it is combined with power system resonance.

TSO must refine is evaluation on the planning level based on the POE (point of evaluation) decided with every customer. This point will be the same point where the customer must respect the emission level agreed together with the system operator.

The emission level, that is, the maximum level of harmonic content that every customer must respect, is derived from planning level. Every customer had its own emission level decided together with the system operator. Except for extraordinary situations, agreed emission level is always lower than planning level at the considered POE.

For converting voltage emission limits to current limits, information on the system harmonic impedance is essential for both customer and system operator. This data is given by the TSO to the customer.

Finally, for each harmonic order h, an individual contribution (E_{Uh}) that is allowed to inject is given to the customer. This contribution is calculated based on the global contribution for each harmonic (G_h), sum of every individual contribution of each harmonic on the EHV/HV system. The individual contribution is obtained from the global one by means of a weighted average:

$$E_{Uh} = G_h \cdot \sqrt[\alpha]{\frac{S_i}{S_{tot}}} \tag{3.6}$$

Where:

E_{Uh} : individual contribution for each harmonic;

G_h : global contribution for each harmonic;

α : factor varying with harmonic order h;

S_i : apparent power of the customer;

S_{tot} : total supply capacity of the substation where the customer is connected.

The contribution E_{Uh} refers to voltage harmonics. If the objective are current harmonics, then the value of the harmonic impedance of the system for every harmonic h is needed:

$$E_{ih} = \frac{E_{Uh}}{Z_h} \tag{3.7}$$

Where Z_h is the value of the impedance of the system related to the harmonic h.

3.4. FLICKER PHENOMENOM

The standard adopted for the flicker limitation is IEC/TR 61000-3-7, this part of the 61000 standard refers to “assessment of emission limits for the connection of fluctuating installations to MV, HV and EHV power system”.

As reported in the document, the problem related to voltage fluctuation fall into two categories:

- "Flicker effect from light sources as a result of voltage fluctuations;
- Rapid voltage changes even within the normal operational voltage tolerances."

Even for flicker, standard sets different limits based on voltage level. For the scope of this thesis, limits of HV ($35kV < V_n < 230kV$) are adopted.

A basic definition for flicker can be extracts from the standard, where is defined as: "impression of unsteadiness of visual sensation induced by a light stimulus whose luminance or spectral distribution fluctuates with time". It is useful to clarify that *flicker* means the effect on the incandescent lamps caused by an electromagnetic phenomenon: the voltage fluctuation.

The following quantities P_{st} and P_{lt} are introduced, they describe, in order, short-term flicker severity and long-term flicker severity.

- P_{st} : is evaluated by an average over an observation period of ten minutes;
- P_{lt} : is evaluated over an observation period of two hours from twelve P_{st} values. It is obtained as follow:

$$P_{lt} = \sqrt[3]{\sum_{i=1}^{12} \frac{{P_{st_i}}^3}{12}} \tag{3.8}$$

For flicker problems, IEC 61000-3-7 define thresholds indicators with a probabilistic approach, using the so-called CPF (Cumulative Probability Function). The nominal measurement period should be one week where 99th and 95th percentile of P_{st} and P_{lt} are measured: the 95th percentile shall never exceed the planning level mentioned below, while the 99th percentile could exceed the level by a factor that must be specified by the system operator.

As for harmonic's standard, also in this case, planning level are defined and individual emission limits are obtained from them. For HV-EHV planning level are the following:

index	HV-EHV
P_{st}	0.8
P_{lt}	0.6

In order to be compliant with the standard, the fluctuating load connected to HV network must reside in at least one of the following three stage of assessments:

-Stage 1: Direct Acceptance

Useful for all customer with a power variation really low compared to the apparent power of the system at the point of common coupling (PCC). Considering the following table:

Table 3-3 direct acceptace limits

Number of voltage changes per minute N	$\frac{\Delta S}{S_{sc}}\ MAX$ [%]
N<10	*0.4*
$10 \leq N \leq 200$	*0.2*
N>200	*0.1*

Where:

- ΔS : power variation of the customer fluctuating load [MVA];
- S_{sc} : short circuit power of the power system at PCC [MVA].

In case of compliance with the limits, the customer is automatically accepted in the electrical network.

-Stage 2: Acceptance based on proportionality with agreed power

As already seen in harmonic's standard, the global limitation level obtained from the planning level decided by the TSO is divided among the customers connected to the grid. The division is made by means of a proportionality with agreed power of every customer as follow:

$$E_{P_{st}} = G_{P_{stHV}} \cdot \sqrt[\alpha]{\frac{S_i}{S_{tot}}} \qquad (3.9)$$

$$E_{P_{lt}} = G_{P_{ltHV}} \cdot \sqrt[\alpha]{\frac{S_i}{S_{tot}}} \quad (3.10)$$

Where:

$E_{P_{st}}, E_{P_{lt}}$: are the flicker emission limits of the considered customer installation;

$G_{P_{stHV}}, G_{P_{ltHV}}$: are the maximum global contribution to the flicker levels of all fluctuating installations that can be connected to the network. These two indices are obtained from the corresponding planning level and transfer coefficient of the network;

S_i : agreed power of the customer installation [MVA];

S_{tot} : total supply capacity of the grid. This term must include future load growth estimation [MVA];

α : summation law exponent.

-Stage 3: Acceptance of higher emission level

Some type of load cannot naturally satisfied stage 2 limitations. In fact, in the previous stage, limits were carved based on typical load characteristic. In some circumstances, TSO may accept loads with high power variations. This is possible only if some factor that increase the acceptable emissions are present, as:

- Some installations that will never produce power variations near to their limits. In this case, they will never saturate the percentage of the global contribution to the flicker level assigned. This allows the TSO to allocate more margin to other customers;
- Global contributions calculation was too conservative, resulting in more power variation available for customers;
- Customer installation exceeds stage 2 limits only in few operational cases.

After the identification of the relative emission limit for long-term and short-term, the customer installation must verify:

- The 95th percentile of the values of P_{st} calculated during a week of operation must be always under $E_{P_{st}}$;

- The 99th percentile of the values of P_{st} calculated during a week of operation may exceed emission limit $E_{P_{st}}$ by a factor between 1-1.5 (in accordance with TSO);
- The 95th percentile of the values of P_{lt} calculated during a week of operation must be always under $E_{P_{lt}}$.

During the week of the measurements, the highest level of flicker emissions must be captured.

3.5. FURNACE OPERATIONAL CHALLENGES

Considering an Electric Arc Furnace, its impact on the external electrical network is tremendous. Maximising its power output lead in a deterioration of the power quality of the external network, due to a unique combination of problems. The condition at the PCC must be repristinated.

The major problems created by an EAF can be summarized as follow:

- Power factor deterioration at PCC;
- Flicker effect on nearby utilities;
- Increasing in harmonics content at PCC;
- Voltage unbalance at PCC;
- Subsynchronous resonance with nearby generators;
- Harmonic resonance with nearby generators.

The power factor deterioration is due to the way of working of an electrical arc furnace. In fact, to maximise its power output and achieve a stable furnace operation, the power factor for the furnace must be maintained between 0.7 to 0.8, resulting in the same amount of reactive power and active power withdrawn:

$$Q = P \cdot \tan\varphi = P \cdot \tan(\cos^{-1} PF) \qquad (3.11)$$

$$Q \cong 1.02 \cdot P \; or \; Q \cong 0.75 \cdot P$$

This abnormous needs of reactive power is also the reason of voltage drop formation at the primary side of furnace transformer. Q requested during EAF operation tends to destabilize voltage at PCC. This is due to the wide and irregular oscillations of the active and reactive components of the absorbed current that, together with the harmonic currents and other non-

fundamental components (non-integer multiples of the network frequency), produce corresponding voltage variations across the impedance of the external network (predominantly reactive). Hence, leading in a fluctuating furnace terminal voltage, with significant distortion and possible unbalance. Such fluctuations and distortions are also one of the reasons of the flicker phenomenon.

Below the real measurements plots of furnace voltages and furnace currents in two cycles of operation are reported, respectively:

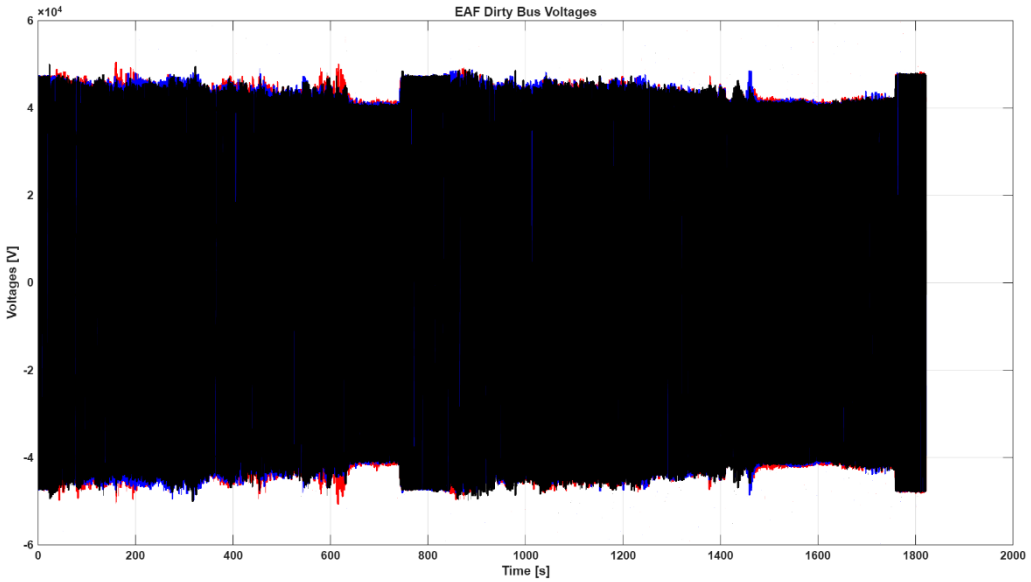


Figure 3-2EAF dirty bus voltages

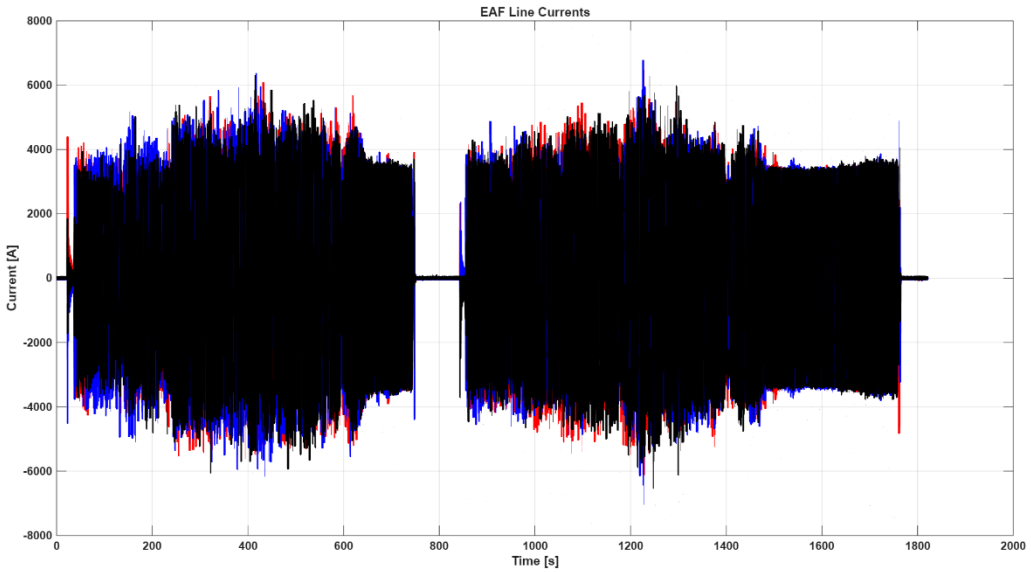


Figure 3-3 - EAF line currents

It can be observed that, during the furnace boring phase and meltdown phase, the furnace voltages are always below their nominal value. The simultaneously observable presence of

the three colours indicating each voltage in the same instant of time, is a visual indicator of unbalance. During tapping and refining, when the currents are approximately nulls, all the three phases of the voltages are at their nominal value and balanced.

This behaviour of the furnace load is strictly related to the physical nature of the electric arc. The arc is the observable phenomenon of the electrical discharge in a gas. De facto, in the furnace the current flows through an ionized gas between the electrodes and the charge, characterized by a non-linear impedance (its resistance decreases as the current increases following an exponential trend). This relationship produces a relatively constant and low arc voltage and high arc currents.

The reason of low PF values for maximum power output is also correlated with the electric arc nature. In AC-EAF, the electrodes alternately act as cathodes and anodes (their status change every half cycle). Every time the current nullifies, the arc extinguishes. The voltage between the electrode tip and the charge, that in this precise moment corresponds with the secondary side voltage of the furnace transformer, should be sufficient to re-ignite the arc. The reignition power of the voltage is strictly correlated with the power factor of the furnace circuit: with a relatively high power factor, the voltage in this instant is too low for re-ignition and the current will stay at zero value until the voltage reaches an adequate magnitude. Although, with a lower PF the voltage can re-ignite the arc immediately, achieving higher efficiency of the process.

A lower power factor results also in a more stable arc. Arc stability is crucial to mitigate flicker, harmonic generation and other electrical disturbances. Even electromagnetic forces contribute to arc displacement.

All these problems, as power factor deterioration, flicker effect and harmonics generation, affect the power quality of the external network. Summarizing, they are mainly related to: arc length and stability, overall circuit impedance and operating voltage and power (power program). The complexity in managing an electric arc furnace dwells in maximizing productivity while minimizing the impact of this load on the grid.

4. DESCRIPTION OF THE EXAMINATED PLANT

4.1. INTRODUCTION

This chapter presents the steelmaking plant considered in the study. As described in Chapter 2, the plant includes an electric arc furnace (EAF) and a ladle furnace (LF), a configuration commonly adopted in steelmaking facilities. These two loads are generally connected to a dedicated bus so that the power-quality disturbances they generate do not affect the other plant equipment. This bus, which includes the EAF, the LF, the filters, the RPCS and all associated protection and measurement devices, is referred to as the *Dirty Bus*. The remaining equipment is connected to a separate bus, referred to as the *Clean Bus*. In the plant considered here, the Clean Bus supplies an emergency feeder, a rolling mill, an exhaust-gas cooling system, and all the other utilities required for the proper operation of the steelmaking shop.

These two buses are typically electrically separated on the MV side and supplied through dedicated HV/MV transformers However, both the Dirty Bus and the Clean Bus are connected to the same high-voltage network at the point of common coupling (PCC). The main system voltage levels are 132 kV for the HV busbar and 30 kV for the MV busbars.

As shown in the single line diagram, the system already includes two filters rated at 20 MVAr each. One of the planned interventions consists of replacing the existing units with two new filters as part of the plant revamping.

The remainder of this chapter focuses on the main components that influence the electrical behaviour and power flow of the system. In particular, the analysis considers:

- The step-down transformer HV/MV of the dirty bus and the clean bus, its reactance and how it interacts with the power flow of the system;
- The series impedance of the electric arc furnaces and how the power flow of the system is affected by it;
- The furnace transformer and its interaction with the power flow of the system;
- The furnace impedance and its contribution in the power flow of the system.

Together with the single-line diagram and the overall system description, the analysis of these components provides the technical basis for identifying the plant's current power-quality issues. It also supports the selection and sizing of the new reactive power compensation system developed in the following chapters.

4.2. SINGLE-LINE DIAGRAM OF THE PLANT

Reported below, the single line diagram of the steelmaking factory. A lot of devices are present, especially on the clean bus. For the aim of this work, the clean bus will be schematized as a simple load injecting or absorbing active and reactive power.

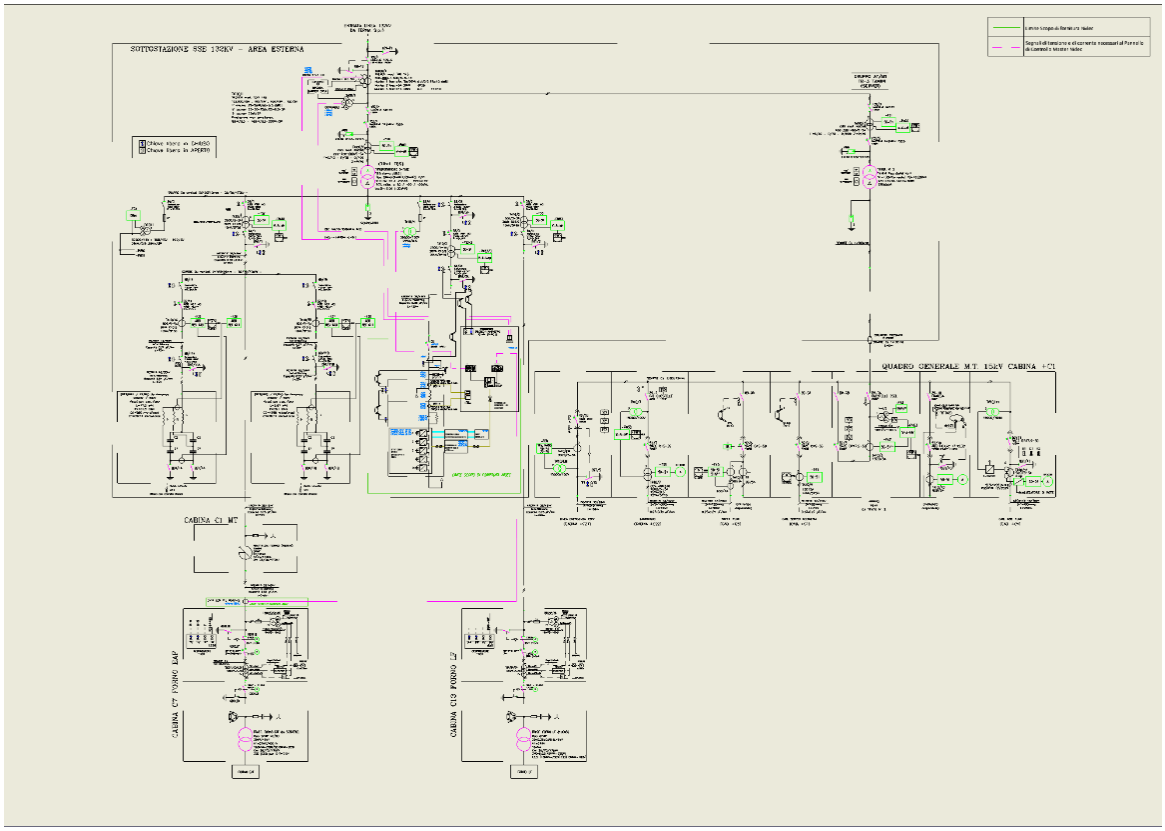


Figure 4-1 - SLD of the studycase factory, provided by NIdec

In DIgSILENT, this SLD has been reduced at its minimum, with just the loads and parameters useful for this work:

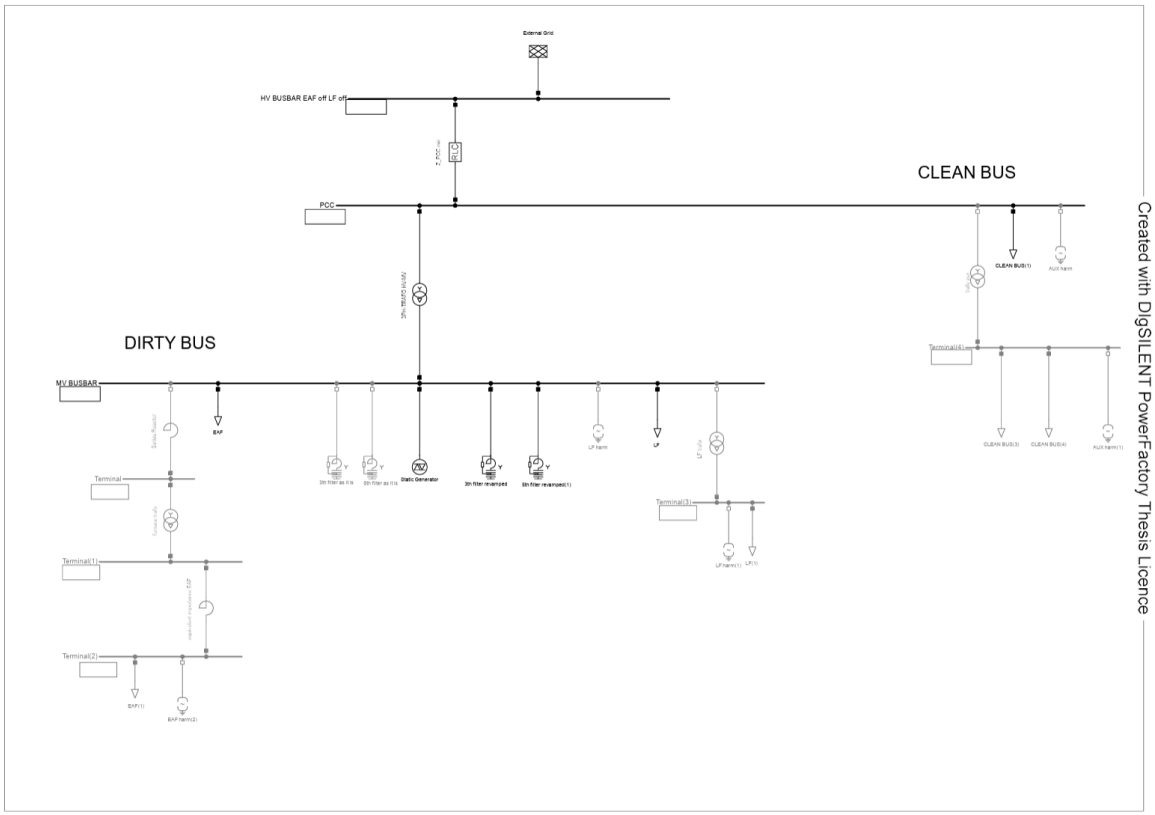


Figure 4-2 - SLD of the factory schematize on DigSilent Powerfactory

4.3. HIGH VOLTAGE NETWORK

For the High voltage network, the following data are necessary to properly evaluate the system behaviour.

Table 4-1 - high voltage network PCC parameters

HIGH VOLTAGE NETWORK **PCC**	Minimum short-circuit power	MVA	1971
	X/R ratio for the minimum short-circuit power	-	10
	Maximum short-circuit power	MVA	3425
	Reference performance short-circuit power	MVA	2850
	X/R ratio for the short-circuit power	-	10
	Nominal voltage	kV	132
	Maximum voltage	kV	132 + 10%
	Network frequency	Hz	50

In particular, the short-circuit power of the HV network represents one of the fundamental parameters to evaluate the robustness of the grid where the EAF is connected. A greater value of the short-circuit power identifies a grid that is not affected by the variation in the voltage due to the dynamic behaviour of the furnace. A high value of P_{cc} means a grid less subject to flicker phenomena, voltage instability and harmonics distortion. Also, a related low equivalent impedance is related to a network with high short-circuit power.

Another useful parameter is the $\frac{X}{R}$ ratio, a high ratio means a predominant inductive part of the equivalent impedance, while low values are related with a more resistive behaviour. The correct range is around 5 to 15, lower values correspond with a too resistive grid, while higher values accentuate flicker phenomena, amplify harmonics spectrum and increase the time constant of the system.

The correct evaluation of these two parameters (short-circuit power and $\frac{X}{R}$ ratio) is essential to correctly predicting the dynamic behaviour of the grid. In the considered case, P_{cc} is equal

to *2850 MVA*, with a minimum of *1971 MVA* and a maximum of *3425 MVA*. An electric arc Furnace with an apparent power in the range of 100 MVA, together with these values of short-circuit power, will surely cause problem at the PCC. In this scenario, the installation of an RPCS is mandatory to be compliant with the standards. Considering real installation of electric arc furnaces on the networks, problems caused on the grid for each value of short-circuit power can be summarized.

For instance, in the following table, the categorization of P_{cc} values for an EAF of 100 MVA are reported:

Table 4-2 - short circuit power properties

Short circuit power at PCC	Score	Effect
< 250 MVA	Very low	Severe flicker effect, unstable voltage
250–500 MVA	Low	Visible effect at PCC, RPCS mandatory
500–1000 MVA	Normal	Acceptable only with RPCS to be fully compliant
1–2 GVA	Good	Stable grid, flicker effect really low
> 2 GVA	Desiderable	No visbile effect at PCC

Regarding the $\frac{X}{R}$ ratio, in the reported case the value is equal to 10, corresponding to a typical value for an industrial utility. Also for this value, real-case scenarios suggest:

Table 4-3 - X/R ratio properties

X/R ratio external grid	Score	Considerations
3 – 5	Low	Too resistive grid, no stability
5 – 10	Normal	Typical value of industrial utilities
10 – 15	Good	Good grid stability
> 15 – 20	High	Very inductive grid, amplification of flicker
> 20 – 25	Very high	Problems on flicker and harmonics

Another essential parameter to properly define the grid behaviour is the network impedance. It is possible to define a value of the network impedance for every useful value of short circuit power, proceeding in the following way:

- Minimum short-circuit power:

  $V_{HV} = 132\ kV$;

  $S_{cc\ min} = 1971\ MVA$;

  $\frac{X}{R} = 10$;

The network reactance is given by the formula:

$$X_{L\,min} = \frac{{V_{HV}}^2}{S_{cc\,min}} \cdot \sin\varphi = 8.796\ \Omega \tag{4.1}$$

The phase shift is obtained by exploiting the relationship:

$$\tan\varphi = \frac{X}{R} \tag{4.2}$$

The network inductance is obtained by dividing the reactance by the pulsation:

$$L_{min} = \frac{X_{L\,min}}{\omega} = \frac{X_{L\,min}}{2 \cdot \pi \cdot f} = 27.99\ mH \tag{4.3}$$

Considering the grid frequency: $f = 50\ Hz$

The network resistance is then computed using the $\frac{X}{R}$ ratio:

$$R_{min} = \frac{X_{L\,min}}{\frac{X}{R}} = 0.8796\ \Omega \tag{4.4}$$

- Maximum short-circuit power:

  $V_{HV} = 132\ kV$;

  $S_{cc\,max} = 3425\ MVA$;

  $\frac{X}{R} = 10$;

  The network reactance is given by the formula:

$$X_{L\,max} = \frac{{V_{HV}}^2}{S_{cc\,max}} \cdot \sin\varphi = 5.062\ \Omega \tag{4.5}$$

The phase shift is obtained by exploiting the relationship:

$$\tan\varphi = \frac{X}{R}$$

The network inductance is obtained by dividing the reactance by the pulsation:

$$L_{max} = \frac{X_{L\,max}}{\omega} = \frac{X_{L\,max}}{2 \cdot \pi \cdot f} = 16.11\ mH \tag{4.6}$$

Considering the grid frequency: $f = 50\ Hz$

The network resistance is then computed using the $\frac{X}{R}$ ratio:

$$R_{max} = \frac{X_{L\,max}}{\frac{X}{R}} = 0.5062\ \Omega \tag{4.7}$$

- Performance short-circuit power:

  $V_{HV} = 132\ kV$;

  $S_{cc\,min} = 2850\ MVA$;

  $\frac{X}{R} = 10$;

  The network reactance is given by the formula:

$$X_{L\,perf} = \frac{{V_{HV}}^2}{S_{cc\,perf}} \cdot \sin\varphi = 6.083\ \Omega \tag{4.8}$$

The phase shift is obtained by exploiting the relationship:

$$\tan\varphi = \frac{X}{R}$$

The network inductance is obtained by dividing the reactance by the pulsation:

$$L_{perf} = \frac{X_{L\,perf}}{\omega} = \frac{X_{L\,perf}}{2 \cdot \pi \cdot f} = 19.364\,mH \tag{4.9}$$

Considering the grid frequency: $f = 50\,Hz$

The network resistance is then computed using the $\frac{X}{R}$ ratio:

$$R_{perf} = \frac{X_{L\,perf}}{\frac{X}{R}} = 0.6083\,\Omega \tag{4.10}$$

It is important to note that with decreasing short-circuit power, the network impedance increases. This behaviour is well expected because a lower short-circuit power means a grid more affected by the loads connected to it, dynamics represented by a higher impedance: for the same current, a higher voltage drop is obtained.

For a conservative analysis, the lowest short-circuit power should always be considered for the calculation of network impedance. In the considered case, this minimum value occurred once in six years. Hence, in order to not oversizing the RPCS, the value called performance short-circuit power is adopted.

Instead, the value of the maximum short-circuit power had been calculated because it is necessary to properly design the protection system of the devices connected to the system (RPCS and filters) in case of faults that occurs on HV-side.

4.4. MAIN COMPONENTS OF THE PLANT

4.4.1. HV/MV STEP-DOWN TRANSFORMER

The step-down transformer connecting the transmission system to the dirty bus is an essential component of the system. In the case reported, it was already installed and the nominal plate data reported:

Table 4-4 - dirty bus step-down trafo parameters

STEP-DOWN TRANSFORMER DIRTY BUS	Nominal power	MVA	130
	Primary side nominal voltage (HV)	kV	132
	Secondary side nominal voltage (MV)	kV	30
	Tap-changer steps	-	± 2 x 2.5%
	Short-circuit voltage (v_{cc} %) HV – MV	%	16.09
	Short-circuit power HV – MV (copper losses)	kW	336.447
	No-load (P_{fe})	kW	39.5
	No-load ($I_{0\%}$)	%	0.05
	Vector group	-	Yd11
	Neutral at secondary side (MV)	-	Isolated

The device is a three-phase transformer manufactured by Tamini, the rated apparent power changes with the type of cooling system used. With this transformer, three types of cooling system are present:

- ONAN: Oil Natural-Air Forced, is a type of cooling system that does not need any motor to stimulate the convection movement of air on the external side and the oil on the internal one. The rated apparent power is lower in that case, decreasing at 80 MVA.

- OFAF1: Oil Natural-Air Forced, in this case the oil placed in contact with the internal side is moved by a motor to increase the heat exchange, the apparent power of the transformer can arrive at 100 MVA.

- OFAF2: Oil-Natural-Air Forced, as before, the oil is constantly moved but with a higher speed, the apparent power of the transformer achieve 130 MVA.

Also, five positions of tap are present as reported on the table:

Table 4-5 - tap-changer positions of the step-down trafo

-5%	-2,5%	/	+2,5%	+5%
125 kV	128,7 kV	132 kV	135,3 kV	138,6 kV

In this study case, only the nominal tap position ($V = 132\ kV$) is considered.

The vector group is $Yd - 11$ meaning that the primary windings of the transformer are connected in star configuration, while the secondary windings are connencted in delta configuration. This is common choice for step-down transformer; the primary Y ending impose sinusoidal line voltages while the delta endings at the secondary side obliged the magnetizing current to be sinusoidal as well. The 11 indicate the displacements between the line voltages on each side. For instance, the three-phase line voltages of the secondary are rotated clockwise by a 330° angle with respect to the primary three-phase line voltages. In other words, the secondary side voltage system is 30° leading the primary one (or 330° lagging).

For power flow calculations performed in the next chapters, the impedance values of the transformer are necessary. With the following formula it is possible to achieve the values of the primary side and the secondary one:

$$x_{tr} = \frac{V^2}{A} \cdot V_{cc\%} \tag{4.11}$$

With:

- x_{tr}: impedance of the transformer for the selected side [Ω]
- V: nominal voltage of the selected side $[kV]$
- A: apparent power of the transformer $[MVA]$
- $V_{cc\%}$: short-circuit voltage of the transformer

That, it becomes for the primary side:

$$x_{tr_1} = \frac{{V_{HV}}^2}{A} \cdot V_{cc\%} = \frac{132^2}{130} \cdot 16.09\% = 21.565\ \Omega$$

For the secondary side:

$$x_{tr_2} = \frac{{V_{MV}}^2}{A} \cdot V_{cc\%} = \frac{30^2}{130} \cdot 16.09\% = 1.114\ \Omega$$

4.4.2. SERIES IMPEDANCE

The inductive reactance value of the whole system is a crucial parameter in a factory where an Electric Arc Furnace operates. Its value strongly influences the arc stability of the EAF: the higher it is, the greater the stability of the arc burning.

The optimal value of inductive reactance changes with the working point operation of the furnace, it is a common practice to install a series reactor upstream the furnace transformer to increase inductive reactance and stabilize the electric arc. This practice leads to a better furnace operation, reducing flicker effect and harmonics content. On the contrary, a greater value of the total inductive reactance will obviously lower the Power Factor of the power supply system seen at the PCC.

The series reactor should have a specific value of resistance and reactance; this latter value commonly ranges between 25 to 30 times the value of the furnace power supply system impedance. Some power programs provide to shunt the series reactor once the EAF is stable, in this way, a more energy efficient operation is followed.

The series reactor in the presented case has the following data:

Table 4-6 - EAF series reactor parameters

EAF SERIES REACTOR	Nominal voltage	kV	30
	Nominal current	A	2309.4
	Typical impedance (absolute value)	Ω	1.146
	Typical value (relative value respect to the absolute one)	%	65
	Tap changer type	-	No-load

As it could be observed, it presents a tap changer to properly tune the reactance based on the power program with which the arc furnace is operated.

The tap positions change, in this case, the impedance of the reactor. On the data plate is reported its typical value, coinciding with the third tap position. Also, the impedance percentage is reported in relation of the maximum value it can assume.

Table 4-7 - tap position of the reactor

Tap Position	4	3 (typical)	2	1
Z [Ω]	0.887	1.146	1.436	1.762
Z [%]	50.3	65	81.5	100

4.4.3. FURNACE TRANSFORMER

Transformers designed for electric arc furnaces are always three-phase current transformer. These devices are more stressed in comparison to usual transformer due to the natural short-circuit that occurs during the furnace operations: arc ignition, boring phase and meltdown phase. For these reasons, the furnace transformer is the most important device present in the electrical circuit of an EAF.

The following characteristics are strongly recommended:

- Large transformation ratio between primary and secondary voltages, keeping a high current intensity;
- Adjust the input power in relation to the current needed by the EAF in each operational process;
- Winding insulation designed to menage long-term overload (125% of the power rating) without any damage caused by the temperature increasing;
- High mechanical stability in front of variable dynamic stress that can occur during short-circuit events.

In addition, furnace transformers are always equipped with on-load tap-changer (OLTC) with a large number of taps. The objective is to control the input power in a broad range of its values and be able to adjust it in relation with the load.

For these reasons, furnace transformers are typically custom designed for each steelmaking factory. In the considered case, the specific parameters reported on the data plate are listed:

Table 4-8 - furnace trasformer parameters

POWER TRANSFORMER OF THE ELECTRIC ARC FURNACE **EAF**	- nominal power. primary side	MVA	100
	- nominal voltage. primary side	kV	30
	- maximum voltage. secondary side	kV	1.25
	- maximum short-circuit voltage (v_{cc} %)	%	18.8 (tap 1)
	- minimum voltage. secondary side	kV	0.650
	- minimum short.circuit voltage (v_{cc} %)	%	6.37 (tap 21)
	-Numbers of TAPS	n°	21
	- short-circuit power or X/R ratio	kW	550
	- no-load losses (1.0 x Un)	kW	66.596 (100% Vr)
	-No-load current (1.0 x Un)	%	0.35 (100% Vr)
	- vector group	-	Yd (open)

The tap positions are 21, divided in two sectors:

- Range $650V - 950V$ (tap 1-11) → constant current ($60.8\ A$)
- Range $980V - 1250V$ (tap 12-21) → constant power ($57.7\ MVA$)

In the following table, for every tap position is reported: secondary side nominal voltage, short-circuit voltage, secondary side nominal current.

Table 4-9 – short-circuit voltage and secondary side current characteristic for every tap position

Tap	V_{2n} **[V]**	V_{cc} **[%]**	I_{2n} **[kA]**
1	650	18.8	60.8
2	680	17.7	60.8
3	710	16.7	60.8
4	740	15.8	60.8
5	770	15	60.8
6	800	14.2	60.8
7	830	13.5	60.8
8	860	12.9	60.8
9	890	12.4	60.8
10	920	11.8	60.8
11	950	11.4	60.8
12	980	10.6	58.9
13	1010	9.9	57.2
14	1040	9.3	55.5
15	1070	8.75	54
16	1100	8.25	52.5
17	1130	7.8	51.1
18	1160	7.4	49.8
19	1190	7.02	48.5
20	1220	6.68	47.3
21	1250	6.37	46.2

Even for the furnace transformer it is necessary to calculate its impedance at the primary side as well as at the secondary side. To do so, the same formula used for the HV/MV transformer is considered:

$$x_{tr} = \frac{V^2}{A} \cdot V_{cc\%}$$

In this case, the apparent power is not fixed, at least for the first tap. It is achieved as the product of the rated current and the rated voltage for the considered tap position:

Table 4-10 - current costant vs power costant tap positions

Tap	V_{2n} **[V]**	I_{2n} **[kA]**	**A[MVA]**
1	650	60.8	39.52
2	680	60.8	41.344
3	710	60.8	43.168
4	740	60.8	44.992
5	770	60.8	46.816
6	800	60.8	48.64
7	830	60.8	50.464
8	860	60.8	52.288
9	890	60.8	54.112
10	920	60.8	55.936
11	950	60.8	57.76
12	980	58.9	57.722
13	1010	57.2	57.772
14	1040	55.5	57.72
15	1070	54	57.78
16	1100	52.5	57.75
17	1130	51.1	57.743
18	1160	49.8	57.768
19	1190	48.5	57.715
20	1220	47.3	57.706
21	1250	46.2	57.75

As is could be observe, starting from the 11th position of tap, the apparent power stays in range of 57.7 MVA (constant power range).

The values of the impedance for primary and secondary side of the transformer are then calculated:

Table 4-11 - primary and secondary side impedance for every tap position

Tap	V_{1n} [kV]	V_{2n} [kV]	V_{cc} [%]	A[MVA]	$x_{tr_1}[\Omega]$	$x_{tr_2}[\Omega]$
1	30	0.65	0.188	39.52	4.281377	0.00201
2	30	0.68	0.177	41.344	3.853038	0.00198
3	30	0.71	0.167	43.168	3.481746	0.00195
4	30	0.74	0.158	44.992	3.160562	0.001923
5	30	0.77	0.15	46.816	2.88363	0.0019
6	30	0.8	0.142	48.64	2.627467	0.001868
7	30	0.83	0.135	50.464	2.407657	0.001843
8	30	0.86	0.129	52.288	2.220395	0.001825
9	30	0.89	0.124	54.112	2.062389	0.001815
10	30	0.92	0.118	55.936	1.898598	0.001786
11	30	0.95	0.114	57.76	1.776316	0.001781
12	30	0.98	0.106	57.722	1.652749	0.001764
13	30	1.01	0.099	57.772	1.54227	0.001748
14	30	1.04	0.093	57.72	1.450104	0.001743
15	30	1.07	0.0875	57.78	1.362928	0.001734
16	30	1.1	0.0825	57.75	1.285714	0.001729
17	30	1.13	0.078	57.743	1.215732	0.001725
18	30	1.16	0.074	57.768	1.152887	0.001724
19	30	1.19	0.0702	57.715	1.094689	0.001722
20	30	1.22	0.0668	57.706	1.041833	0.001723
21	30	1.25	0.0637	57.75	0.992727	0.001723

4.4.4. EXISTING FILTERS

As a common practice pursued in previous years, filters in parallel to dirty loads have been placed. Filters act as capacitors banks, injecting reactive power in the network. Moreover,

they can be tuned to mitigate harmonics of a specific order, commonly the first harmonics that appear in the spectrum as the third or the fifth, as well as the seventh one, In the considered case, two filters are present with a nominal reactive power of 20 $Mvar$ each.

They are both C-type filters. The C-type is an evolution of a single-tuned filters, designed to attenuate specific harmonics and limit the current in its inductive branch at nominal frequency. Its configuration includes a tuned LC-branch and, in parallel, another resistive-inductive branch. The aim of this last branch is to reduce the losses and guarantee a longer life of the components.

This typology of filter is particularly indicated for factory with high reactive power, as an Electric Arc Furnace, where it is necessary to optimize the efficiency and reduce the thermal stress. The topology of the C-type filter is the following:

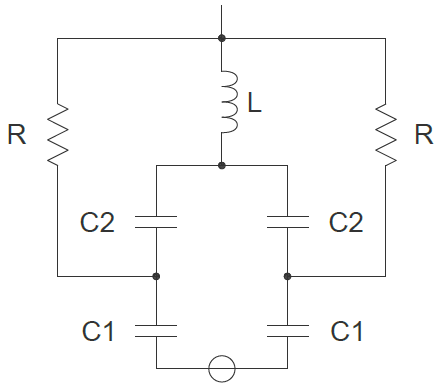


Figure 4-3 C-type topology

The total impedance obtained is:

$$z(f) = \left(\frac{1}{Rv + j\omega L + \frac{1}{j\omega C2}} + \frac{1}{Rd} \right)^{-1} + \frac{1}{j\omega C1} \tag{4.12}$$

Where:

- L: inductance $[H]$
- $C1$: main capacitance $[F]$
- $C2$: secondary capacitance $[F]$

- Rd: damping resistance [Ω]
- Rv: equivalent resistance of L-C2 branch [Ω]

The resonance frequency is defined as the frequency that nullify the imaginary component in the impedance. At that frequency the impedance is equal to the resistance of the filter, at least for the most basic one.

For a C-type, it is defined as the quantity that nullify the imaginary part of the fraction:

$$\frac{1}{Rv + j\omega L + \frac{1}{j\omega C2}} \tag{4.13}$$

$$j\omega L + \frac{1}{j\omega C2} = 0 \rightarrow \omega_r = \sqrt{\frac{1}{LC2}} \tag{4.14}$$

It results that, at resonant frequency, the filter starts conducting harmonics. The total impedance decreases with the increasing in frequency, with a peak at the resonant frequency ω_r.

Defined:

Natural impedance:
$$z_0 = \sqrt{\frac{L}{C2}} = \omega_r \cdot L = \frac{1}{\omega_r \cdot C2} \tag{4.15}$$

Quality Factor:
$$Q = \frac{z_0}{R} = \frac{1}{R} \cdot \sqrt{\frac{L}{C2}} \tag{4.16}$$

It follows that:

- Higher Q: more selective filter, more sensible to frequency variations
- Lower Q: less selective filter, more stable.

The harmonic current absorbed by the filter at the h-harmonic order is:

$$I_h = \frac{V_h}{z(f)} \tag{4.17}$$

The two already installed filters were tuned on, respectively:

- Third harmonic, $Q = 100$
- Fifth harmonic, $Q = 100$

With a damping resistance of:

- Third harmonic, $R_d = 101.2\ \Omega$
- Fifth harmonic, $R_d = 28.1\ \Omega$

4.4.5. FURNACE EQUIVALENT IMPEDANCE

As discussed in chapter 2, below the Furnace transformer various elements are present that define an electric arc furnace. These elements work together to properly deliver power at scraps and forming the metal bath.

It is possible to individuate three principal elements:

- Bus bars
- Flexible cables
- Tubular busses

The sum of the mentioned components forms a real secondary circuit. Its design should minimize the energy losses occurring in it and, simultaneously, ensuring power distribution uniformity between each phase. These last requirements could be achieved only if the inductance of any individual phases is equal and the total reactance and resistance of the secondary circuit have a relative low value. As for any other electrical component, the value of the equivalent resistance is strictly related with the crafting materials, while the equivalent reactance is linked with its geometry. In the case of an EAF, the reactance is mainly inductive and depends on the self-inductance and mutual inductance of the conductors carrying the current. Due to the geometry of the graphite electrodes, usually the inductances of the single phases are not equal, unless the electrodes are placed in a triangular disposition.

It is a common practice to schematize the secondary circuit by means of its equivalent impedance. For the considered study case, we obtain:

Table 4-12 - EAF impedance parameters

secondary circuit impedance EAF	Phase reactance	*mΩ*	*3.45*
	Phase resistance	*mΩ*	*0.33*
	Total impedance	*mΩ*	*0.33 + j 3.45*

5. AS-IT-IS PLANT ANALYSIS

5.1. MEASUREMENTS: POSITION, MEASUREMENTS ANALYSIS AT PCC, DIRTY BUS AND CLEAN BUS

The measurements provided for this study case comes from a measurement campaign performed previously. The two points of measurements and the quantity measured were:

- At PCC: line-to-line voltages and line current
- Upstream the EAF: line-to-line voltages and line current

The sampling period of the instruments were $200\ \mu s$, that implies 100 samples to obtain one period at $50\ Hz$. In total, 9102272 measurements were taken for every quantity.

Since only line-to-line voltages were measured, the corresponding phase voltages were first reconstructed under the assumption of a three-wire system with zero-sequence voltage equal to zero. The reconstructed phase quantities were then transformed into the αβ reference frame.

To obtain the power values, active and reactive, the Akagi transformations for instantaneous values of powers have been utilized. To do so, the power invariant Clarke transformation shall be performed on the instantaneous electrical quantities:

$$\begin{bmatrix} V_\alpha \\ V_\beta \end{bmatrix} = \sqrt{\frac{2}{3}} \cdot \begin{bmatrix} 1 & -\frac{1}{2} & -\frac{1}{2} \\ 0 & \sqrt{\frac{3}{2}} & -\sqrt{\frac{3}{2}} \end{bmatrix} \cdot \begin{bmatrix} V_S \\ V_R \\ V_T \end{bmatrix} \tag{5.1}$$

$$\begin{bmatrix} I_\alpha \\ I_\beta \end{bmatrix} = \sqrt{\frac{2}{3}} \cdot \begin{bmatrix} 1 & -\frac{1}{2} & -\frac{1}{2} \\ 0 & \sqrt{\frac{3}{2}} & -\sqrt{\frac{3}{2}} \end{bmatrix} \cdot \begin{bmatrix} I_S \\ I_R \\ I_T \end{bmatrix} \tag{5.2}$$

The instantaneous active power is defined as the scalar product between the voltages vector and the currents vector:

$$P = \begin{bmatrix} V_\alpha \\ V_\beta \end{bmatrix} \cdot \begin{bmatrix} I_\alpha \\ I_\beta \end{bmatrix} = V_\alpha \cdot I_\alpha + V_\beta \cdot I_\beta \tag{5.3}$$

The instantaneous reactive power, for instance, is defined as the vector product between the voltages vector and the currents vector. The symbolic determinant is exploited:

$$Q = \begin{bmatrix} V_\alpha \\ V_\beta \end{bmatrix} \times \begin{bmatrix} I_\alpha \\ I_\beta \end{bmatrix} = det \begin{bmatrix} V_\alpha & V_\beta \\ I_\alpha & I_\beta \end{bmatrix} = V_\alpha \cdot I_\beta - V_\beta \cdot I_\alpha \tag{5.4}$$

Imposing:

$$\begin{cases} V_S + V_R + V_T = 0 \\ I_S + I_R + I_T = 0 \end{cases}$$

$$\begin{cases} V_T = -(V_S + V_R) \\ I_T = -(I_S + I_R) \end{cases}$$

The transformed quantities become:

$$\begin{cases} V_\alpha = \sqrt{\frac{2}{3}} \cdot \left(V_S - \frac{V_R}{2} - \frac{V_T}{2} \right) = \sqrt{\frac{2}{3}} \cdot \left(V_S - \frac{V_R}{2} + \frac{V_S + V_R}{2} \right) = \sqrt{\frac{3}{2}} \cdot V_S \\ I_\alpha = \sqrt{\frac{2}{3}} \cdot \left(I_S - \frac{I_R}{2} - \frac{I_T}{2} \right) = \sqrt{\frac{2}{3}} \cdot \left(I_S - \frac{I_R}{2} + \frac{I_S + I_R}{2} \right) = \sqrt{\frac{3}{2}} \cdot I_S \end{cases}$$

$$\begin{cases} V_\beta = \sqrt{\frac{2}{3}} \cdot \left(\frac{\sqrt{3}}{2} \cdot V_R - \frac{\sqrt{3}}{2} \cdot V_T \right) = \frac{V_S + 2 \cdot V_R}{\sqrt{2}} \\ I_\beta = \sqrt{\frac{2}{3}} \cdot \left(\frac{\sqrt{3}}{2} \cdot I_R - \frac{\sqrt{3}}{2} \cdot I_T \right) = \frac{I_S + 2 \cdot I_R}{\sqrt{2}} \end{cases} \tag{5.5}$$

The instantaneous active power value becomes:

$$\begin{aligned} P = V_\alpha \cdot I_\alpha + V_\beta \cdot I_\beta &= \frac{3}{2} \cdot V_S \cdot I_S + \frac{(V_S + 2 \cdot V_R)(\cdot I_S + 2 \cdot I_R)}{2} \\ &= I_S \cdot (2 \cdot V_S + V_R) + I_R \cdot (2 \cdot V_R + V_S) \end{aligned} \tag{5.6}$$

The instantaneous reactive power value becomes:

$$\begin{aligned} Q = V_\alpha \cdot I_\beta - V_\beta \cdot I_\alpha &= \sqrt{\frac{3}{2}} \cdot V_S \cdot \frac{I_S + 2 \cdot I_R}{\sqrt{2}} - \frac{V_S + 2 \cdot V_R}{\sqrt{2}} \cdot \sqrt{\frac{3}{2}} \cdot I_S \\ &= -\sqrt{3} \cdot (I_S \cdot V_R - I_R \cdot V_S) \end{aligned} \tag{5.7}$$

The negative sign in the reactive-power expression follows the adopted convention: capacitive reactive power is negative, whereas inductive reactive power is positive.

Finally, the instantaneous values of the powers are reported:

$$\begin{cases} P = I_S \cdot (2 \cdot V_S + V_R) + I_R \cdot (2 \cdot V_R + V_S) \\ Q = \sqrt{3} \cdot (I_S \cdot V_R - I_R \cdot V_S) \end{cases} \tag{5.8}$$

Considering a capacitive reactive power lower than zero.

These transformations allowed to achieve the values of powers at PCC and upstream the furnace.

As mentioned before, only the line-to-line voltages have been measured, the phase voltages needed for the power values have been obtained in the following way:

Supposing:

$$V_S + V_R + V_T = 0$$

$$V_{RS} = V_R - V_S \Longrightarrow V_R = V_{RS} + V_S$$

$$V_{ST} = V_S - V_T \Longrightarrow V_T = V_S - V_{ST}$$

Substituting:

$$V_S + V_R + V_T = 0 \Longrightarrow V_S + (V_{RS} + V_S) + (V_S - V_{ST}) = 0 \Longrightarrow V_S = \frac{V_{ST} - V_{RS}}{3}$$

$$V_R = V_{RS} + V_S \Longrightarrow V_{RS} + \frac{V_{ST} - V_{RS}}{3} \Longrightarrow \frac{2 \cdot V_{RS} - V_{ST}}{3}$$

$$V_S + V_R + V_T = 0 \Longrightarrow V_T = -V_S - V_R$$

Resulting in:

$$\begin{cases} V_S = \dfrac{V_{ST} - V_{RS}}{3} \\ V_R = \dfrac{2 \cdot V_{RS} - V_{ST}}{3} \\ V_T = -V_S - V_R \end{cases} \tag{5.9}$$

As the literature suggests, at the beginning of every cycle of steelmaking, given the power program adopted, it is possible to separate the melting period in two main sub-intervals. In this case, the boring phase has been individuated, as expected, immediately after the fettling of EAF. From 860 seconds to 980 seconds the average active power measured upstream the furnace had the following value:

$$P_{boring} = 58.845\ MW$$

That is, considering the nominal value of the electric arc furnace (validated after in this chapter) of $P_{EAF} = 83.65\ MW$, exactly the 70.35% of it, as expected. Notice that the duration of the period of the boring phase is two minutes.

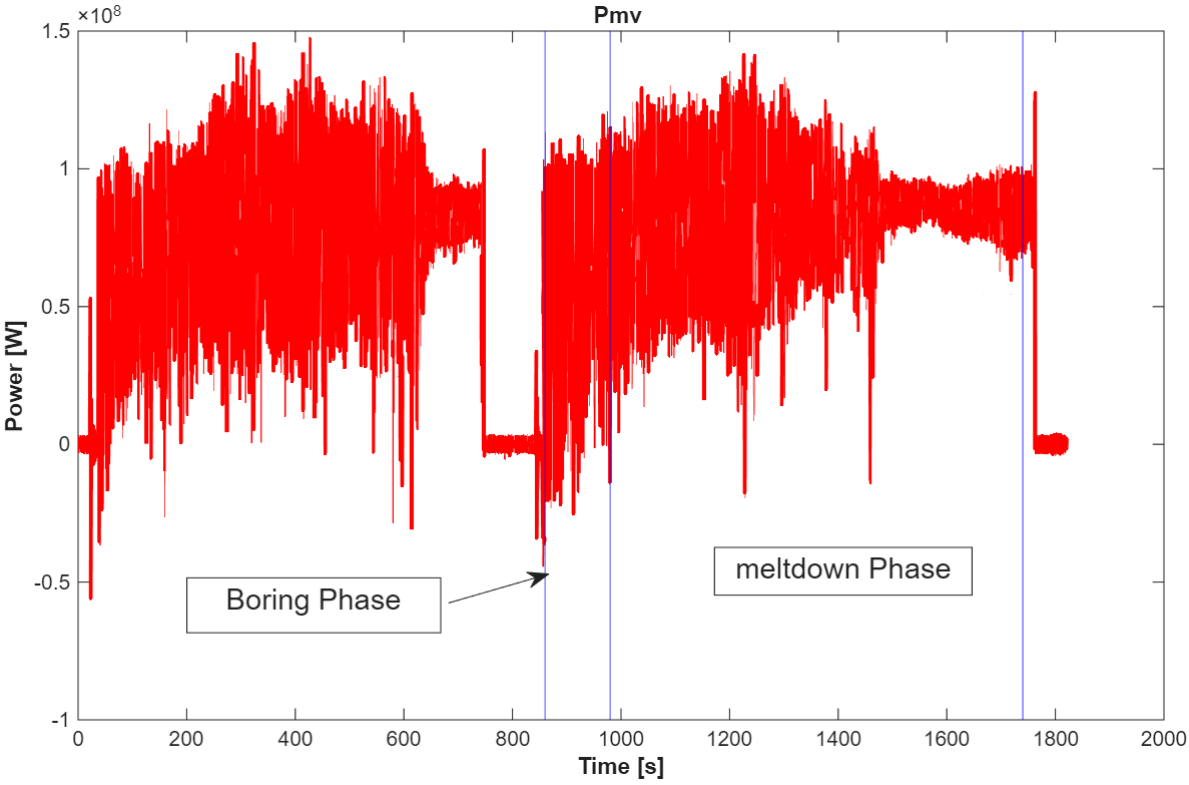


Figure 5-1 boring vs meltdown power spectra

However, for the sake of the power flow analysis, only the ten minutes period where the Electric Arc furnaces is working at the nominal power has been considered. The period considered start at 1140 s and last until 1740 s.

5.2.LOADFLOW

Based on the active and reactive power values, it possible to individuate three different period of working:

- 760 s – 830 s : in this period only the Ladle Furnace is working
- 1140 s – 1740 s : in this period only the Electric Arc Furnace is working
- 1770 s – 1820 s : in this period EAF and LF are disconnected

The graph showing the active and reactive power of the entire period of measurement of 30 minutes is reported below. The different periods of the steelmaking process are clearly

observable: fettling phase and tapping phase, where the powers are near zero; boring phase, where the powers are rising; meltdown phase, where powers are at their maximum and the last phase, where the power is reduced to not damage the walls lining.

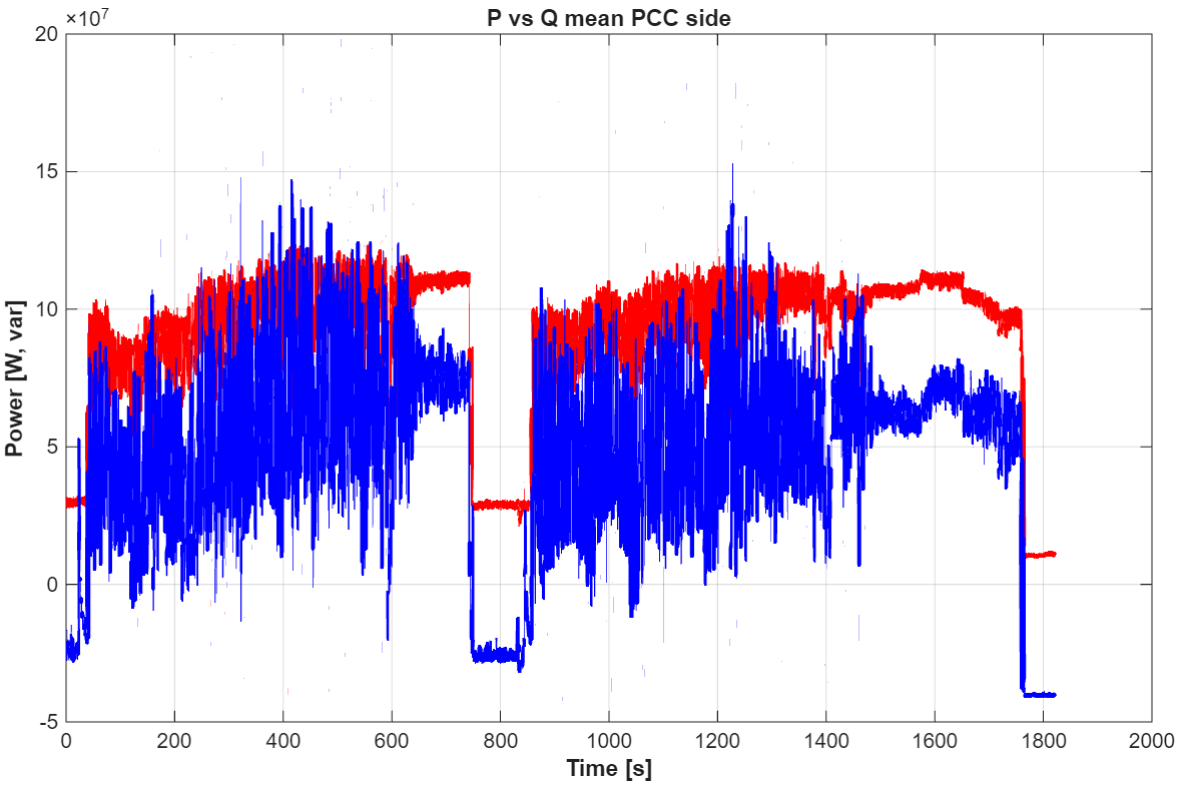


Figure 5-2 active (red) and reactive (blue) power

First period: 760s – 830 s

The assumption did on this period is validated from the reactive power and active power graphs. The reactive power, in fact, is around 25 Mvar capacitive, different from the 40 Mvar expected from the filters installed. Furthermore, the reactive power upstream the EAF is null, so the electric arc furnace is off. Evidence on the graphs are reported below

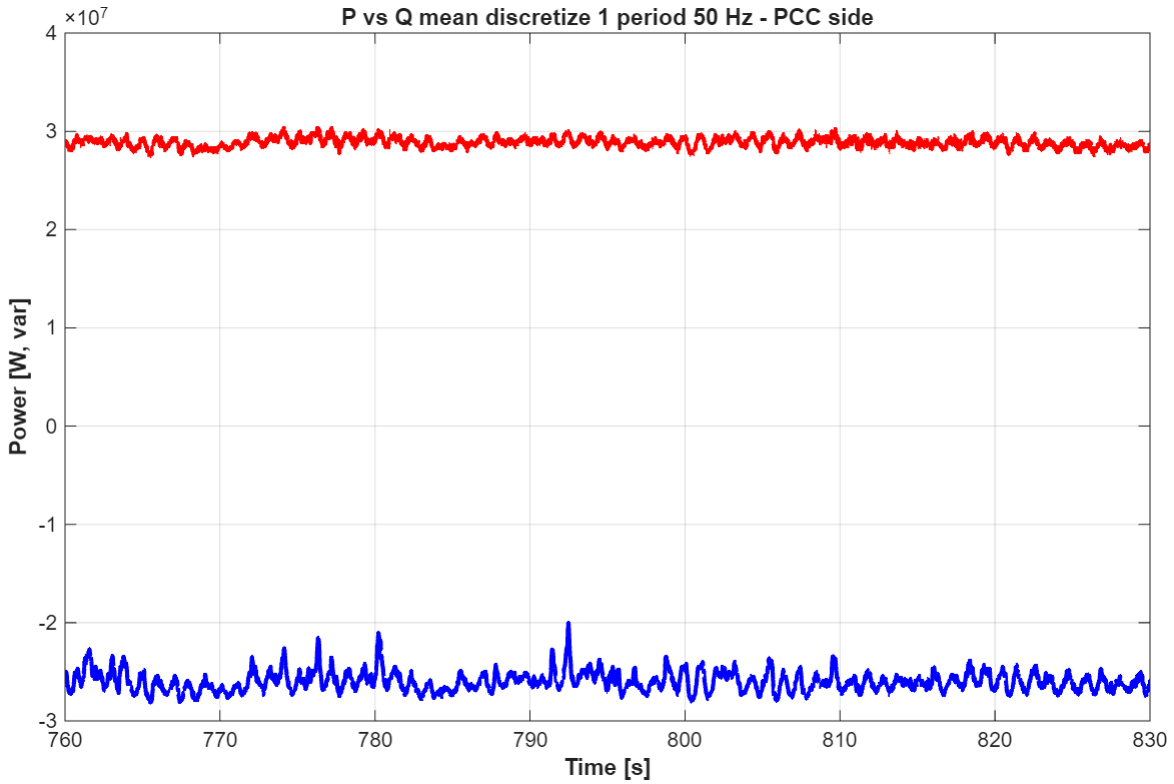


Figure 5-3 Reactive power measures at PCC while EAF off

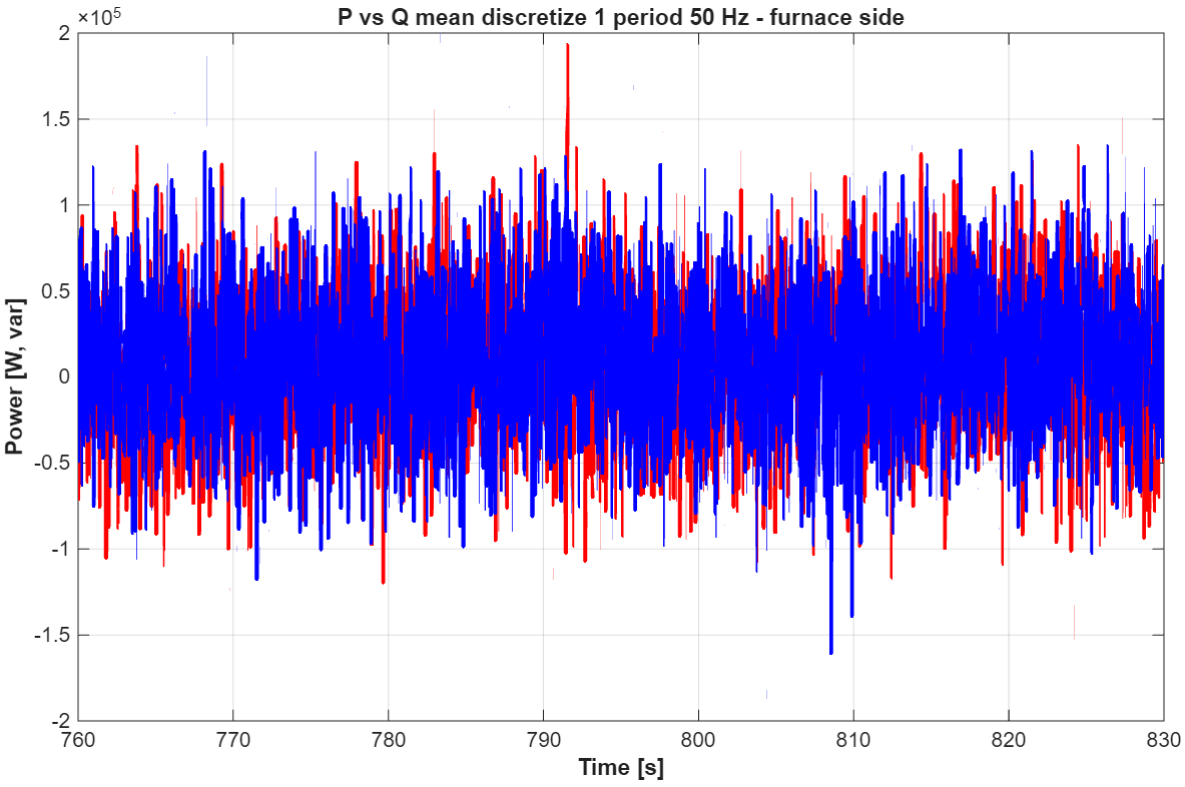


Figure 5-4 Reactive power measures furnace side while EAF off

Second period: 1140 s – 1740 s

On the second period, only the EAF is working because, if the LF was working in parallel, the reactive power measured at PCC would be greater.

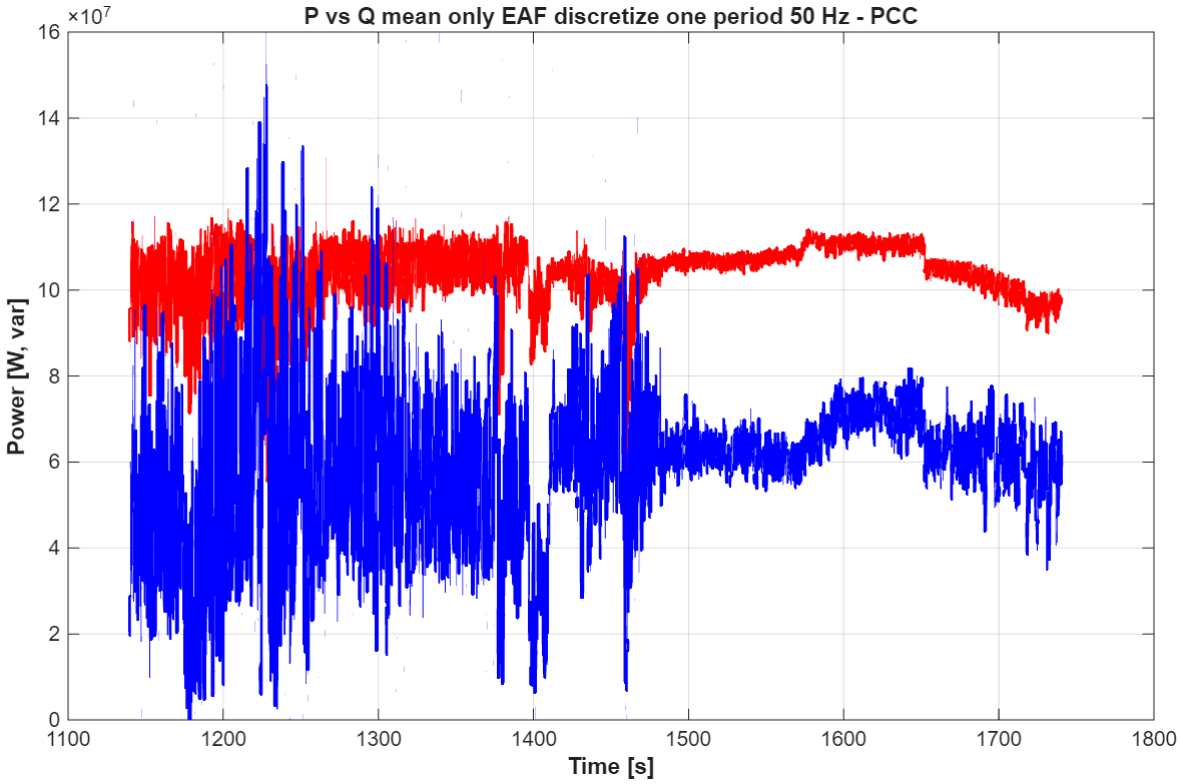


Figure 5-5 Reactive power measure at PCC while only EAF is working

Third period: 1770 s – 1820 s

For the third period, it is easy to observe that no furnaces are connected because the reactive power measured at PCC coincide exactly with the reactive power injected in the grid by the filters 40 Mvar

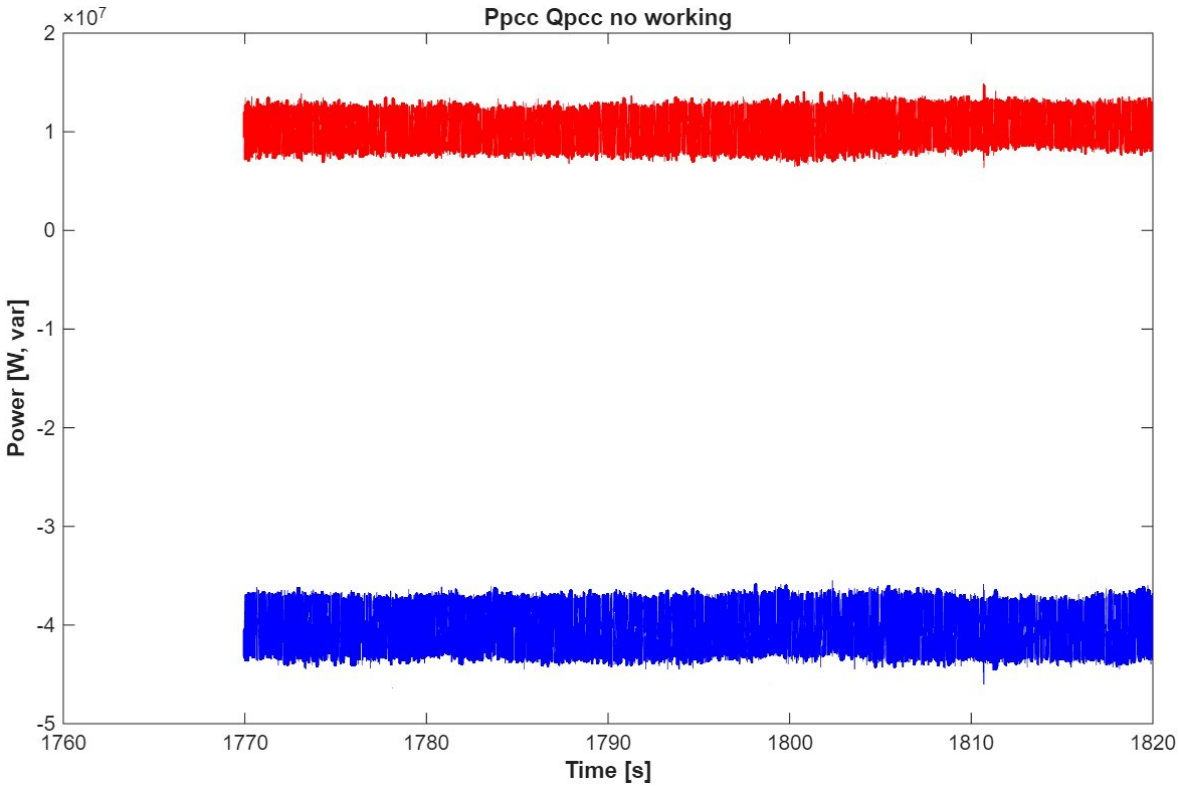


Figure 5-6 Reactive power measures at PCC while no furnaces are working

For the evaluation of the values of the clean bus, the procedure adopted was about matching the phase-to-phase voltage values obtained from a supposed value of reactive power with phase-to-phase voltages measured. Two main values of the clean bus have been individuated: one when the furnaces are working and the other when all the furnaces are off.

For the clean bus value with the furnaces ON, the supposed load has to match two reference voltages: first when only the Ladle Furnace is working and the second one, when only the EAF is working.

During the period 1, from 760 s to 830 s, the RMS value of the phase-to-phase voltages were:

$$V_{RMS_{measured}} = 136.19\ kV$$

With a supposed value of the clean bus of:

$$P = 18.2\ MW$$

$$Q = 9.5\ Mvar$$

The rms voltage observable at PCC is equal to:

$$V_{RMS_{calculated}} = 136.3\ kV$$

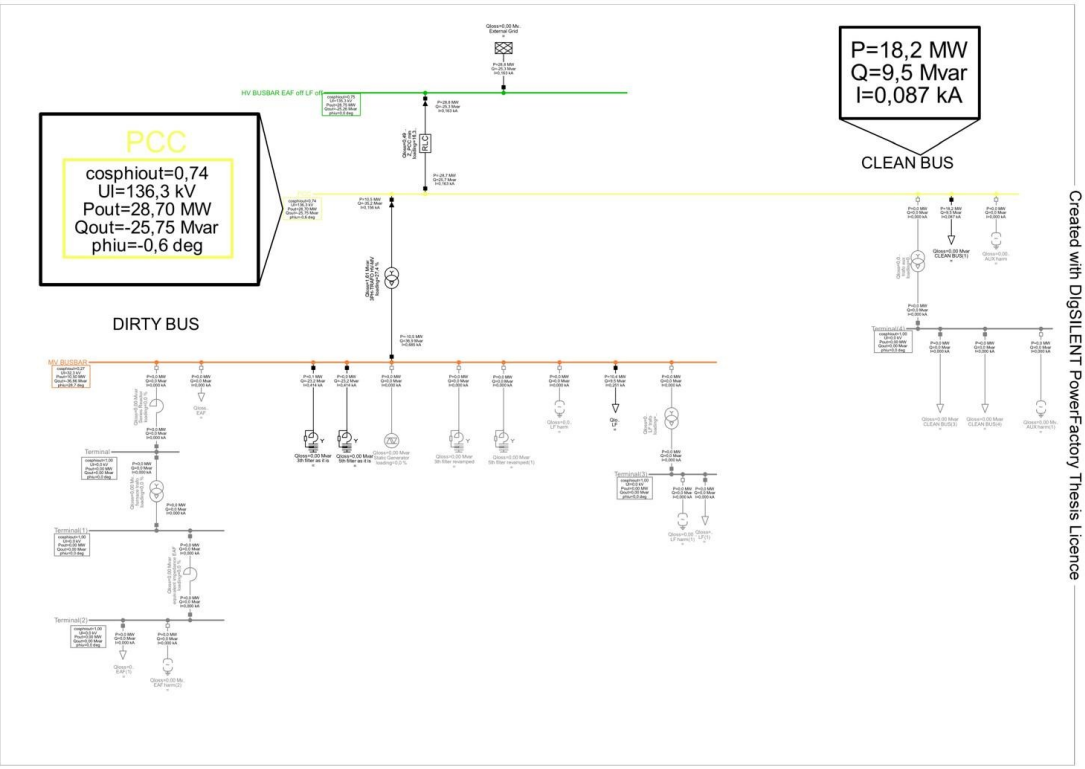


Figure 5-7 voltages at PCC with supposed clean bus loads - period 1

In order to validated this assumption, the measured voltage and the calculated one in scenario 2 have to match, with the same values of powers for the clean bus.

During period 2, from 1140 s to 1740 s, the RMS value of the phase-to-phase voltages was:

$$V_{RMS_{measured}} = 132.4\ kV$$

And with the same input data of P and Q of the clean bus in the software, the RMS value of the voltage at PCC is equal to:

$$V_{RMS_{calculated}} = 132.1\ kV$$

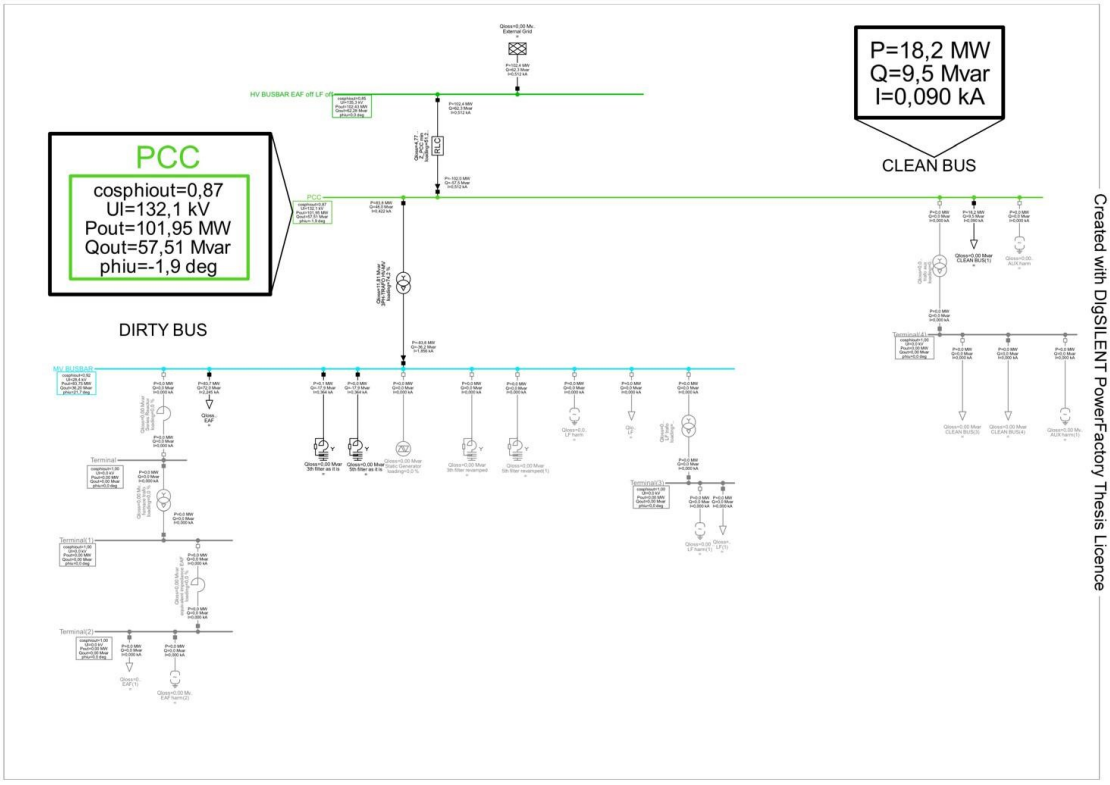


Figure 5-8 voltages at PCC with supposed clean bus loads - period 2

In the third scenario, when all the furnaces are not working, the initial hypothesis on the values of the clean bus was a lower active and the reactive power. This assumption was due to all ancillary loads that only works in parallel with the furnaces (i.e. rolling mills).

During period 3, from 1770 s to 1820 s, the RMS value of the phase-to-phase voltages was:

$$V_{RMS_{measured}} = 137.24\ kV$$

With a supposed value of the clean bus of:

$$P = 10.5\ MW$$

$$Q = 5.2\ Mvar$$

The RMS voltage value calculated is:

$$V_{RMS_{calculated}} = 137.0\ kV$$

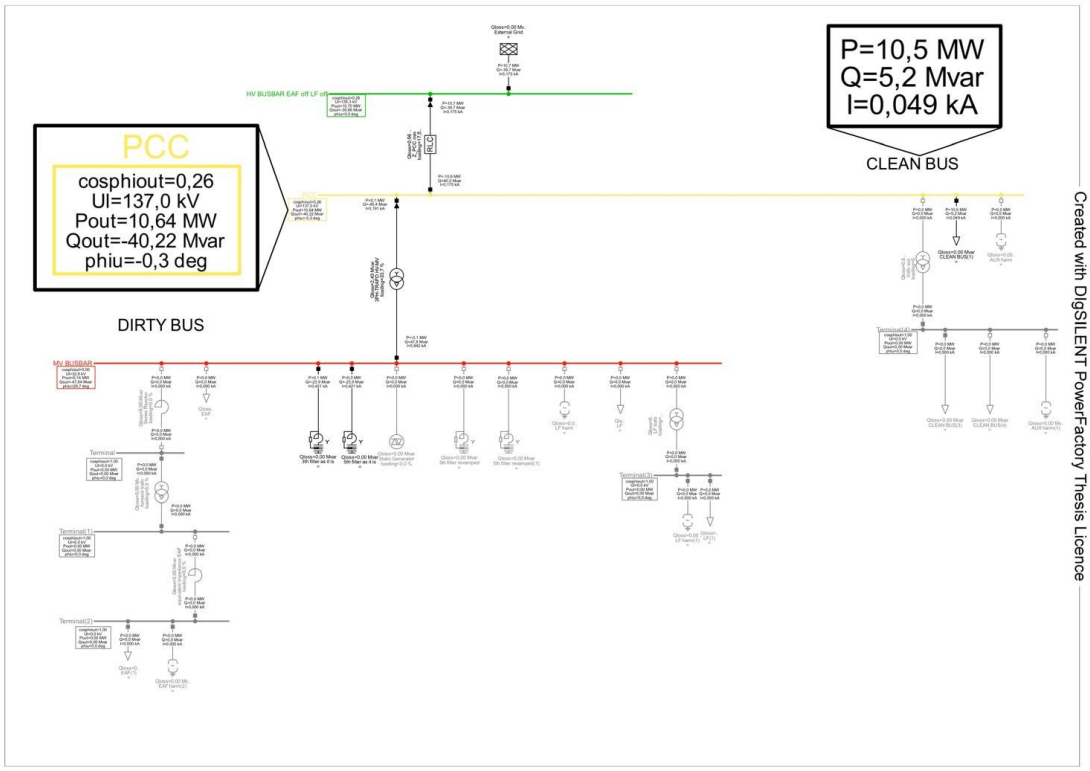


Figure 5-9 voltages at PCC with supposed clean bus loads - period 3

This stage can also be performed by hand with a trial-and-error approach, solving for every supposed power the power flow equation of the system, until the voltage value of the slack bus (PCC) was equal to the measured one, with a chosen tolerance.

In the next two sub-chapters, the supposition of the P and Q value of every load made in this chapter along with the three defined periods, must be validated. To do so, with the supposed value of P and Q of every load, filters contribution, transformer losses and clean bus contribution, in all of the three scenarios the active and reactive power, as well as the power factor, must match with the corresponding measured quantity.

This analysis was intentionally carried out in two stages. First, an analytical calculation was performed, reproducing the traditional approach, without exploiting any type of tools or software. Only after establishing the analytic baseline, the calculations of every scenario have been performed also by software. In this case, the software used was DIgSILENT PowerFactory, a professional software environment widely adopted in power system engineering. It provides a comprehensive suite of simulation tools, including steady-state power flow analysis and harmonic analysis, allowing the electrical behaviour of the network

to be assessed under realistic operating conditions, with a level of detail that is difficult to achieve analytically.

5.2.1. ANALYTIC CALCULATION

For the analytic calculation, starting from a supposed value of P and Q of every load, it is possible to achieve the active and reactive power at PCC. For the transformer contribution, only the HV/MV transformer must be considered because the point where the quantities have been measured was upstream the furnace transformer, so their losses have been already taken into account. Instead, with the following calculations, the losses in the HV/MV transformer can be obtained:

It is possible to calculate the reactive current and the active current with the following formula:

$$I_{active} = \frac{P}{\sqrt{3} \cdot V}$$

$$I_{reactive} = \frac{Q}{\sqrt{3} \cdot V} \tag{5.10}$$

$$I_{total} = \sqrt{{I_{active}}^2 + {I_{reactive}}^2}$$

where P and Q are the powers seen by the transformer, obtained as:

$$P_{trafo} = P_{EAF} \; or \; P_{LF} \tag{5.11}$$

Based on the connected load in the considered period:

$$Q_{trafo} = Q_{EAF} \; or \; Q_{LF} \; - Q_{filters} \tag{5.12}$$

and V is the phase-to-phase voltage upstream the EAF.

Then the losses in the transformer are achieved exploiting its impedance value. Based on the reference voltage used to calculate the current, the primary or the secondary side impedance must be selected:

$$Q_{loss} = 3 \cdot x_{tr} \cdot {I_{total}}^2 \tag{5.13}$$

First period:

in this scenario, with the ladle furnace working and the EAF no working. The phase-to-phase voltage upstream the EAF is 33.043 kV. We obtain:

- Contribute from the filters: $Q = 46.4\ Mvar$
  Their values differ from the nominal one because the voltage where the filters are connected is different (higher voltages implies greater capacitive power injected, lower voltages imply lower value of the reactive power injected)
- Losses in the transformer HV/MV:
  - $I_{active} = 181.19\ A$
  - $I_{reactive} = -645.44\ A$
  - $I_{total} = 670.39\ A$

  Leading to: $Q_{loss} = 1.502\ Mvar$
- Contribute from the Ladle Furnace: $Q = 9.5\ Mvar\ ;\ P = 10.4\ MW$
- Contribute from the electric Arc Furnace: $Q = 0\ Mvar\ ;\ P = 0\ MW$
- Contribute from the clean bus: $Q = 9.5\ Mvar\ ;\ P = 18.2\ MW$

Summing up all the contributions, the values of active and reactive power at the PCC obtained are:

$$P_{PCC} = P_{LF} + P_{clean\ bus} = 28.6\ MW$$

$$Q_{PCC} = Q_{LF} + Q_{loss} - Q_{filters} + Q_{clean\ bus} = -25.9\ Mvar$$

Second period:

in this scenario, only the electric arc furnace is working, the ladle furnace is turned off. The phase-to-phase voltage upstream the EAF is 29.209 kV. We obtain:

- Contribute from the filters: $Q = 35.8\ Mvar$
  Their values differ from the nominal one because the voltage where the filters are connected is different (the nominal voltage of the filters is 30 kV, in this case the voltage is lower, this implies a lower capacitive power injected)
- Losses in the transformer HV/MV:
  - $I_{active} = 1653.44\ A$

- $I_{reactive} = 715.38\ A$
- $I_{total} = 1801.56\ A$

Leading to: $Q_{loss} = 10.85\ Mvar$

- Contribute from the Ladle Furnace: $Q = 0\ Mvar\ ;\ P = 0\ MW$
- Contribute from the electric Arc Furnace: $Q = 71.992\ Mvar\ ;\ P = 83.65\ MW$
- Contribute from the clean bus: $Q = 9.5\ Mvar\ ;\ P = 18.2\ MW$

Summing up all the contributions, the values of active and reactive power at the PCC obtained are:

$$P_{PCC} = P_{EAF} + P_{clean\ bus} = 101.85\ MW$$

$$Q_{PCC} = Q_{LF} + Q_{loss} - Q_{filters} + Q_{clean\ bus} = 56.54\ Mvar$$

Third period:

in this scenario, neither the electric arc furnace nor the ladle furnace is working. The active and reactive powers absorbed by the clean bus are different, due to auxiliary utilities that are commonly working in parallel with the furnaces, as rolling mills or cooler for exhaust gasses. The phase-to-phase voltage upstream the EAF is 33.518 kV. We obtain:

- Contribute from the filters: $Q = -47.8\ Mvar$
  Their values differ from the nominal one because the voltage where the filters are connected is different (in this scenario, the phase-phase voltage is the highest because no heavy load is connected near the filters)
- Losses in the transformer HV/MV:
  - $I_{active} = 0\ A$
  - $I_{reactive} = -823.36\ A$
  - $I_{total} = 823.36\ A$

  Leading to: $Q_{loss} = 2.27\ Mvar$

- Contribute from the Ladle Furnace: $Q = 0\ Mvar\ ;\ P = 0\ MW$
- Contribute from the electric Arc Furnace: $Q = 0\ Mvar\ ;\ P = 0\ MW$
- Contribute from the clean bus: $Q = 5.8\ Mvar\ ;\ P = 10.7\ MW$

Summing up all the contributions, the values of active and reactive power at the PCC obtained are:

$$P_{PCC} = P_{clean\ bus} = 10.7\ MW$$

$$Q_{PCC} = Q_{loss} - Q_{filters} + Q_{clean\ bus} = -39.73\ Mvar$$

Comparing the previously obtained values of active and reactive power in every period with the measured values at PCC, it is possible to verify the correctness of the power flow analysis performed:

Table 5-1 values of power at PCC, measured vs calculated

values of power at PCC				
		calculated	measured	delta%
first period	P[MW]	28.6	28.871	0.94%
	Q[Mvar]	-25.89802	-25.987	0.34%
second period	P[MW]	101.85	103.96	2.03%
	Q[Mvar]	56.54	58.213	2.88%
third period	P[MW]	10.7	10.648	0.49%
	Q[Mvar]	-39.73	-40.288	1.37%

These results validate the assumed clean-bus power in the two operating conditions considered: one furnace operating and both furnaces switched off.

The calculation of the power factor in every scenario is straightforward:

$$PF = \frac{P}{A} \tag{5.14}$$

Where:

$$A = \sqrt{P^2 + Q^2} \tag{5.15}$$

It results in:

Table 5-2 Power Factor in every period

Power Factor	
first period	0.74
second period	0.87
third period	0.26

5.2.2. DIGSILENT CALCULATION

As already mentioned during the calculation of the losses in the transformer, the measurement of the currents at the medium busbar had been performed upstream the electric arc furnace. For this reason, to be consistent with the analytic calculations, the loads must be attached at the medium voltage busbar: furnaces transformers losses as well as furnace reactor losses had been already taken into account in the current's measurements.

The HV/MV transformer has been implemented with the same data reported in chapter 4:

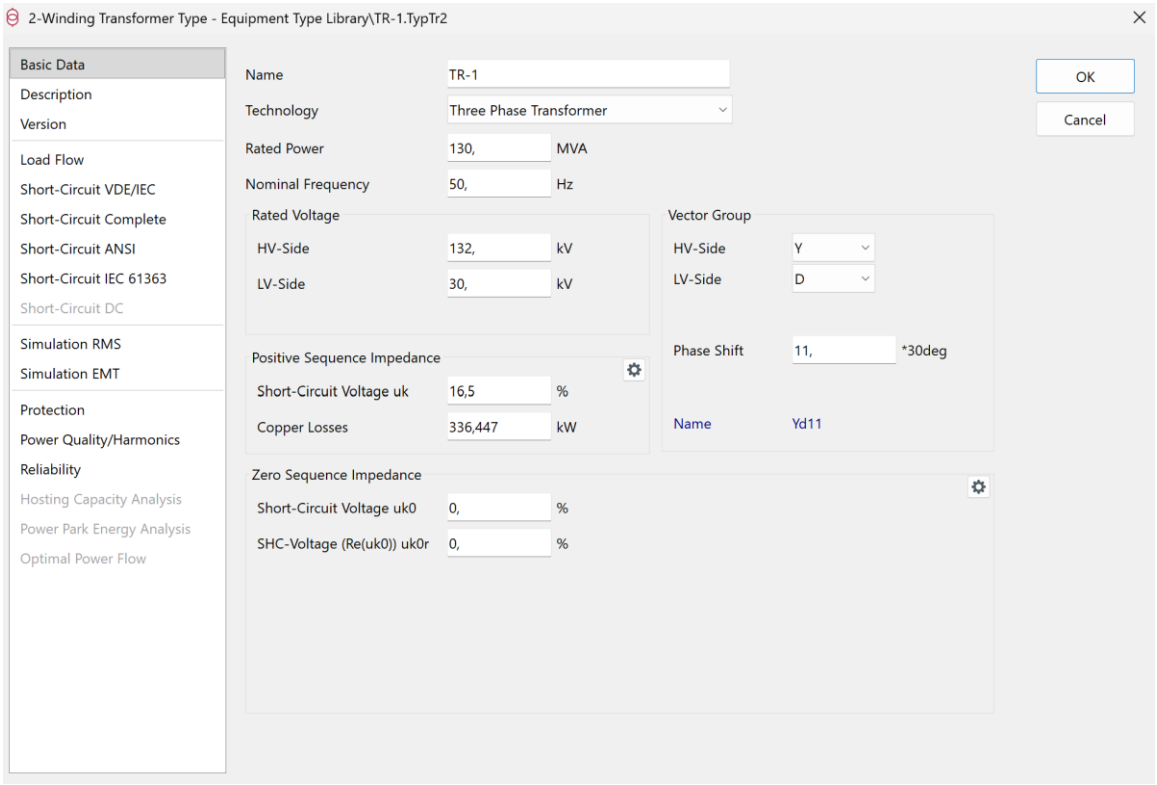


Figure 5-10 DIgSILENT tab of trasformer data 1

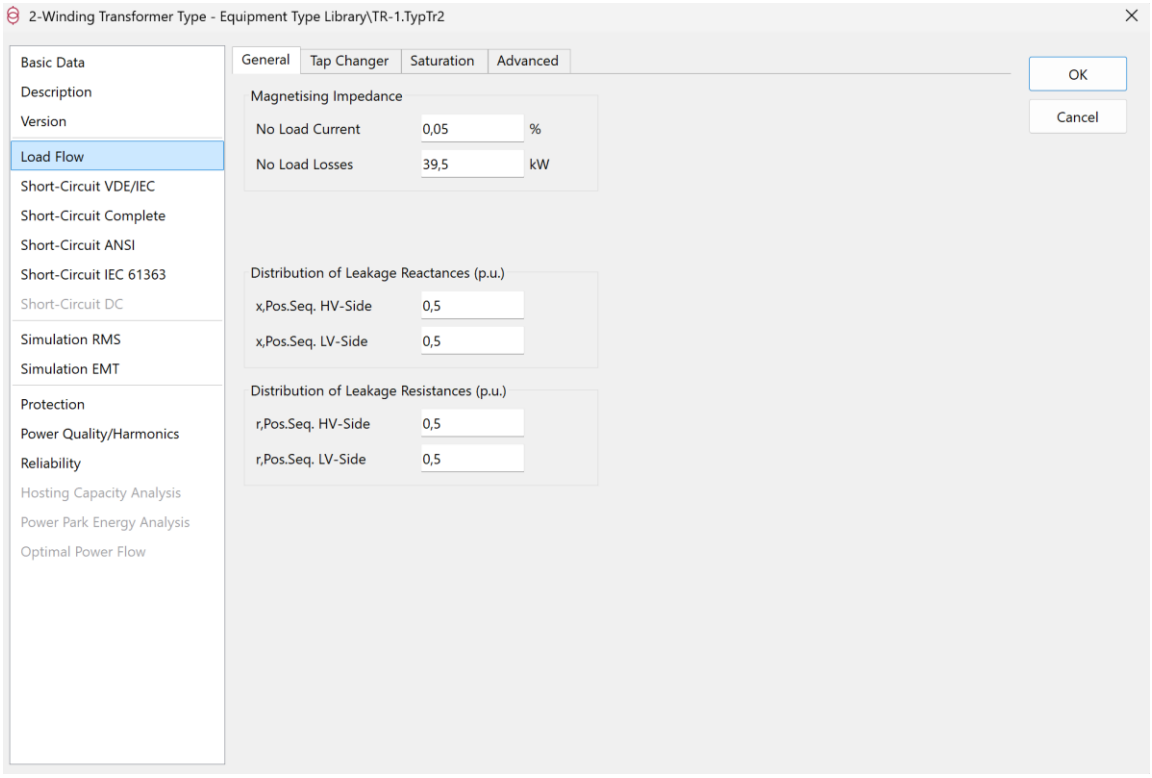


Figure 5-11 DIgSILENT tab of trasformer data 2

First scenario:

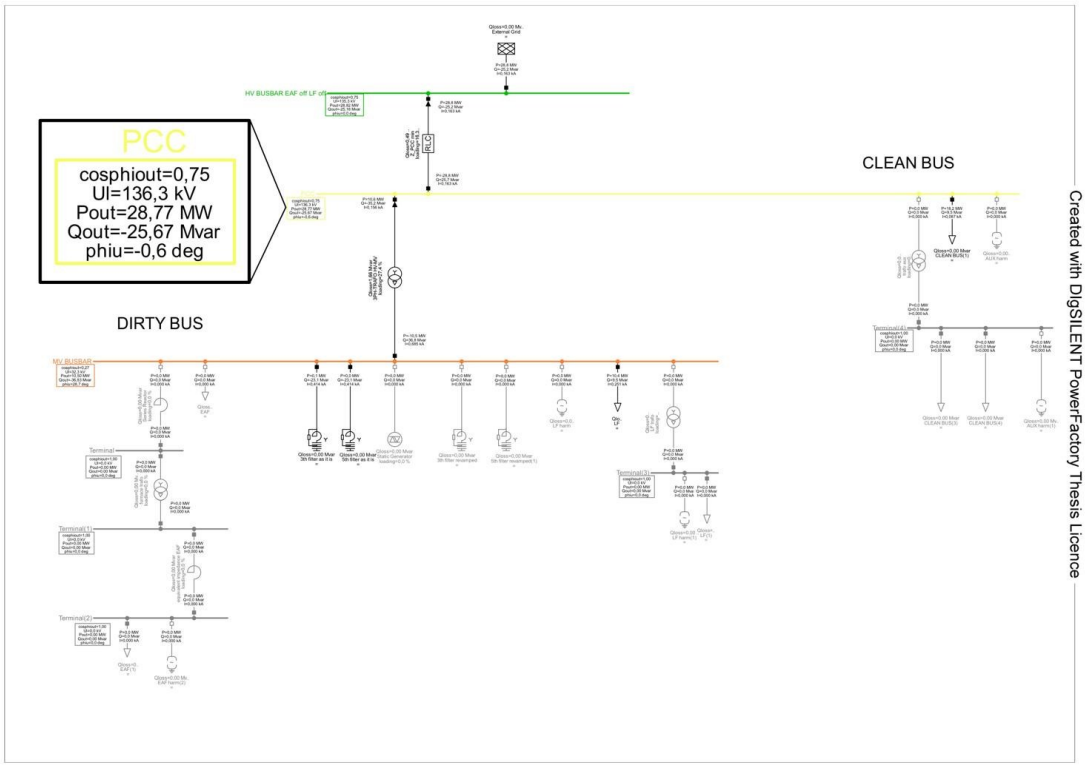


Figure 5-12 1° scenario simulation

To simulate the first scenario, when only the Ladle furnace is working, the loads representing the EAF is disconnected.

The results obtained of active power and reactive power at PCC are, in order:

$$P = 28.77\ MW$$

$$Q = -25.67\ Mvar$$

Compared with the calculated one, the discrepancy between the analytical power flow analysis and the analysis performed by the software results in a negligible difference:

$$\Delta P_{\%} = \frac{|P_{analytic} - P_{software}|}{|P_{analytic}|} = 0.59\%$$

$$\Delta Q_{\%} = \frac{|Q_{analytic} - Q_{software}|}{|Q_{analytic}|} = 0.88\%$$

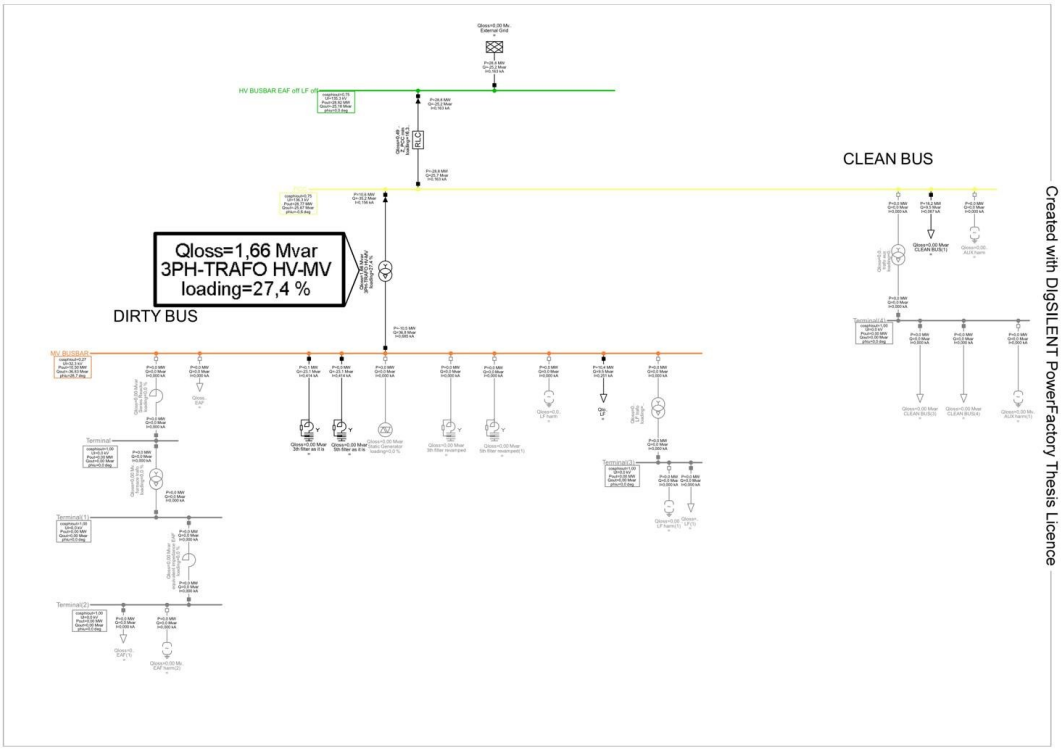


Figure 5-13 1° scenario - transformer losses

Also, the losses in the HV/MV transformer calculated analytically are similar with the transformer losses observable on the software:

$$Q_{loss_{software}} = 1.66\ Mvar$$

$$Q_{loss_{analytic}} = 1.502\ Mvar$$

Second scenario:

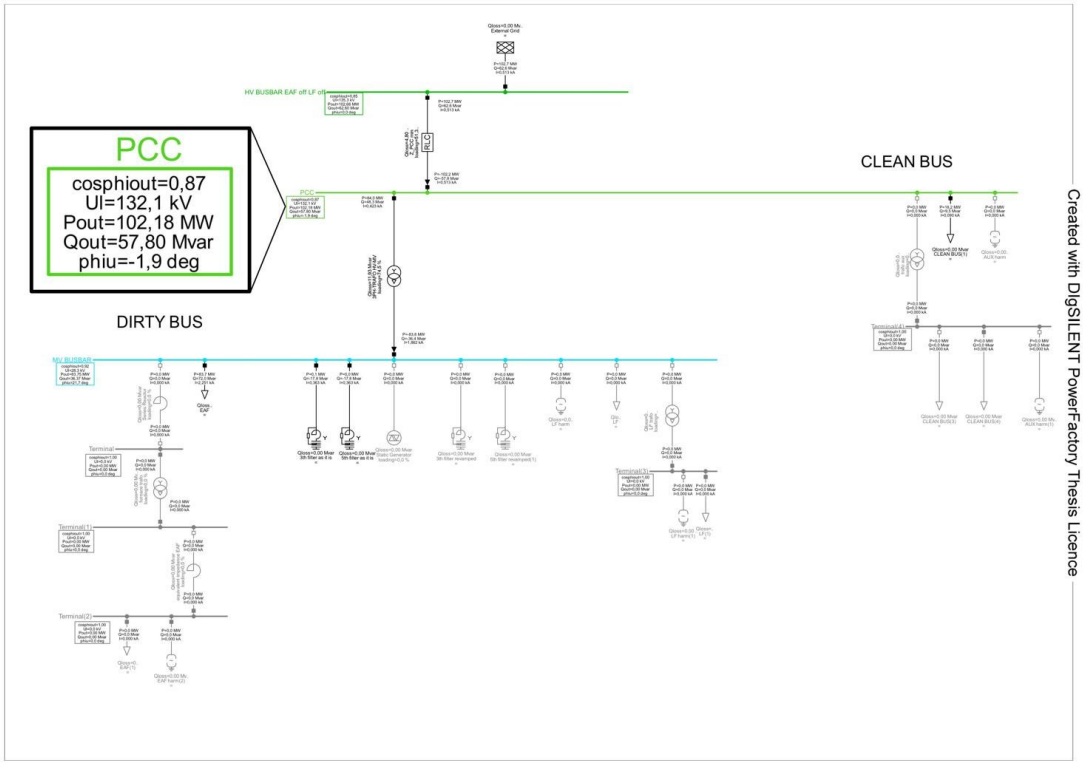


Figure 5-14 2° scenario simulation

In this scenario, as for the analytic calculation, only the EAF is working. To do so, on the single line diagram of the software, all the other loads have been disconnected. The clean bus is settled as for the first scenario, because in both of them there is a furnace working.

In this period as well is useful to compare the result with their analytic counterpart. In this case, the values obtained of active power and reactive power at PCC are, in order:

$$P = 102.18\ MW$$

$$Q = 57.80\ Mvar$$

Compared with the calculated one, the discrepancy between the analytical power flow analysis and the analysis performed by the software results in a negligible difference:

$$\Delta P_{\%} = \frac{\left|P_{analytic} - P_{software}\right|}{\left|P_{analytic}\right|} = 0.32\%$$

$$\Delta Q_{\%} = \frac{|Q_{analytic} - Q_{software}|}{|Q_{analytic}|} = 2.23\%$$

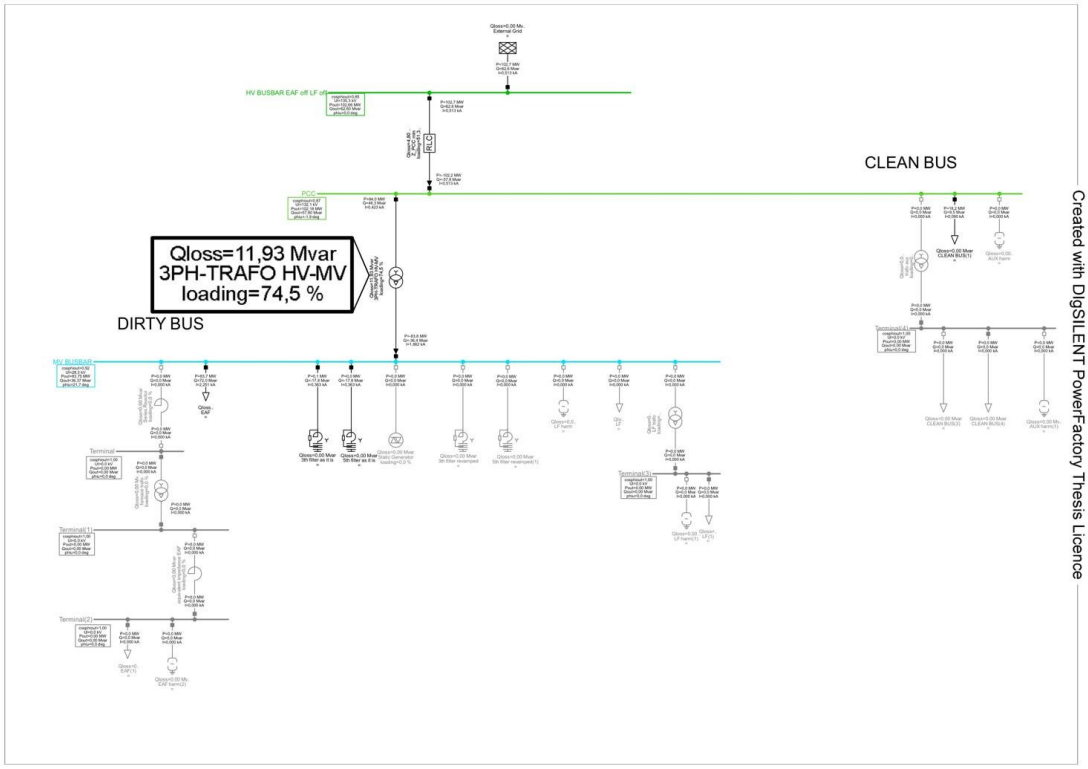


Figure 5-15 2° scenario - transformer losses

For the losses on the HV/MV transformer in the second period, the results are the following:

$$Q_{loss_{software}} = 11.93\ Mvar$$

$$Q_{loss_{analytic}} = 10.85\ Mvar$$

It can be noticed that the major discrepancy between the reactive power at PCC calculated analytically and the one calculated by the software is due to the different value of the transformer losses:

$$\Delta Q_{loss} = 1.08\ Mvar$$

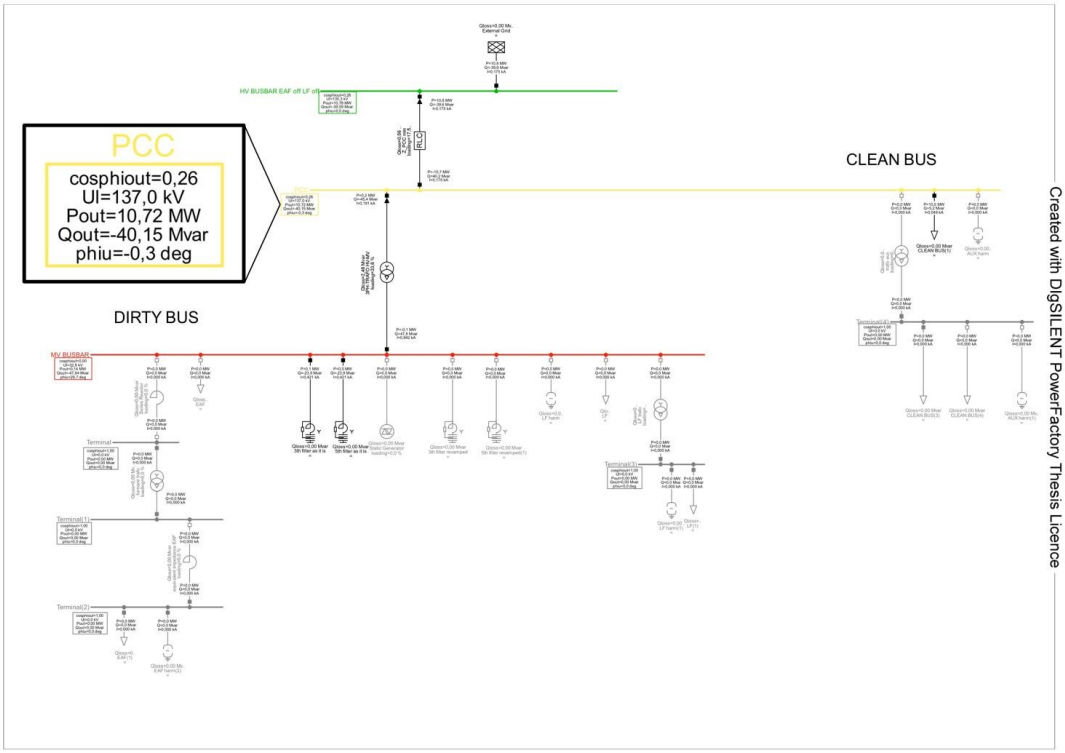


Figure 5-16 3° scenario simulation

In the last period, no furnaces are connected, only the old filters and the clean bus are considered in the power flow. As mentioned before, the clean bus in this scenario has a different value.

The results obtained of active power and reactive power at PCC are, in order:

$$P = 10.72\ MW$$

$$Q = -40.15\ Mvar$$

Compared with the calculated one, the discrepancy between the analytical power flow analysis and the analysis performed by the software results in a negligible difference:

$$\Delta P_{\%} = \frac{|P_{analytic} - P_{software}|}{|P_{analytic}|} = 0.19\%$$

$$\Delta Q_{\%} = \frac{|Q_{analytic} - Q_{software}|}{|Q_{analytic}|} = 1.06\%$$

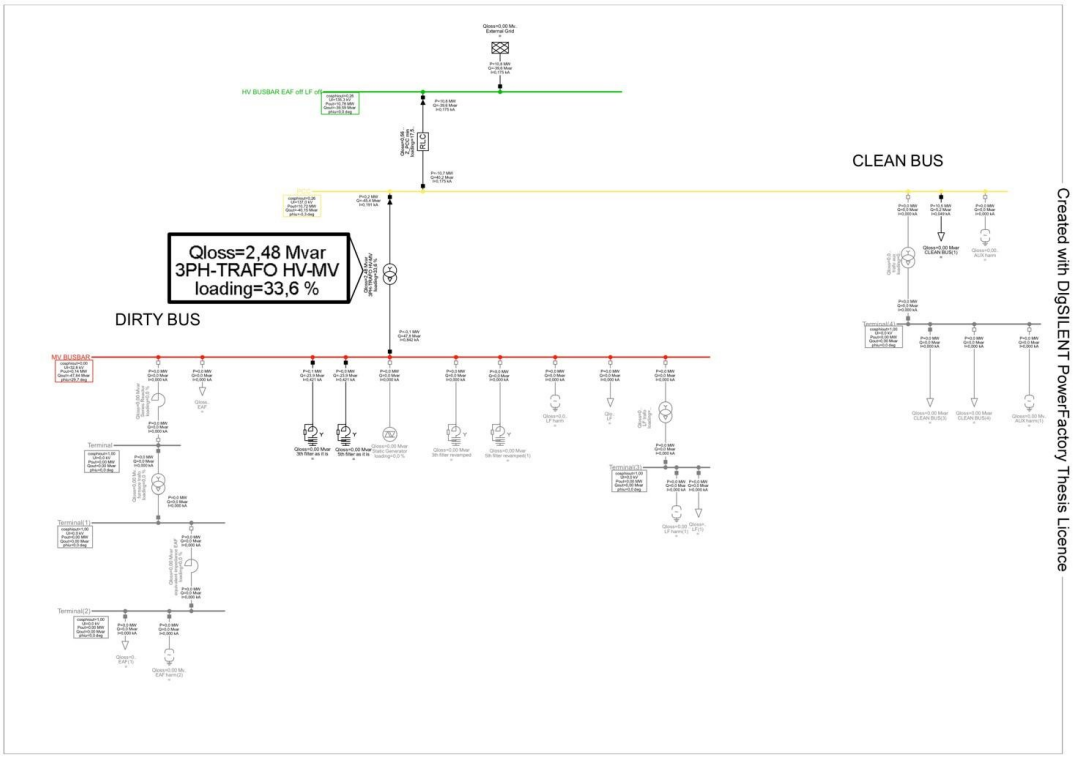


Figure 5-17 3° scenario - transformer losses

In this case, the differences in the transformer losses are:

$$Q_{loss_{software}} = 2.48\ Mvar$$

$$Q_{loss_{analytic}} = 2.27\ Mvar$$

Where only the current due to the reactive power contribution is present. In fact, no active loads are present on the dirty bus downstream the transformer in this scenario.

Reported below, a table summing up all the results obtained from the analytic analysis and the one performed with the software:

Table 5-3 analytic vs software power values

values of power at PCC				
		analytic	software	delta%
first period	P[MW]	28.6	28.77	0.59%
	Q[Mvar]	-25.89802	-25.67	0.88%
second period	P[MW]	101.85	102.18	0.32%
	Q[Mvar]	56.54	57.80	2.23%
third period	P[MW]	10.7	10.72	0.19%
	Q[Mvar]	-39.73	-40.15	1.06%

As expected, it can be noticed that the result obtained with DigSilent, in average, are closer to the measured values. However, the discrepancy between analytic and software approach is so small that the reactive power compensation needed from the STATCOM to be compliant at PCC is the same in any case. This topic will be further explored in chapter 7.

Table 5-4 software vs measured power values

values of power at PCC				
		Calculated via software	measured	delta%
first period	P[MW]	28.77	28.871	0.35%
	Q[Mvar]	-25.67	-25.987	1.22%
second period	P[MW]	102.18	103.96	1.71%
	Q[Mvar]	57.80	58.213	0.71%
third period	P[MW]	10.72	10.648	0.68%
	Q[Mvar]	-40.15	-40.288	0.34%

5.3. HARMONIC ANALYSIS

For the harmonic analysis, the worst-case operating condition is considered. Accordingly, all loads capable of injecting harmonic currents are assumed to be connected and operating simultaneously.

The main elements that provide harmonics currents are the electric arc furnace, the ladle furnace and the clean bus. Below are reported the list, for every harmonic order, of the contribution of the current rated on the fundamental one.

Table 5-5 percentage of harmonics currents for every harmonics order until the 50th

Order	I_{EAF} *30kV*	I_{LF} *30kV*	$I_{clean\ bus}$ *132kV*
	$I_{\%}$	$I_{\%}$	$I_{\%}$
1	*100%*	*100%*	*100%*
2	*3.10%*	*3.87%*	*0.76%*
3	*7.20%*	*2.79%*	*0.63%*
4	*1.80%*	*1.86%*	*0.30%*
5	*5.20%*	*1.41%*	*2.60%*
6	*2.25%*	*0.80%*	*0.16%*
7	*2.50%*	*0.66%*	*1.10%*
8	*1.50%*	*0.42%*	*0.04%*
9	*1.00%*	*0.29%*	
10	*0.50%*	*0.25%*	
11	*0.40%*	*0.22%*	*1.95%*
12	*0.30%*	*0.19%*	
13	*0.20%*	*0.17%*	*1.07%*

14	*0.19%*	*0.14%*	
15	*0.18%*	*0.10%*	
16	*0.17%*	*0.12%*	
17	*0.16%*	*0.08%*	
18	*0.15%*	*0.10%*	
19	*0.14%*	*0.10%*	
20	*0.12%*		
21	*0.11%*		
22	*0.10%*		
23	*0.09%*		
24	*0.09%*		
25	*0.08%*		
26	*0.06%*		
27	*0.05%*		
28	*0.05%*		
29	*0.04%*		
30	*0.04%*		
31	*0.03%*		
32	*0.03%*		
33	*0.03%*		
34	*0.03%*		
35	*0.03%*		
36	*0.02%*		
37	*0.02%*		
38	*0.02%*		
39	*0.02%*		
40	*0.02%*		
41	*0.02%*		
42	*0.02%*		
43	*0.02%*		
44	*0.02%*		
45	*0.01%*		
46	*0.01%*		
47	*0.01%*		
48	*0.01%*		
49	*0.01%*		
50	*0.01%*		

As observable, in the table all the harmonics contributions until the 50^{th} order are reported. If, for the considered load, no contribution is given for a specific order, its value is not reported. Mind that, as expected, the most critical load is the EAF and its harmonic contribution persist up to the last order considered (50^{th}).

The rated current given as value base value for all loads were:

$$30\ kV \rightarrow I_{EAF} = 1924\ A$$

$$30\ kV \rightarrow I_{LF} = 290\ A$$

$$132\ kV \rightarrow\ I_{clean\ bus} = 103\ A$$

For a more detailed representation of the harmonic phenomenon, all of these values have been reported to the voltage where the loads that they represent are located on the single line diagram. Exploiting the voltage ratio of the various transformer, the currents obtained are:

$$1.25\ kV \rightarrow I_{EAF} = 46176\ A$$

$$0.33\ kV \rightarrow I_{LF} = 26364\ A$$

$$16.298\ kV \rightarrow\ I_{clean\ bus} = 822\ A$$

The position of the current generator of the electric arc furnace is downstream the series reactor and the furnace transformer:

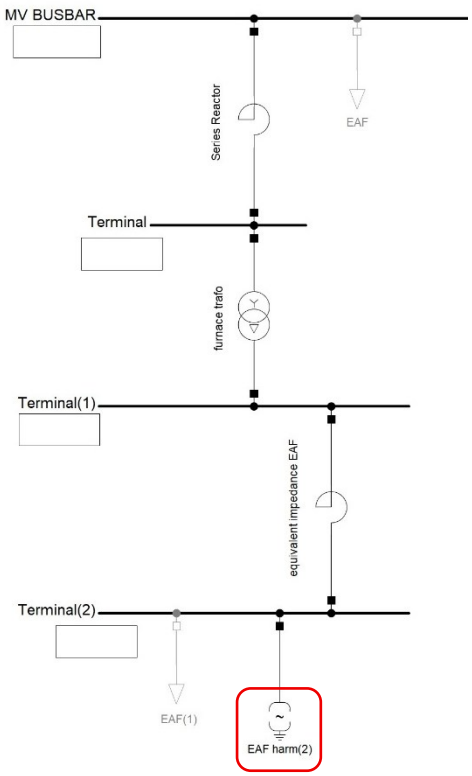


Figure 5-18 EAF harmonic current source position on the SLD

The same procedure has been applied for the harmonic source of the ladle furnace, its position is downstream the LF transformer:

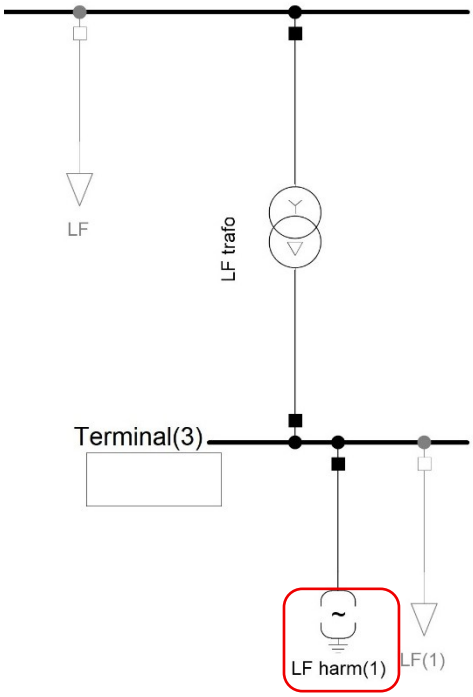


Figure 5-19 LF harmonic current source position on the SLD

Finally, also the clean bus harmonic source has been placed downstream its transformer, in this case at medium voltage level:

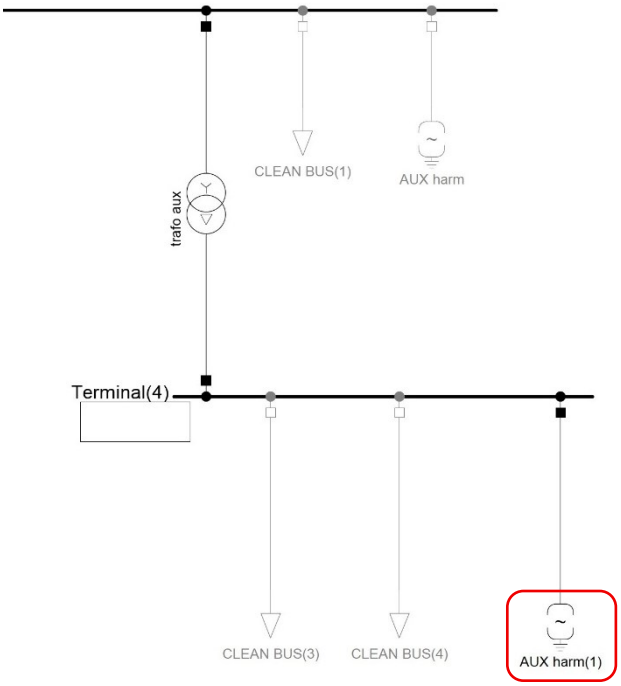


Figure 5-20 clean bus harmonic current source position on the SLD

With all loads connected and with the harmonics currents sources properly designed, it is possible to perform a harmonic load flow analysis on DIgSILENT. As expected, the THD at PCC is already compliant with the standard:

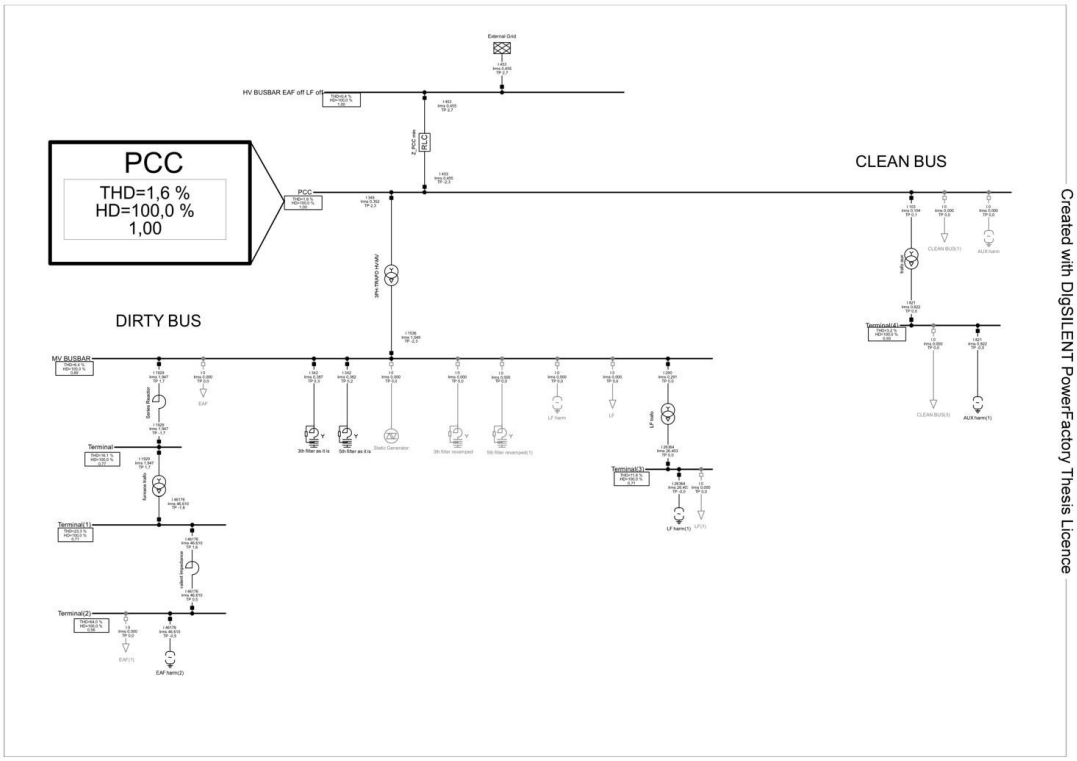


Figure 5-21 THD in the AS-IT-IS situation

De facto, the customer required a revamping of the old filters in order to be compliant with the standard limits for every single harmonic. Considering the standard already discussed in chapter 3, IEC 61000-3-6, it is evident that, in this situation, the 8th harmonic is above its limit:

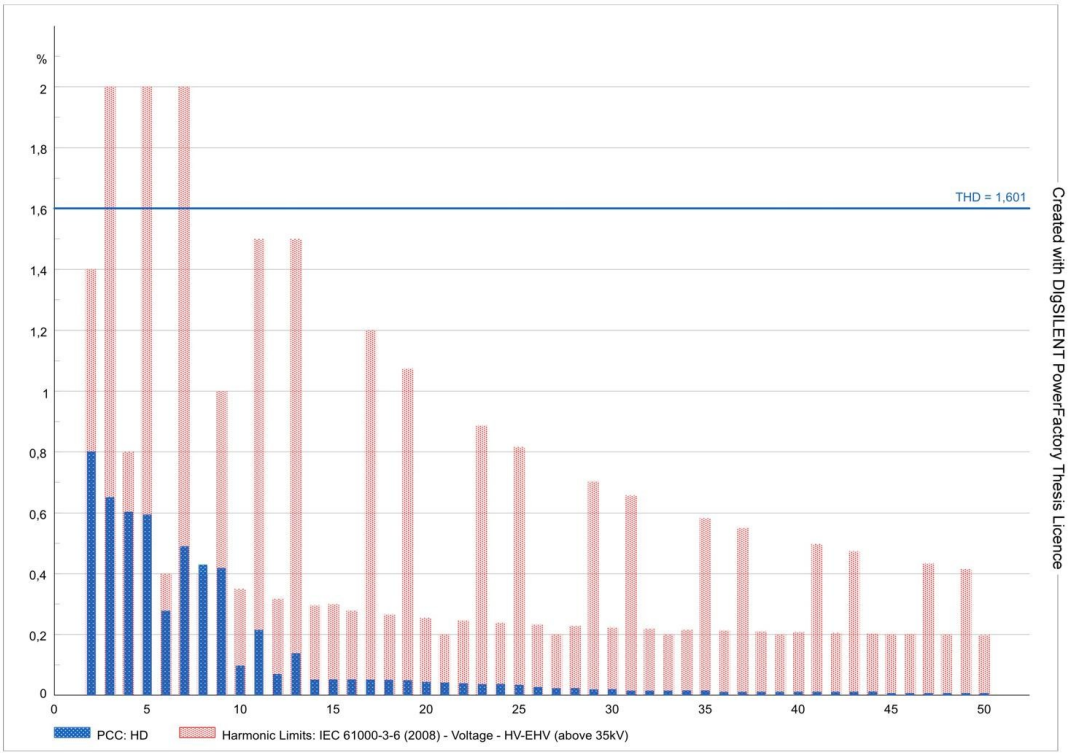


Figure 5-22 single harmonic order percentage vs standard

In the old case, the filters had a rated reactive power of *20 Mvar* each, and they were tuned, respectively, on the 3rd and on the 5th harmonic.

5.4. FLICKER ANALYSIS

As discussed in chapter 3, voltage flicker is a slightly perceptible fluctuation in the electric lamps' luminosity. This is mainly caused by rapid variation in the supply voltage: in industrial power system equipped with heavy loads, such as EAF system, this phenomenon is inevitable. When this voltage fluctuations occur within specific frequency ranges and with the correct amplitude, the human eye could be annoyed by these oscillations in brightness. Because flicker is ultimately a physiological disturbance, its evaluation requires a measurement process that mimics the response of human visual system: the flickermeter.

The operation of the flickermeter is strictly defined in a dedicated standard (IEC 61000-4-15): this document defines the internal architecture that the instrument must include. In particular: the dynamic model of the lamp, the demodulation process, the statistical block and the mathematical formulation used to compute the "short-term flicker index" (P_{st}) and the "long-term flicker index" (P_{lt}).

As already mentioned in chapter 3, the adopted standard (IEC 61000-3-7), which establishes the compatibility level for both P_{st} and P_{lt}, in the considered case are, respectively, 1,0 and 0.8. Although the conceptual structure of the flickermeter is defined clearly in the IEC61000-4-15, reproducing its exact behaviour by a mathematical model is extremely complicated. The simulation of each of the components of the flickermeter introduces uncertainties and errors and, been the P_{st} formula a non-liner combination of the output of these blocks, even a small variation of these outputs from their empirical counterparts can results in errors and deviation of the short-term flicker index by its real value. For these reasons, an already developed MatLab script provided by Nidec R&D department has been used to predict the short-term flicker index and the Instantaneous Flicker Severity (IFS).

The script accepts as input the vector of the phase-to-phase voltages at the reference point (in this case it will be the PCC), the sampling frequency with which the voltage vector values has been collected, the frequency of the network and the frequency with which the simulated light bulb is working. For the output values, the P_{st} for each phase and the vector containing the IFS values for each phase at any voltage sample is provided.

In the considered study-case, the P_{st} measured at PCC with a flickermeter in the as-it-is situation is obtained as the mean of the P_{st} measured on each phase:

- Phase a: $P_{st_a} = 4.11$
- Phase b: $P_{st_b} = 4.15$
- Phase c: $P_{st_c} = 3.67$

Resulting in:

$$P_{st} = 4.033$$

To be sure that the script provides consistent result, the P_{st} of each phase under the same conditions of work has been calculated:

- Phase a: $P_{st_a} = 4.09$
- Phase b: $P_{st_b} = 4.28$
- Phase c: $P_{st_c} = 3.79$

Resulting in:

$$P_{st} = 4.053$$

With an error lower than 0.5%.

Considering:

- $200\mu s$ as sampling frequency
- $50Hz$ as nominal frequency
- $230Hz$ as frequency of the simulated light bulb

Comparing the real IFS (with subscript "r") with the simulated one for each phase, the two curves are merely distinguishable:

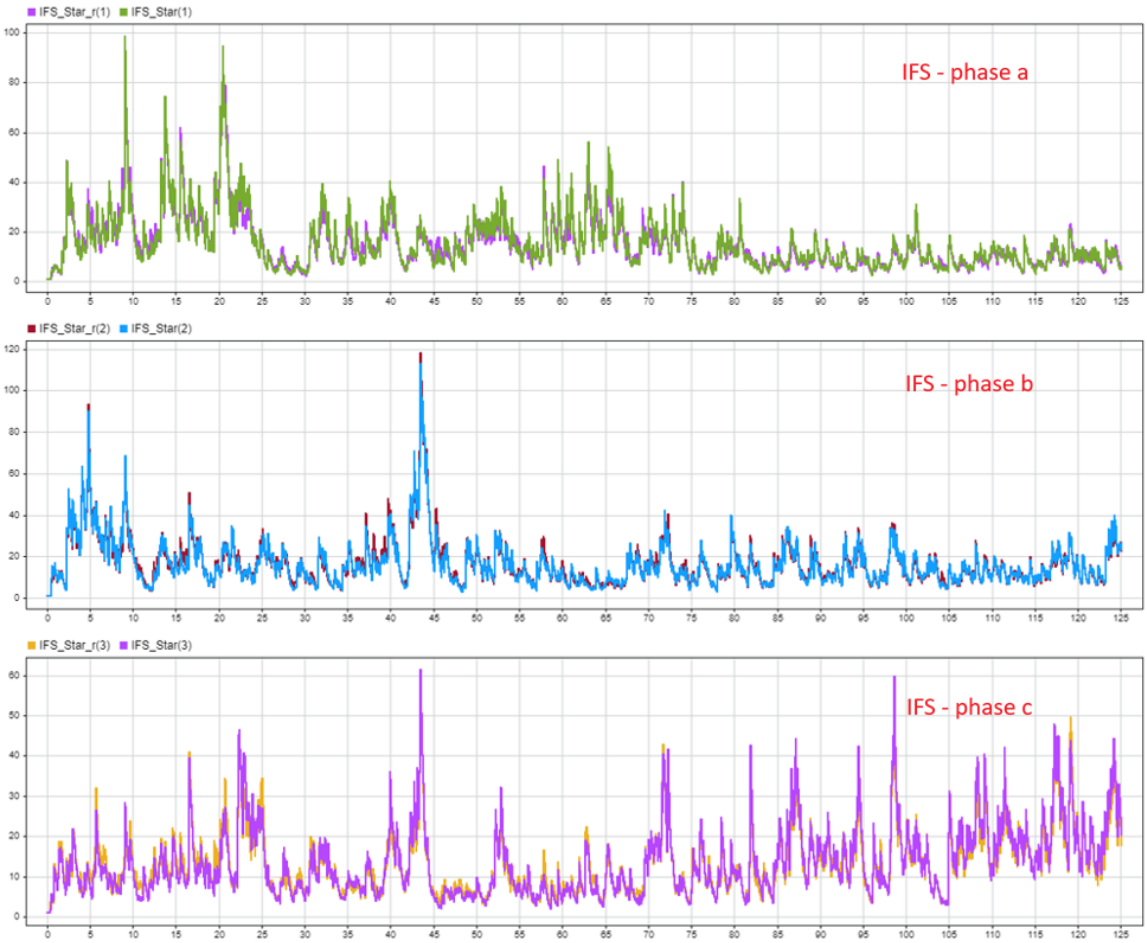


Figure 5-23 IFS measured vs simulated

An outstanding indicator of the flicker effect is obtained performing the Fortescue symmetrical component transformation. With the Fortesque matrix, the three-phase system is divided into three new three phase systems:

Direct component: it represents the nominal system, if the starting system is balanced and symmetrical, only this component would be different from zero.

Inverse component: It represents the imbalance; it is a three-phase system that rotates in the opposite direction to the direct one.

Zero component: It does not rotate; its three vectors coincide. In fact, it is null when no neutral conductor is present in the system.

For the evaluation of the Flicker effect, the most important component is the Direct one. In a symmetrical and balanced three-phase system, it should be constant and its variation is directly responsible for the amplitude variations perceived by the flickermeter. The negative sequence component, on the other hand, highlights any imbalance introduced by the furnace operation, which may amplify or distort the flicker effect.

Reported below, the positive and negative sequence of the voltage at the medium voltage busbar and at PCC gives an idea of the imbalance present in the system:

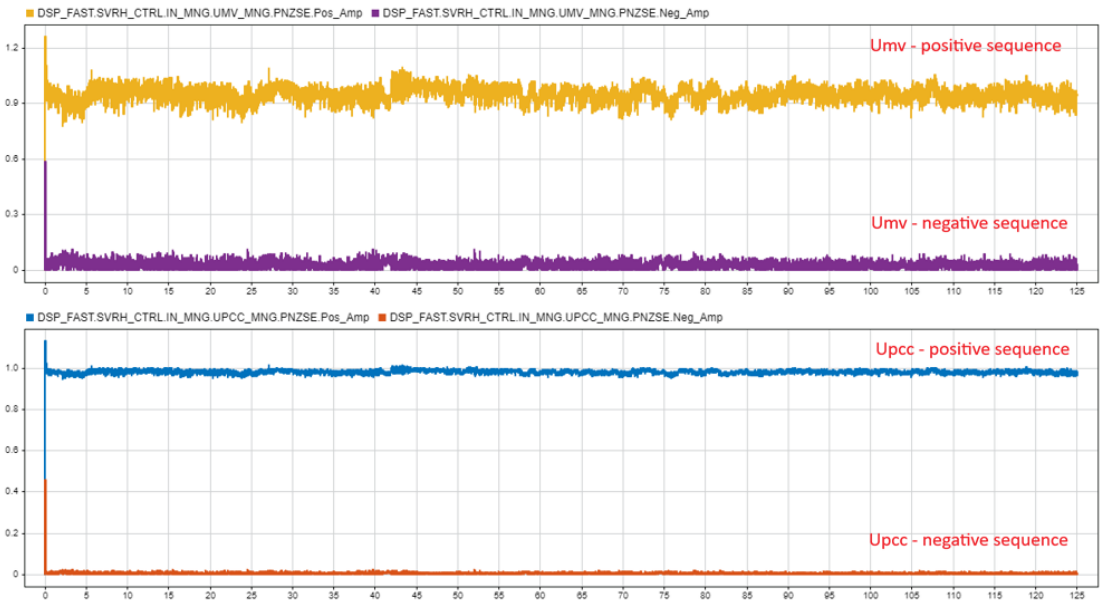


Figure 5-24 PCC and MV positive and negative voltage

The considered network is mainly influenced by the Electric Arc Furnace. To attenuate the distortion observed on the voltages, a standard procedure is controlling the RPCS in order to match the positive sequence of the current produced by the EAF. In particular, adopting a STATCOM as a solution, the converter would match the EAF current reactive part.



Figure 5-25 positive and negative curret of EAF with details of reactive component

For the voltages and currents graphs as well as for the P_{st} and for the IFL, a period of 125 seconds starting from 400 s and ending at 525 s, while the meltdown phase was in place, has been considered. Also in this case, the worst-case scenario approach will be considered, to assure the fully compliance during any period of working.

6. STATCOM CONVERTER

6.1.INTRODUCTION

Nowadays the Electrical Distribution System (EDS) is facing demand of: more availability of power, better Power Quality, high reliability, low cost and less environmental impact. However, many users continue to experience severe technical and economic consequences resulting from a poor Power Quality. To improve Power Quality in the EDS, it is necessary to install, in immediate proximity of the disturbances source, a reactive shunt device compensator capable to compensate, in a fast and accurate way, the reactive power fluctuations and current load unbalance.

This chapter introduces the STATCOM as a solution for industrial Power Quality applications and then develops the analysis from operating principles to practical implementation. First, the main reactive-power compensation technologies are compared and the fundamental operating principle of the STATCOM is explained. The SILCOVAR-H architecture and its Cascaded H-Bridge topology are then presented, followed by the design role of the decoupling reactor and the adopted phase-shifted PWM strategy. The discussion therefore connects the required compensation functions with the converter topology, the principal components and the associated control principles.

In the recent years Power Quality issues have become more and more important both in practice and in research. Binding rules and regulations are imposing on suppliers (Grid Owner's/ Transmission System Operator) and consumers (Industrial plant) the obligation to keep required Power Quality at Point of Common Coupling (PCC). Moreover, the growing interest on Power Quality comes not only from the legal regulations, but also by the fact that many consumers have experienced technical and economic problems due to poor Power Quality. In fact Electrical Disturbances such as harmonics, current unbalance and flicker can prevent the electrical equipment to operate properly; on the other hand, large and fast reactive power variations at PCC induce grid voltage fluctuations decreasing the power transfer capacity and resulting, in the worst case, in the outages or voltage collapse of the Power System.

In general, Power Quality is a matter of common interest involving suppliers and consumers. In particular, for suppliers the Power Quality shall be a reliable and effective process to deliver electrical power to consumers; for consumers the Power Quality shall be a means to improve productivity and bring benefits.

To improve Power Quality at PCC different solutions are available and each one is different for the costs, reliability and performances. One obvious way is reinforcing the power grid by building new lines, installing new and bigger transformers, or moving the point of common coupling to a higher voltage level. Such measures, however, are very expensive and time consuming, if they are permitted. A straightforward and cost-effective way to improve Power Quality is installing, in immediate proximity of the disturbances source, a reactive shunt device compensator, especially developed to compensate, in a fast and accurate way, the reactive power fluctuations and load current unbalancing.

6.1.1. RPCS DEFINITON

Reactive Power Compensation Systems (RPCS) include several shunt-connected technologies with different operating principles, dynamic performances and installation requirements. The following comparison introduces mechanically switched capacitors and reactors, SVCs and STATCOMs in order to explain why converter-based compensation is particularly suitable for rapidly varying industrial loads.

Among the different devices available to manage reactive power, mechanically switched capacitors (MSC) and reactors (MSR) are simple and widely used solutions in industrial plants. It must be remarked, however, that this solution has several drawbacks: the reactive current depends linearly on the grid voltage, as shown in the below figure, consequently the reactive power decreases with the square of the grid voltage; it is possible to have only step variations of the reactive power output by switching one or more components; each insertion causes severe grid voltage transients decreasing dynamic stability of power network; in order to avoid grid voltage oscillations, the anti-resonance frequency of the network impedance must be accurately taken into account; finally, frequent maintenance operations on the breakers are mandatory.

A TCR (Thyristor Controlled Reactor) added to a fixed capacitor bank (SVC) provides a better solution in terms of smoothness of reactive power output and dynamic performances, although the latter are limited by the firing angle delay control of thyristor, which results in a time lag or transportation lag with respect to the input reference signal.

The STATCOM is the most recent solution, which allows the injection of reactive current almost independently of the grid voltage, and the fastest dynamic performances thanks to semiconductor devices controlled in turn on and turn off; it is capable of balancing grid

current without injecting current harmonics; it requires less space than the SVC. The STATCOM solutions will be widely discussed in the following paragraphs.

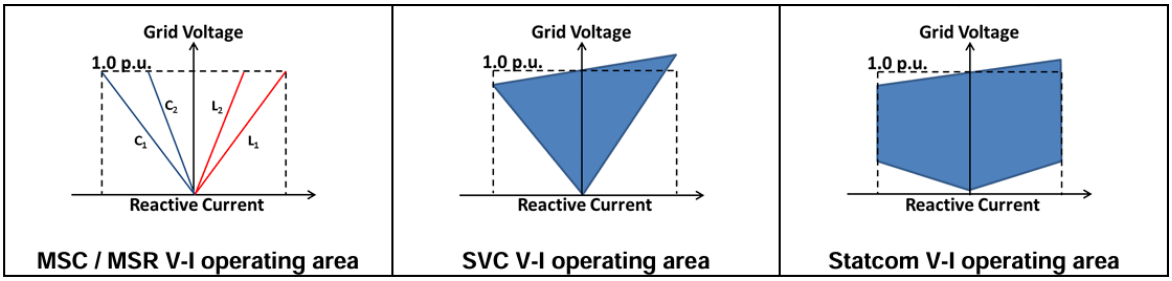


Figure 6-1 capability curve with different RPCS technologies – Nidec conversion

6.1.2. STATCOM TECHNOLOGY OVERVIEW

A STATCOM can be represented as a Voltage Source Converter (VSC) connected in shunt to the grid through a coupling reactance, consisting of a dedicated reactor, the leakage reactance of a coupling transformer, or a combination of both. The VSC is composed of power-electronic switching devices and dc capacitors. Through an appropriate switching and modulation strategy, the converter synthesizes a controllable three-phase ac voltage from the energy stored in the dc capacitors. At the fundamental frequency and in steady-state reactive operation, the converter voltage is controlled approximately in phase with the grid voltage. The voltage-magnitude difference across the coupling reactance then determines the reactive-current direction: a converter voltage lower than the grid voltage produces inductive operation, whereas a higher converter voltage produces capacitive operation. A small phase-angle displacement is additionally required to exchange the active power needed to regulate the dc-link voltages and supply converter losses. These relationships are developed in Section 6.3.1 when the decoupling reactor is discussed.

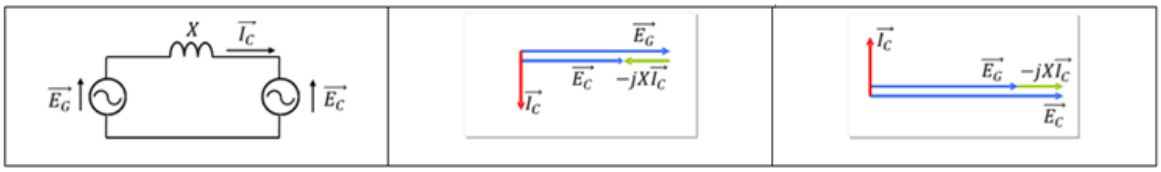


Figure 6-2 STATCOM working principle – Nidec conversion

At fundamental frequency and during purely reactive operation, the converter voltage is controlled approximately in phase with the grid voltage. The voltage difference across the coupling reactance determines the direction and magnitude of the reactive current. When the converter voltage magnitude is higher than the grid voltage magnitude, the STATCOM

supplies capacitive current to the grid. When it is lower, the STATCOM absorbs inductive current from the grid. If the two voltage magnitudes are equal, the reactive current exchange is ideally zero. The detailed voltage and power relationships are developed in Section 1.3.1, where the function of the decoupling reactor is discussed.

Thus, the basic operating principle of the STATCOM resembles the one of the synchronous compensator, but it is, obviously, static and has a much faster response (the output voltage can change almost instantaneously). Moreover the STATCOM can manage negative sequence components, both in voltage and current. So from the power-system point of view, the STATCOM operating principle is therefore comparable to that of a synchronous compensator, although no rotating mass is involved and the output can be modified within a fraction of the fundamental-frequency cycle. Contrary to capacitor- or reactor-based compensation, whose reactive current varies directly with the grid voltage, the STATCOM is primarily current-limited. Consequently, within its converter voltage and current capability, it can maintain a high reactive-current contribution during undervoltage conditions. The final reactive-power capability remains dependent on the actual grid voltage and on the limits of the converter, dc capacitors, coupling reactor and transformer.

In industrial Power Quality applications, the STATCOM is controlled as a fast current source. The load currents and the grid voltages are measured continuously, and the controller determines the compensating-current components required at each instant. The resulting STATCOM current is superimposed on the load current so that the current drawn from the upstream network is smoother, more balanced and closer to the required power factor. For rapidly varying loads, such as electric arc furnaces, the main objectives are the compensation of the fluctuating positive-sequence reactive current and the reduction of the negative-sequence current responsible for load unbalance.

Reactive-current compensation and negative-sequence-current control reduce the voltage drops produced by the disturbing load across the network impedance and therefore mitigate voltage fluctuations and flicker at the PCC. Residual voltage fluctuations may also be caused by rapid variations in the load active power. A conventional STATCOM with dc capacitors can exchange active power only temporarily, mainly to regulate its internal dc voltage and cover converter losses. Significant smoothing of the load active-power fluctuations requires

explicitly designed energy-storage capability and must therefore be treated as a dedicated function rather than as an inherent characteristic of the STATCOM.

In addition to reactive-power control, the STATCOM can perform the following functions in industrial Power Quality applications:

- Power Factor Correction at the PCC: the STATCOM regulates the reactive current exchanged with the grid in order to maintain the required power factor within its operating capability.
- Fast Reactive-Power Compensation: the STATCOM tracks rapid variations in the load reactive-power demand and injects the corresponding compensating current.
- Voltage Support: by supplying capacitive current during voltage depressions or absorbing inductive current during overvoltage conditions, the STATCOM contributes to voltage regulation and dynamic voltage recovery.
- Load Balancing: the STATCOM controls the negative-sequence components of its output current so that the upstream grid currents remain as balanced as practicable.
- Flicker Mitigation: rapid compensation of fluctuating reactive current and load unbalance reduces the voltage fluctuations produced by disturbing loads at the PCC.
- Active Filtering: where included in the control strategy and converter rating, the STATCOM can compensate selected low-order harmonic and non-fundamental current components generated by the load.

These operating principles can be implemented through different VSC topologies and modulation strategies.

6.2.NIDEC STATCOM: SILCOVAR-H

For medium-voltage industrial Power Quality applications, multilevel voltage-source converters offer significant advantages in terms of output waveform quality, semiconductor voltage stress, modularity and scalability. Within this framework, the Nidec SILCOVAR-H is a medium-voltage STATCOM based on a Cascaded H-Bridge topology and IGBT power modules. The converter is designed to generate a controllable three-phase voltage and to exchange reactive current with the grid through the coupling reactance, thereby implementing the compensation functions introduced in the previous section.

The SILCOVAR-H is proposed in two typical configurations: building solution and container solution. A render of those is presented below:

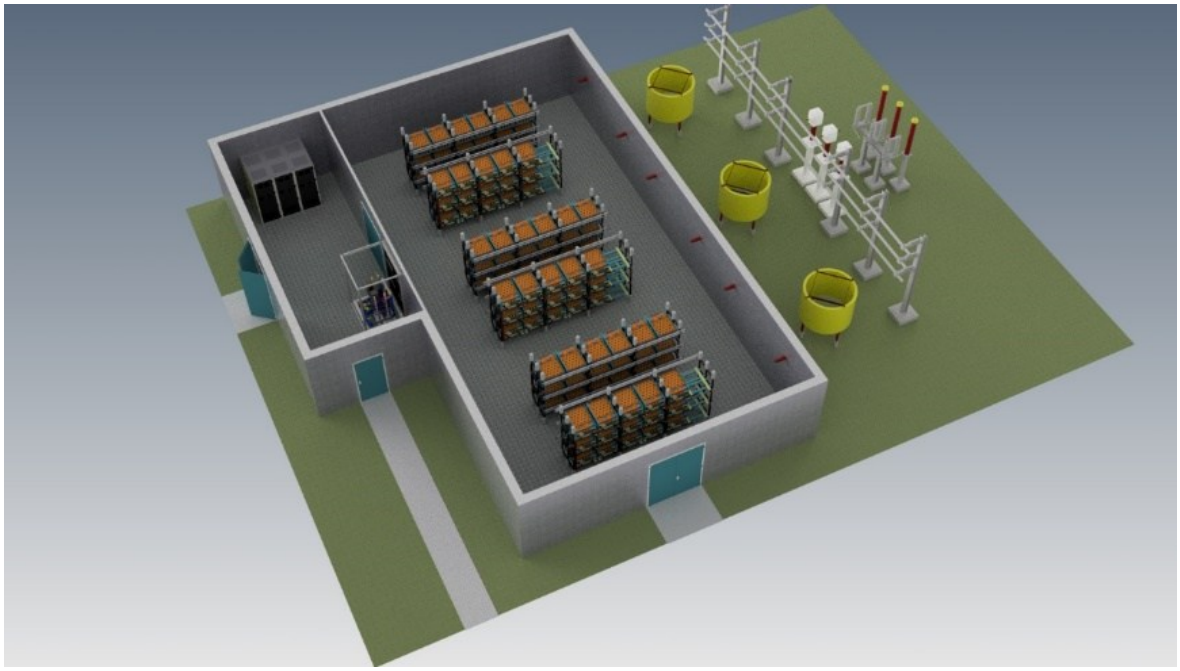


Figure 6-3 3D building solution layout

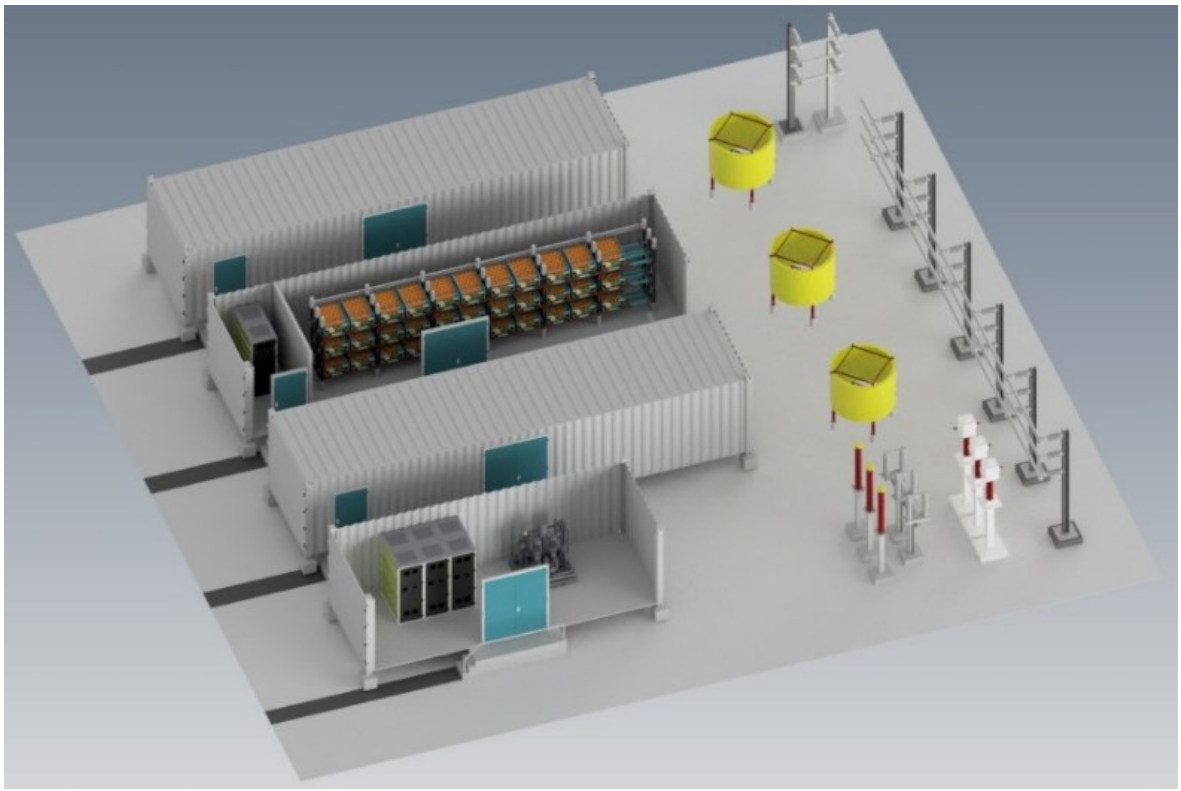


Figure 6-4 3D container solution layout

6.2.1. SILCOVAR-H ARCHITECTURE

The SILCOVAR-H is a voltage-source converter with multilevel medium-voltage PWM modulation. Its power section is composed of identical Full H-Bridge cells connected in series. Depending on the rated voltage, current and required functions, the three converter branches can be arranged in star or delta configuration and can be connected to the grid either directly or through a coupling transformer. The complete system also includes the control and auxiliary circuits, the cooling system, the pre-charge equipment and the output decoupling reactors.

The modular architecture allows the converter voltage and power ratings to be adapted by selecting the number and current rating of the power modules. Each module is a factory-assembled power-electronic unit that contains the dc-link capacitors, four IGBT positions with antiparallel diodes, local control and firing boards, discharge devices and a heat sink. Air cooling is used for the lower-current product range, whereas water cooling is adopted for the higher-current ratings.

A render of one block tower and one phase is reported in figure 6-5

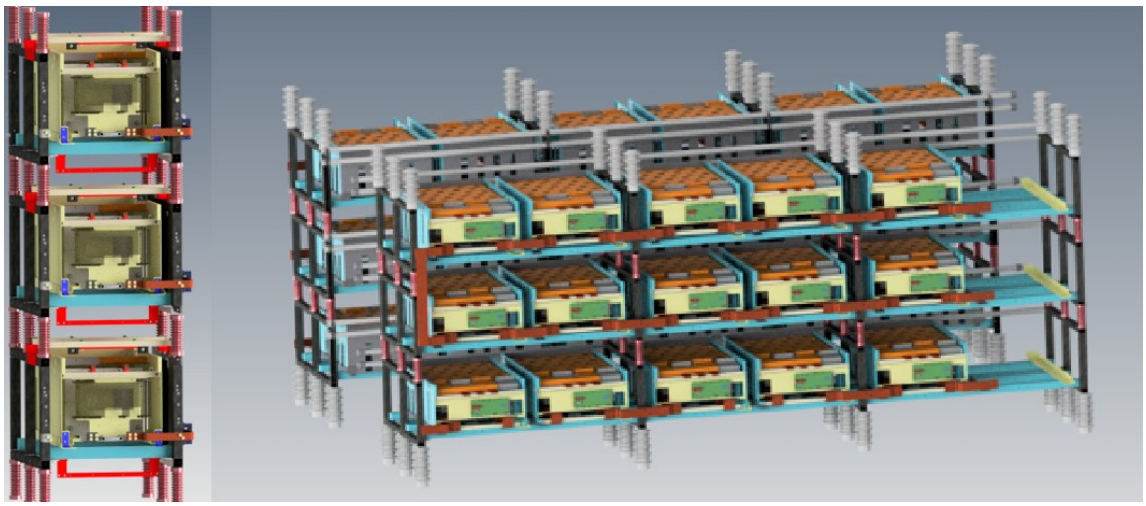


Figure 6-5 power modules layout of a single phase

6.2.2. CASCADED H-BRIDGE TOPOLOGY

A single Full H-Bridge power module consists of four controlled semiconductor positions. Appropriate switching combinations apply a positive dc-link voltage, a negative dc-link voltage or a zero voltage to the ac terminals of the module. Therefore, the instantaneous output of one cell can assume the values +E, 0 or −E, where E denotes the dc-link voltage of that module.

The ac terminals of the power modules belonging to the same converter branch are connected in series. The branch voltage is consequently obtained as the algebraic sum of the individual cell voltages. Unlike motor-drive CHB converters, in which isolated dc sources are commonly supplied by a multi-secondary transformer and diode rectifiers, the dc links of a STATCOM are floating capacitive energy-storage elements. Their average voltages are maintained by the converter control through a small active-power exchange with the grid, sufficient to compensate internal losses.

The cascading principle distributes the total converter voltage among several power modules. This provides three important engineering benefits:

- each semiconductor device is exposed only to the voltage of its own dc link rather than to the total converter voltage;
- each switching transition changes the branch voltage by one cell voltage, reducing voltage steps and electromagnetic interference;
- the equivalent converter switching effect is distributed among the cells, providing a high-quality waveform without imposing the full equivalent switching frequency on each device.

If N identical H-Bridge modules are connected in series and their dc-link voltages are equal, the branch voltage can theoretically assume 2N + 1 discrete levels, ranging from −NE to +NE. As N increases, the staircase waveform approaches a sinusoidal reference and the voltage harmonic content is progressively reduced. Phase-shifted carrier PWM can be used to distribute switching events among the cells and to obtain a higher equivalent output switching frequency than the switching frequency of each individual module.

For one H-Bridge cell, the principal switching states are:

- +E when the diagonal pair S1–S2 is conducting;

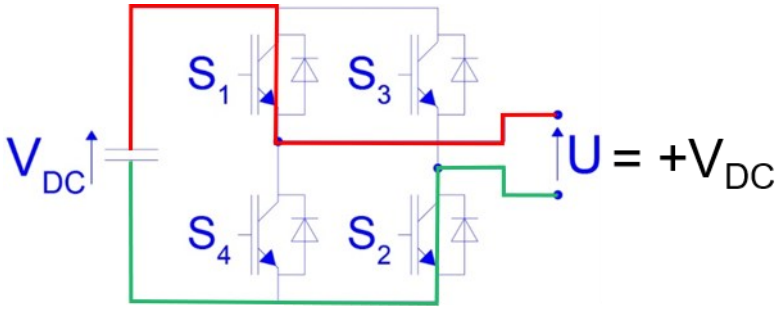


Figure 6-6 +Vdc configuration

• −E when the diagonal pair S3–S4 is conducting;

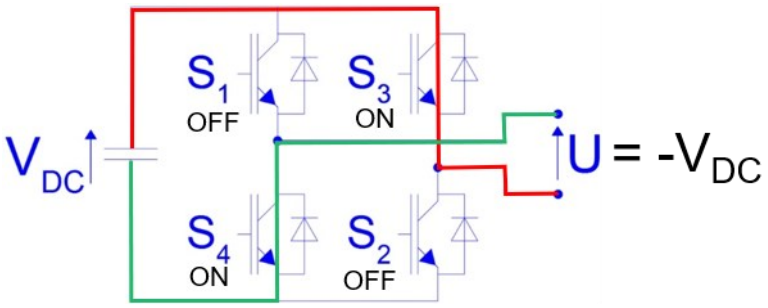


Figure 6-7 -Vdc configuration

• 0 when either same-side switching combination is selected, subject to the adopted modulation and dead-time logic.

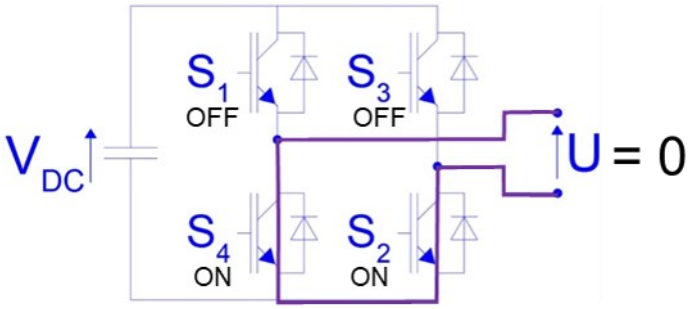


Figure 6-8 null configuration

Several switching combinations may generate the same total branch voltage. These redundant states are exploited by the control system to balance the dc-link capacitor voltages and to distribute switching losses among the power modules. Hardware availability is instead improved by equipping the converter with an additional module and a dedicated electromechanical bypass arrangement. If a power module is declared faulty, it can be isolated and bypassed; provided that the remaining healthy modules retain sufficient voltage capability, the converter can resume operation without the faulty cell.

6.2.3. STAR AND DELTA CONFIGURATION

The three cascaded branches of the SILCOVAR-H can be connected either in star or in delta. In the star arrangement, one end of each branch is connected to a common floating point, whereas the other ends are connected to the three grid phases. In the delta arrangement, the three branches form a closed loop between the phase-to-phase terminals. The selected configuration influences the voltage applied to each branch, the relationship between branch and line currents, the number of required modules and the set of control functions available. The delta configuration is particularly suited to high-power applications and permits the

circulation of internal zero-sequence current components without injecting them into the grid, which is useful for dc-link voltage balancing and unbalanced-load compensation.

From an installation perspective, the modular power sections can be arranged in cabinets, containers or dedicated buildings. For the larger ratings, the H-Bridge modules are water cooled and installed in modular mechanical structures. The series electrical interconnections, fibre-optic control links and coolant distribution are integrated into the power section, while the supervisory control and cooling units are located in a segregated low-voltage area. This separation permits scalable plant layouts while preserving maintainability and personnel safety.

6.3. MAIN COMPONENTS

The preceding sections have described the SILCOVAR-H architecture, the operating principle of its Cascaded H-Bridge power modules and the implications of star and delta branch connections. The following sections focus on the principal elements that determine the electrical interaction between the converter and the grid: the decoupling reactor and the modulation and control system.

6.3.1. DECOUPLING REACTOR

In order to have the possibility to exchange power with the grid, a reactor in series with the converter is needed. There are various types of filters that fully cover this role, from the more advanced as an LCL to a simple reactor as an LR. Below is reported an elementary case, where the reactor is simply an inductor in series with the STATCOM, it becomes obvious that it plays a crucial role in the power exchange between the converter and the grid. In fact, without this element, the exchange is not possible.

If an inductor is considered, the following relationship between voltages and power can be written:

From the power law applied on the grid side:

$$\dot{E_G} \cdot \dot{I}^* = P_G + jQ_G \qquad (6.1)$$

$$\rightarrow \dot{I} = \frac{P_G - jQ_G}{\dot{E_G}^*}$$

From Ohm law between converter and grid:

$$\dot{Z} \cdot \dot{I} = \dot{E}_{conv} - \dot{E}_G$$
$$\rightarrow \dot{I} = \frac{\dot{E}_{conv} - \dot{E}_G}{\dot{Z}} \tag{6.2}$$

Comparing the two identities:

$$\frac{P_G - jQ_G}{\dot{E}_G{}^*} = \frac{\dot{E}_{conv} - \dot{E}_G}{\dot{Z}}$$

$$P_G - jQ_G = \frac{\dot{E}_{conv} \cdot \dot{E}_G{}^* - |E_G|^2}{\dot{Z}} = \frac{E_{conv} \cdot E_G \cdot e^{j\gamma} - |E_G|^2}{jX_L}$$

With γ defined as the load angle, displacement between converter voltage and grid voltage.

$$P_G - jQ_G = \frac{E_{conv} \cdot E_G \cdot \cos\gamma - |E_G|^2 + j(E_{conv} \cdot E_G) \cdot \sin\gamma}{jX_L}$$

Simplifying the imaginary operator:

$$P_G - jQ_G = \frac{E_{conv} \cdot E_G \cdot \sin\gamma}{X_L} - j \cdot \frac{E_{conv} \cdot E_G \cdot \cos\gamma - E_G{}^2}{X_L} \tag{6.3}$$

Adopting small angle approximation: $\sin\gamma = \gamma;\ \cos\gamma = 1$

$$\begin{cases} P_G = \dfrac{E_{conv} \cdot E_G}{X_L} \cdot \gamma \\ Q_G = \dfrac{E_{conv} \cdot E_G - E_G{}^2}{X_L} \end{cases} \tag{6.4}$$

Controlling the STATCOM with the same angle of the grid voltage, the delivered active power is null ($\gamma = 0$).

It is now clear that, if the voltage of the STATCOM is lower than the voltage of the grid:

$$E_{conv} < E_G \rightarrow Q_G < 0$$

The STATCOM absorbs reactive power, acting as an inductor.

If, instead, the STATCOM voltage is greater than the grid voltage:

$$E_{conv} > E_G \rightarrow Q_G > 0$$

The STATCOM injects reactive power in the system, acting as a capacitor.

This is the main role of the decoupling reactor and, along with this function, other advantages are achieved. All the advantages can be summarized as follows:

- Controlled reactive power exchange: The reactor enables a stable and controllable exchange of reactive power between the STATCOM and the grid;
- Current limitation and protection: The series inductor limits the current during transients, voltage sags and fault conditions, protecting the converter's semiconductor devices from overcurrent stress;
- Dynamic decoupling between converter and grid: The reactor isolates the fast converter dynamics from the grid, ensuring stable operation;
- Harmonic filtering: The inductor naturally attenuates high-frequency components generated by the PWM control of the converter, reducing harmonic injection into the grid;
- Balanced current injection under unbalanced voltages: The decoupling reactor allows the STATCOM to inject balanced currents even when the grid voltage is unbalanced.

If, instead of multilevel converter, a traditional solution is considered, the decoupling reactor incorporates also another crucial role. In fact, by properly sizing the inductor, the current ripple can be attenuated. In multilevel converter instead, this is not necessary: the multilevel topology assure a current with a contained ripple due to the almost sinusoidal output voltage. This is a significant advantage, the inductor can be sized only to properly guarantee the power exchange without the constraint imposed by the current ripple.

The sizing of the inductor is obtained imposing a chosen voltage drop on the reactor. Considering the system parameters:

- $V_{MV} = 30\ kV$
- $f_{grid} = 50\ Hz$

- $I_{statcom} = 1500\ A$, considering the maximum allowable current of the power electronic modules installed.

Considering a safety margin of 10% on the STATCOM current, its value becomes:

$$I_{statcom} = 1650\ A$$

Then, the chosen voltage drops in percentage related to the MV nominal voltage is:

$$\Delta V_{\%} = 8\%$$

Obtaining:

$$\Delta V = 2400\ V$$

Exploiting the Ohm's Law applied to the reactor:

$$V = \omega L \cdot I \tag{6.5}$$

Resulting in:

$$L = \frac{V}{I \cdot 2\pi f} = \frac{2400}{1650 \cdot 2\pi \cdot 50} = 4.63\ mH$$

The reactance assumes the following value:

$$X_L = \omega L = 1.45\ \Omega$$

A reactor of this value must be placed in all the three phase of the STATCOM.

There are different types of reactors based on their construction methods. For most of the cases, they fall in two main categories: iron core and air core. The main difference is the presence of iron core in the construction that, in presence of electromagnetic fields, can interfere with the EMI limits.

The proposed solution is an air core reactor and, as any other electric devices, must respect EMI limits. In this case, the ICNIRP limits are considered, as reported below (figure 6-9, figure 6-10).

The main objective of this publication is to establish guidelines for limiting exposure to electric and magnetic fields (EMF) that will provide protection against all established adverse health effects.

Tables 3 and 4 summarize the reference levels for occupational and general public exposure, respectively, and the reference levels are illustrated (Figures. 2 and 3)

The reference levels assume an exposure by a uniform (homogeneous) field with respect to the spatial extension of the human body."

Table 3. Reference levels for occupational exposure to time-varying electric and magnetic fields (unperturbed rms values).

Frequency range	E-field strength E (kV m^{-1})	Magnetic field strength H (A m^{-1})	Magnetic flux density B (T)
1 Hz–8 Hz	20	$1.63 \times 10^5/f^2$	$0.2/f^2$
8 Hz–25 Hz	20	$2 \times 10^4/f$	$2.5 \times 10^{-2}/f$
25 Hz–300 Hz	$5 \times 10^2/f$	8×10^2	1×10^{-3}
300 Hz–3 kHz	$5 \times 10^2/f$	$2.4 \times 10^5/f$	$0.3/f$
3 kHz–10 MHz	1.7×10^{-1}	80	1×10^{-4}

Notes:
- f in Hz.
- See separate sections below for advice on non sinusoidal and multiple frequency exposure.
- To prevent indirect effects especially in high electric fields see chapter on "Protective measures."
- In the frequency range above 100 kHz, RF specific reference levels need to be considered additionally.

Table 4. Reference levels for general public exposure to time-varying electric and magnetic fields (unperturbed rms values).

Frequency range	E-field strength E (kV m^{-1})	Magnetic field strength H (A m^{-1})	Magnetic flux density B (T)
1 Hz–8 Hz	5	$3.2 \times 10^4/f^2$	$4 \times 10^{-2}/f^2$
8 Hz–25 Hz	5	$4 \times 10^3/f$	$5 \times 10^{-3}/f$
25 Hz–50 Hz	5	1.6×10^2	2×10^{-4}
50 Hz–400 Hz	$2.5 \times 10^2/f$	1.6×10^2	2×10^{-4}
400 Hz–3 kHz	$2.5 \times 10^2/f$	$6.4 \times 10^4/f$	$8 \times 10^{-2}/f$
3 kHz–10 MHz	8.3×10^{-2}	21	2.7×10^{-5}

Notes:
- f in Hz.
- See separate sections below for advice on non sinusoidal and multiple frequency exposure.
- In the frequency range above 100 kHz, RF specific reference levels need to be considered additionally.

Figure 6-9 reference levels of EMF for occupational and general public [11]

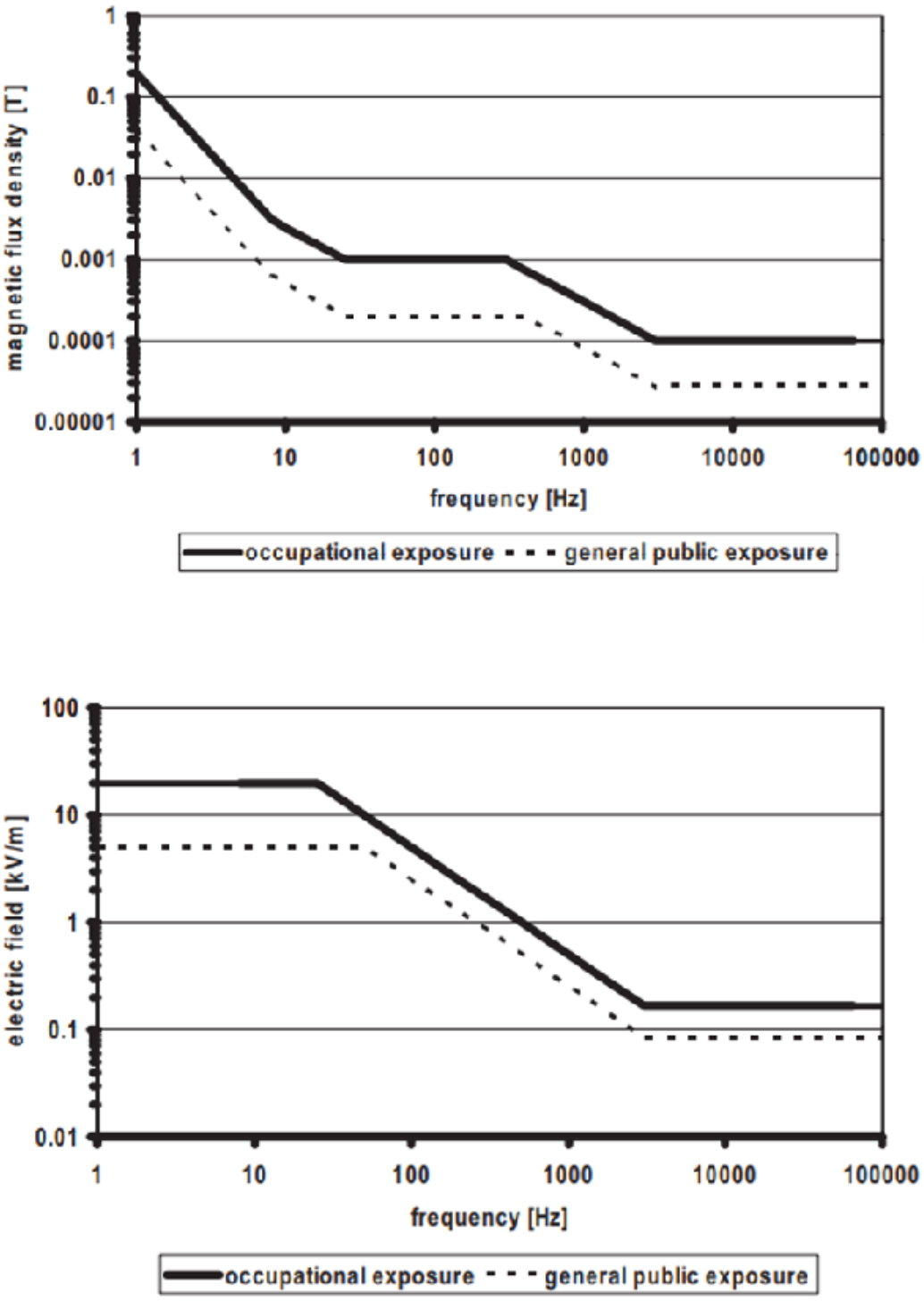


Figure 6-10 E and B fileds limits over frequency [11]

What really matters in the layout design is the so-called MAGNETIC CLEARANCE CONTOUR (MC), this distance is the edge where the magnetic field of the reactor does not cause thermal and electrodynamic effects on neighbouring metallic parts. All these values

are obtained starting from ICNIRP guidelines and provided by the reactor manufacturer. In particular, there are two parameters concerning the layout design, based on the metallic element near the installation:

- MC1: for small metallic parts;
- MC2: for metallic parts forming closed loops.

The proposed decoupling reactor of $4.63\,mH$, air core type, has the following measurements:

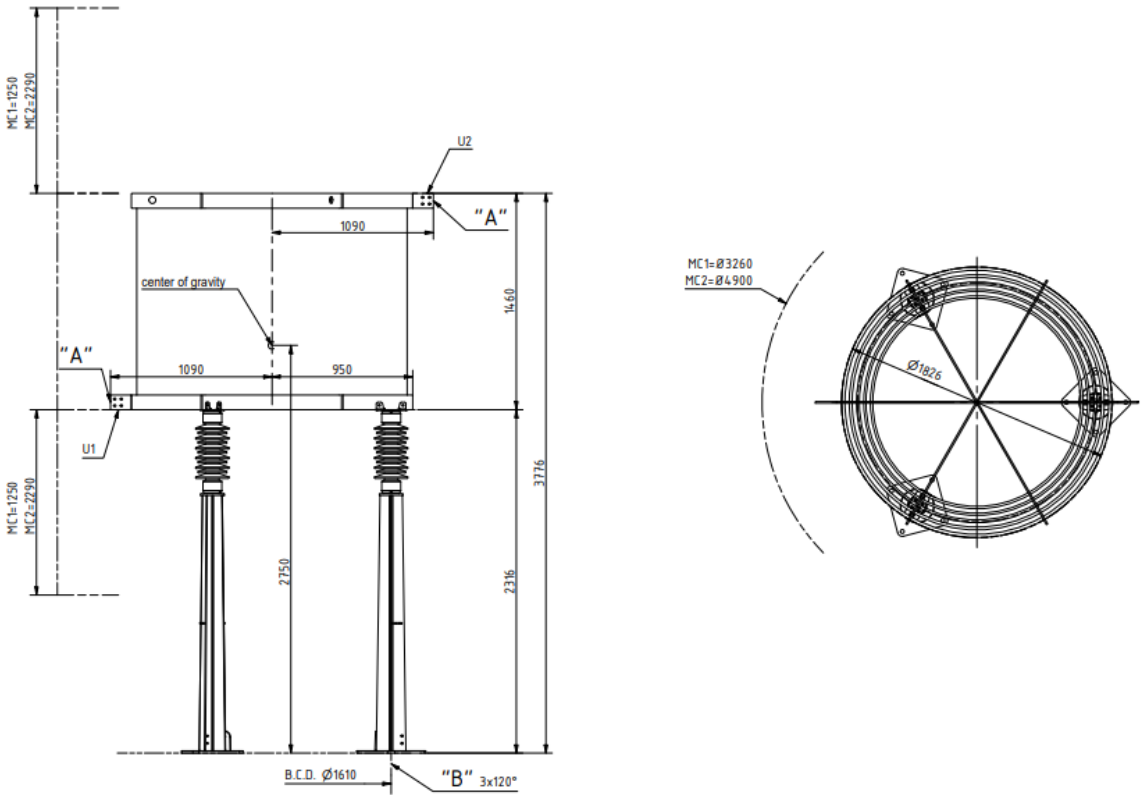


Figure 6-11 decoupling reactor drawing – Nidec corporation

A clearer vision of the coil can be appreciated with its rendering:

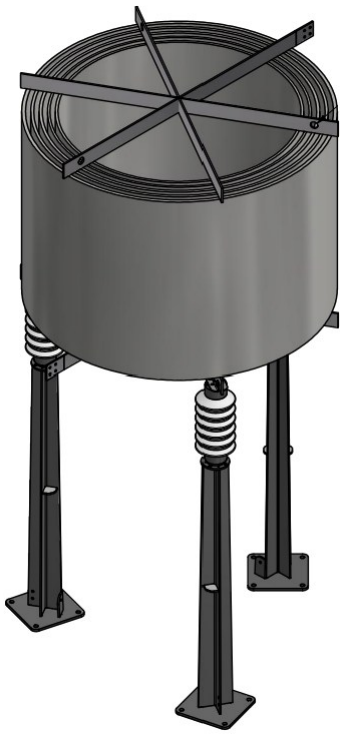


Figure 6-12 decopling reactor 3D rendering - Nidec corporation

Considering the connection between each phase and its own decoupling reactor, the rendering is reported below.

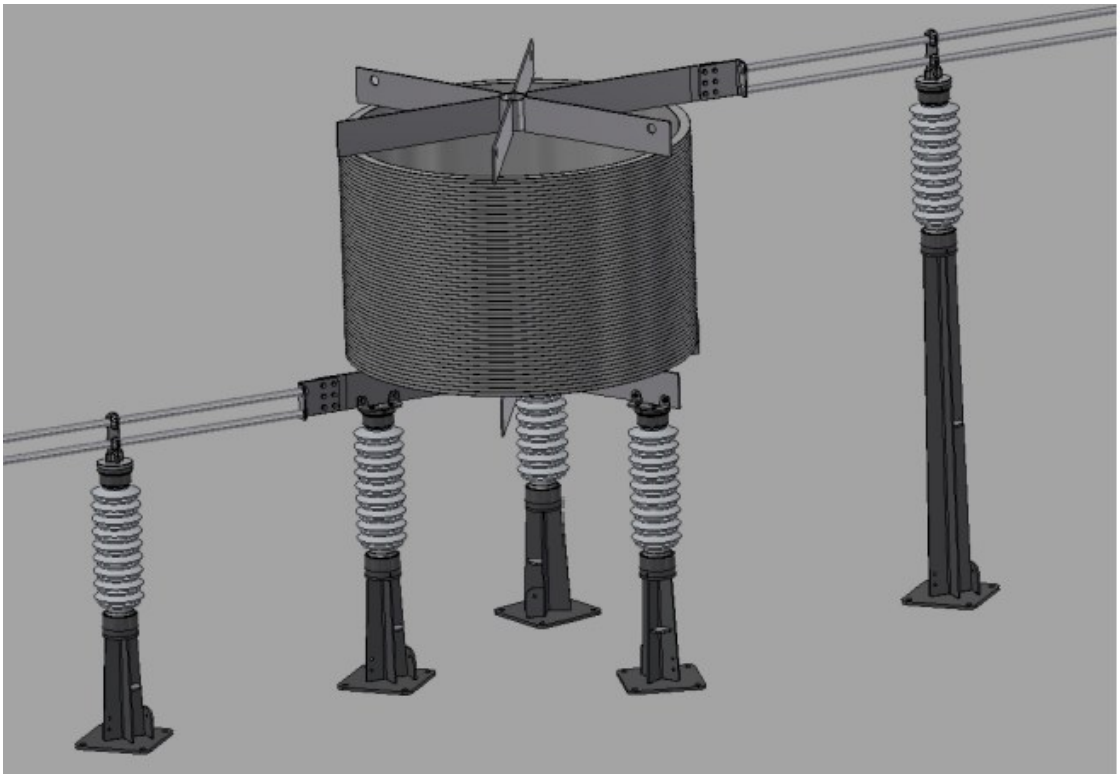


Figure 6-13 rendering of phase and reactor connection - Nidec corporation

6.3.2. CONTROL

The control method adopted in the SILCOVAR-H uses PWM (Pulse Width Modulation). In its basic form, PWM compares a high-frequency periodic carrier, typically triangular, with a modulating signal representing the desired fundamental output voltage. The comparison determines the switching states applied to the converter cells.

The first signal is called “carrier”, for most of the controls is triangular and its frequency is in the range of kHz. Its value ranges from 0 to 1.

The second one is called “modulating signal” and have the same frequency of the output sinewave ($50\ Hz$ or $60\ Hz$). This signal is divided by the maximum value it can assume; the idea is to obtain a signal that vary from 0 to 1, 0 when no voltage should be observed in the output, 1 when all the dc-link voltage must be present.

Then, a comparator compares modulating and carrier signals, when the modulating is higher than the carrier, the H-bridge is commanded ON (S1, S3 ON). Otherwise, when the carrier is higher, is commanded OFF (S2, S4 ON). It is clear that the output wave does not only contain the target waveform but also an unwanted high-frequency component.

The higher is the frequency of these components, the easiest is to filter them out. For this reason, the "frequency modulation ratio" is introduced:

$$mf = \frac{f_{carrier}}{f_{modulating}} \tag{6.6}$$

A higher mf means unwanted components at higher frequencies. It is known that, using a bipolar PMW (one carrier for both the half-bridges) the harmonic content appears as a sidebands centered around mf, while, using an unipolar PWM (one carrier for each half-bridge) the harmonic content sidebands appear around $2mf$.

The drawbacks of high values of mf are clear: the higher is the switching frequency of the transistor, the higher are the losses in those devices. This is one of the main reasons multilevel technology has been developed and, in this case, exploited. In fact, with a correct control method adopted in parallel with a multilevel converter, it is possible to achieve an higher dominant harmonic in the inverter output voltage without increasing the frequency of the carrier in each power modules.

In SILCOVAR-H, phase shifted PWM is adopted. In general, a multilevel converter with n voltage levels requires $(n-1)$ triangular carrier. In this type of modulation, all the triangular carriers have the same frequency and the same magnitude, but they are displaced each other by a phase-shift of:

$$\varphi_{cr} = \frac{360°}{(n-1)} \tag{6.7}$$

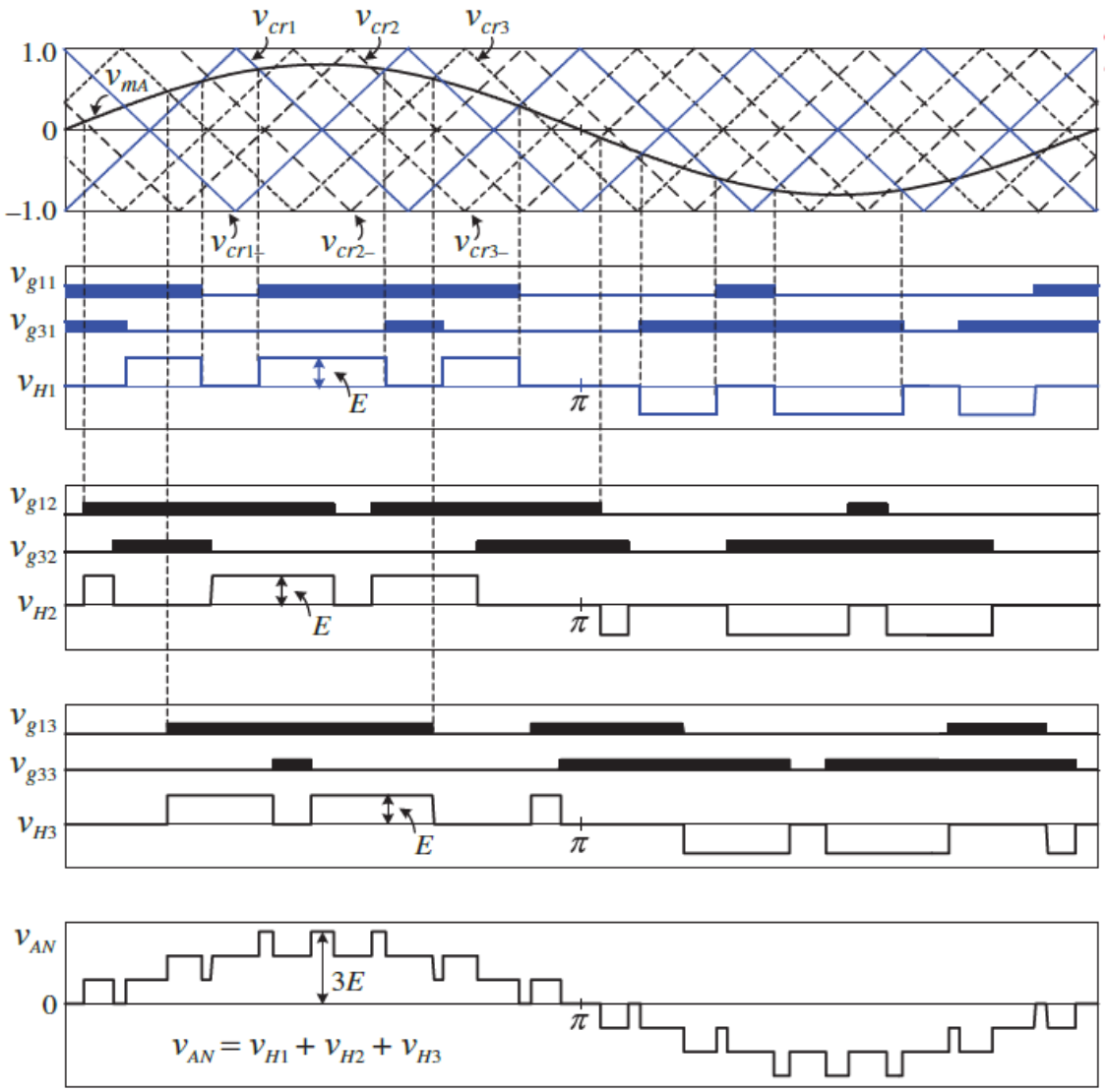


Figure 6-14 resulting phase voltage on a 3-level converter CHB phase shifted PWM [9]

Along the $(n-1)$ carrier signal, three modulating signal (one for each phase) is needed. The inverter phase voltage can be obtained from:

$$V_{AN} = \sum_{i=1}^{H} V_{H_i} \tag{6.8}$$

With this type of modulation, the dominant harmonics in V_{AN}, that defines the inverter switching frequency obtained, is:

$$f_{inv_{sw}} = (n-1) f_{cr} \tag{6.9}$$

There are other types of PWM techniques that can be implemented in a multilevel converter, as level shifted PWM. However, phase shifted PWM guarantee an equal wear of the power modules without the implementation of switching patterns.

The analysis presented in this chapter has linked the Power Quality functions of the STATCOM to the main design features of the SILCOVAR-H. The Cascaded H-Bridge architecture provides the voltage scalability and waveform quality required for medium-voltage operation, whereas the decoupling reactor governs the current and power exchange with the grid. Phase-shifted PWM distributes switching events among the series-connected cells, increasing the equivalent output switching frequency without imposing the same frequency on each semiconductor device. These elements form the physical and control basis for the compensation functions developed in the subsequent analysis.

7. PLANT ANALYSIS WITH RPCS

7.1. ANALYTIC LOADFLOW CALCULATION

For conservative reasons, the customer required a power factor at PCC equal or greater than 0.98. This value is significantly higher than the one required for standard compliance, however, it is a common practice to impose a margin above the minimum threshold to ensure adequate safety over the coming years.

For the calculation of the compensating reactive power needed, the procedure is straightforward.

Given an active power value, if the objective is 0.98 of power factor, then the reactive power to be compliant at PCC needs to match the following value:

$$PF = \cos(\varphi) \rightarrow \varphi = \arccos(PF) \tag{7.1}$$

$$Q = P \cdot \tan(\varphi) \rightarrow Q = P \cdot \tan\big(\arccos(PF)\big) \tag{7.2}$$

The compensating power is achieved by subtracting the real value of reactive power seen at PCC with the target value defined above.

Applying this procedure to the three operating scenarios yields the maximum capacitive and inductive reactive-power requirements of the STATCOM. According to the sign convention adopted in this chapter, positive STATCOM reactive power denotes capacitive injection into the network, whereas negative STATCOM reactive power denotes inductive absorption from the network. In the latter condition, the STATCOM behaves as an inductive load.

Scenario 1:

$$P_{PCC} = 28.6\ MW$$

$$Q_{PCC} = -25.9\ Mvar$$

A negative value of reactive power at the PCC indicates that reactive power flows from the system towards the grid, according to the sign convention adopted in this analysis.

So, the reactive power to be compliant at PCC must be:

$$Q_{compliant} = P \cdot \tan\big(\arccos(0{,}98)\big) = 5.81\ Mvar$$

The STATCOM must be able to withdraw an inductive reactive power equal to:

$$Q_{statcom} = Q_{PCC} - Q_{compliant} = -31.71\ Mvar$$

Scenario 2:

$$P_{PCC} = 101.85\ MW$$

$$Q_{PCC} = 56.54\ Mvar$$

In this case, the reactive power had the same sign of the active power. This means that they are both flowing from the grid to the system.

The reactive power to be compliant at PCC must be:

$$Q_{compliant} = P \cdot \tan\big(\arccos(0{,}98)\big) = 20.68\ Mvar$$

The STATCOM must be able to inject a capacitive reactive power equal to:

$$Q_{statcom} = Q_{PCC} - Q_{compliant} = 35.86\ Mvar$$

Scenario 3:

$$P_{PCC} = 10.7\ MW$$

$$Q_{PCC} = -39.73\ Mvar$$

As already mentioned, in this case, the reactive power at PCC is nearly identical with the rated power of the filters. This situation is, in fact, the most critical point of work of the STATCOM in its inductive area (only considering its compensating role and not the flicker attenuation effect).

The reactive power to be compliant at PCC must be:

$$Q_{compliant} = P \cdot \tan\big(\arccos(0{,}98)\big) = 2.17\ Mvar$$

The STATCOM must be able to inject a capacitive reactive power equal to:

$$Q_{statcom} = Q_{PCC} - Q_{compliant} = -41.90\ Mvar$$

Also in this case, for conservative reasons,it is better to consider the worst-case scenario. As said above, the value of the compensating inductive reactive power that the STATCOM must be able to withdraw is individuated in case 3. For its value of capacitive reactive power that must be able to inject, the case where electric arc furnace, ladle furnace, as well as clean bus are all working in parallel must be considered.

In this case, the powers at PCC will be:

$$P_{PCC} = P_{EAF} + P_{LF} + P_{clean\ bus} = 83.65 + 10.4 + 18.2 = 112.25\ MW$$

$$Q_{PCC} = Q_{EAF} + Q_{LF} + Q_{clean\ bus} - Q_{filters} + Q_{loss\ trafo}$$

$$Q_{PCC} = 71.992 + 9.5 + 9.5 - 40 + 14.09 = 65{,}09\ Mvar$$

Considering the nominal value of the filters (in reality their contribution will be lower because the voltage at MV busbar where they are connected is lower than the rated one) and considering the sum of the loss on the transformer of scenario 1 and scenario 2 as the total losses.

So:

$$P_{PCC} = 112.25\ MW$$

$$Q_{PCC} = 65.09\ Mvar$$

In this case, the reactive power to be compliant at PCC must be:

$$Q_{compliant} = P \cdot \tan\big(\arccos(0.98)\big) = 22.79\ Mvar$$

The STATCOM must be able to inject a capacitive reactive power equal to:

$$Q_{statcom} = Q_{PCC} - Q_{compliant} = 42.29\ Mvar$$

Although this is merely a coincidence, it is noteworthy that the STATCOM ends up needing to inject the same capacitive and inductive reactive power, thus resulting in an almost perfectly symmetrical capability curve.

Summing up the results, the STATCOM must be able to adjust its reactive power between these limits:

$$-41{,}90\ Mvar \leq Q_{statcom} \leq 42{,}29\ Mvar$$

7.2. LOADFLOW ANALYSIS DIGSILENT

To properly implement the STATCOM in DIgSILENT, the Static Generator block was used. In order to guarantee a power factor of 0.98 at the PCC, an external controller was added. With the block configured to operate at constant PF and referenced to the PCC, the STATCOM continues to inject or absorb reactive power until the required amount is reached to ensure that the target power factor is achieved at the PCC.

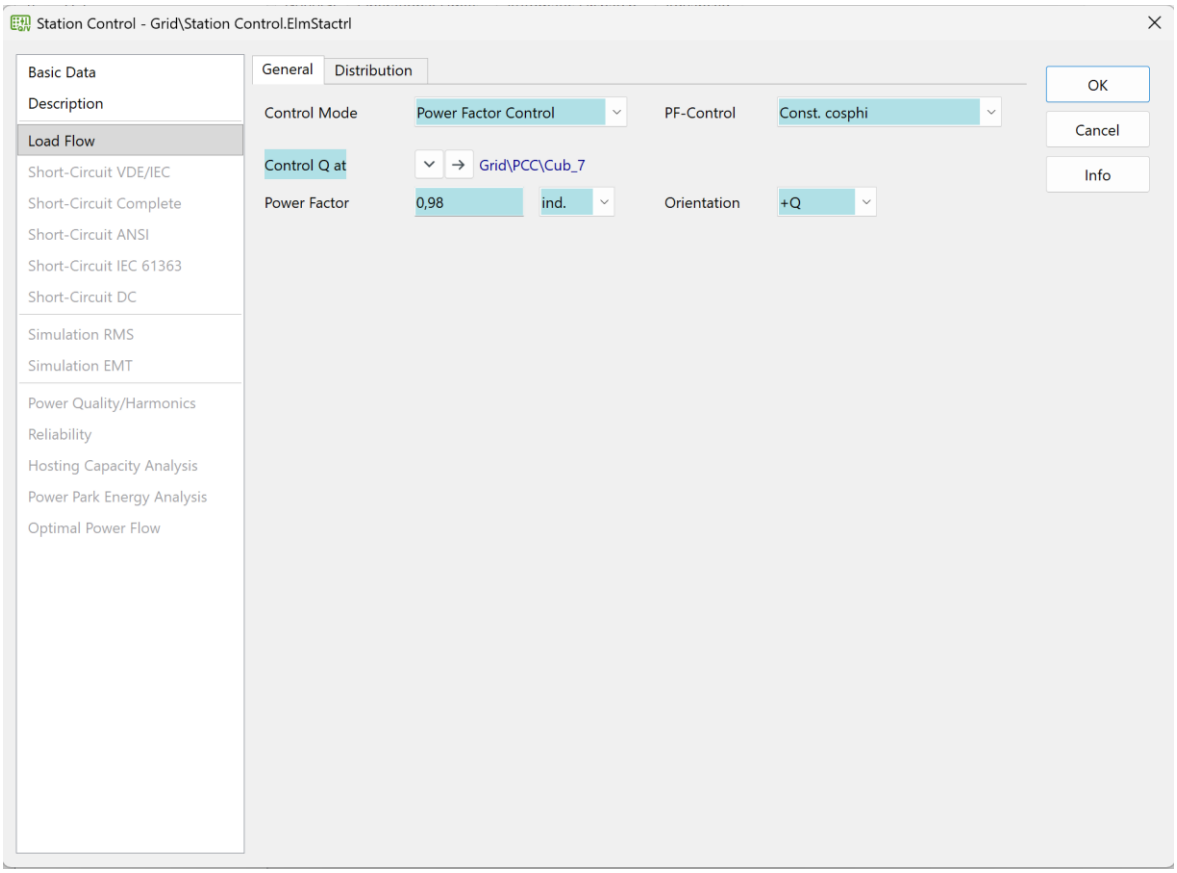


Figure 7-1external control implemented in the software

To be consistent with the analytic calculation, the orientation of Q (+Q) was adopted. With that configuration, a capacitive reactive power is defined as positive while an inductive reactive power holds a negative sign.

It can be expected that the reactive power compensation values the STATCOM will be required to provide will, in magnitude, always be lower than those analytically calculated. This is due to the losses in the HV/MV transformer which, since the STATCOM injects reactive power into the medium voltage busbar, will be smaller than those computed in the

'as-it-is' situation. In other words, the reactive current flowing through the transformer will be lower compared to the case in which the STATCOM is not operating.

The transformer losses can be estimated by assuming that the STATCOM fully compensates the reactive-power demand at the medium-voltage busbar. This approximation is not exact because the STATCOM controller regulates the power factor at the PCC: if loads connected to other busbars require additional reactive power, part of the STATCOM current will necessarily flow through the transformer. The assumption also implies balanced voltage conditions at the busbar to which the STATCOM is connected.

With the assumption of a null reactive current flowing through the transformer together with a nominal value of 30kV at MV busbar, it is possible to evaluate the new losses.

Scenario 1:

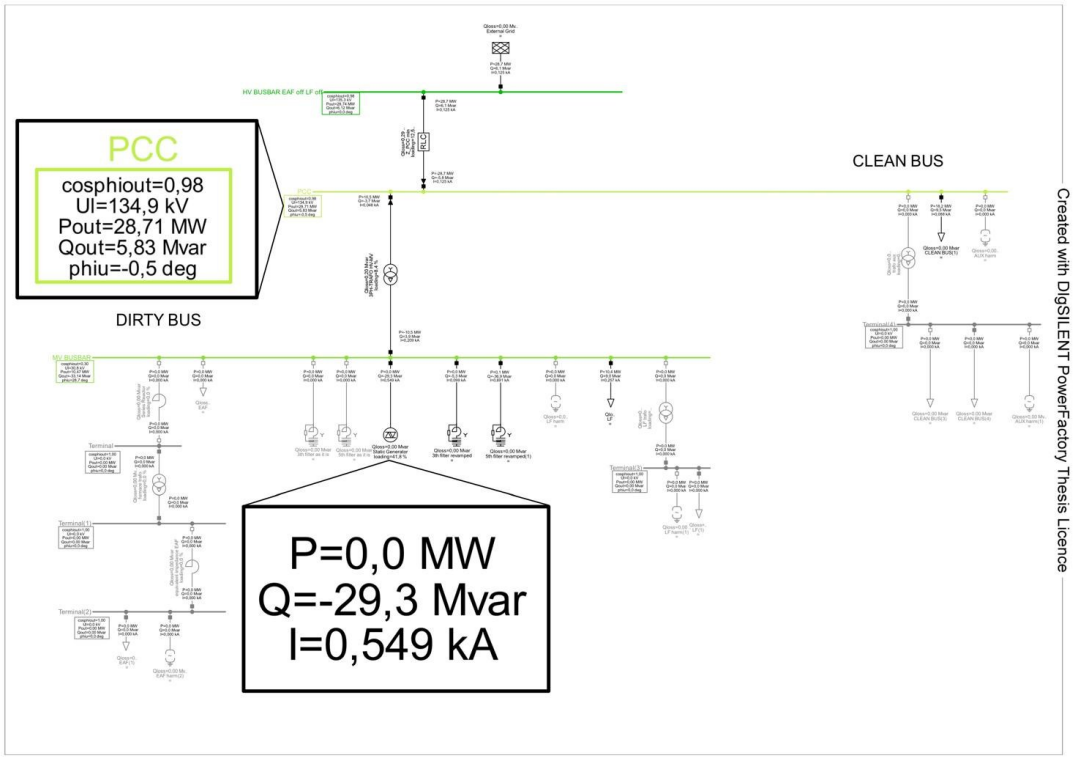


Figure 7-2 1st scenario Q of the STATCOM for PF correction

The value of the compensating reactive power is coherent with the analytical one of $-31.71\ Mvar$

As anticipated, the value the STATCOM must inject is lower, in magnitude, than its analytic counterpart.

The estimated analytical losses on the transformer were:

$I_{active} = 181.19\ A$,

$I_{reactive} = 0\ A$,

$I_{total} = 181.19\ A$,

Leading to: $Q_{loss} = 0.11\ Mvar$

On the software, the losses are:

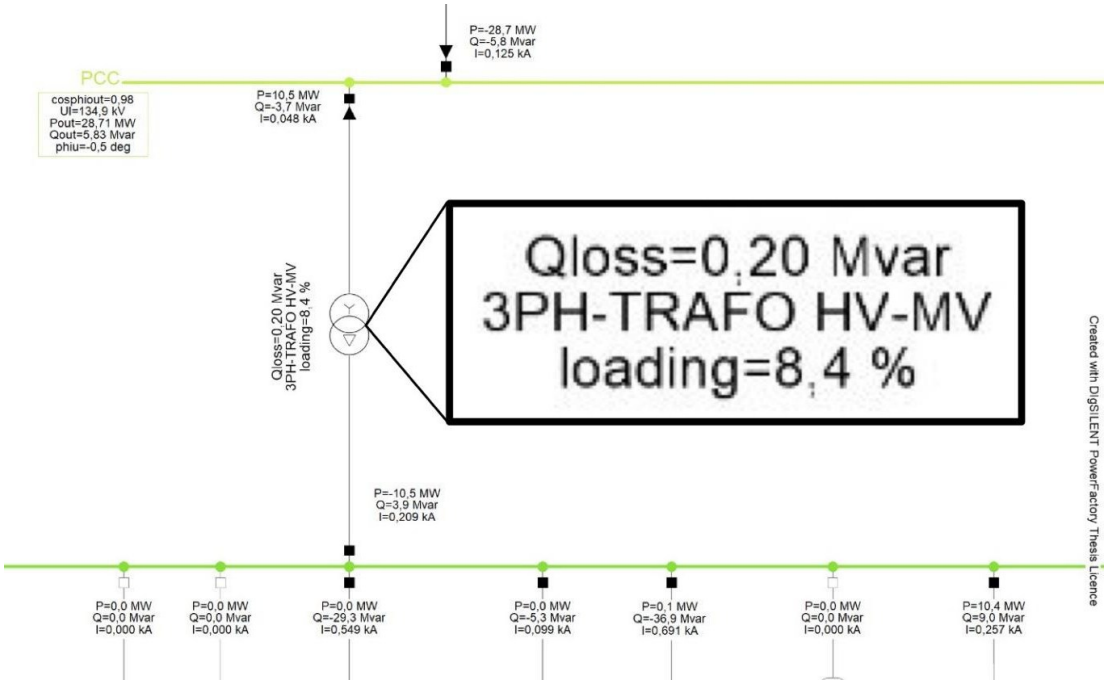


Figure 7-3 1st scenario, losses on the transformer with STATCOM ON

Scenario 2:

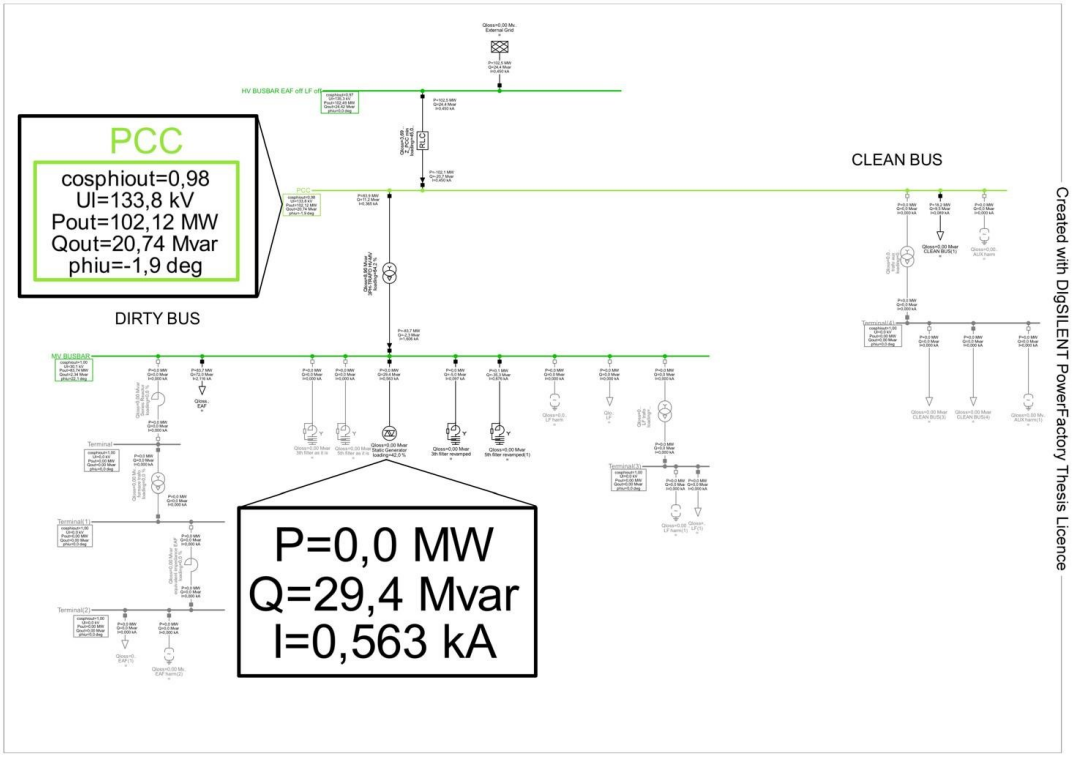


Figure 7-4 2nd scenario Q of the STATCOM for PF correction

In this scenario, the STATCOM has to act as a reactive power generator, injecting 29,4 $Mvar$, the calculated value was 35.86 $Mvar$

Also in this case, the losses decreased respected to the "as it is" situation.

In fact, the estimated analytical losses on the transformer were:

$I_{active} = 1653.44\ A$,

$I_{reactive} = 0\ A$,

$I_{total} = 1653.44\ A$,

Leading to: $Q_{loss} = 9.14\ Mvar$

Confirmed by the software with a really similar value:

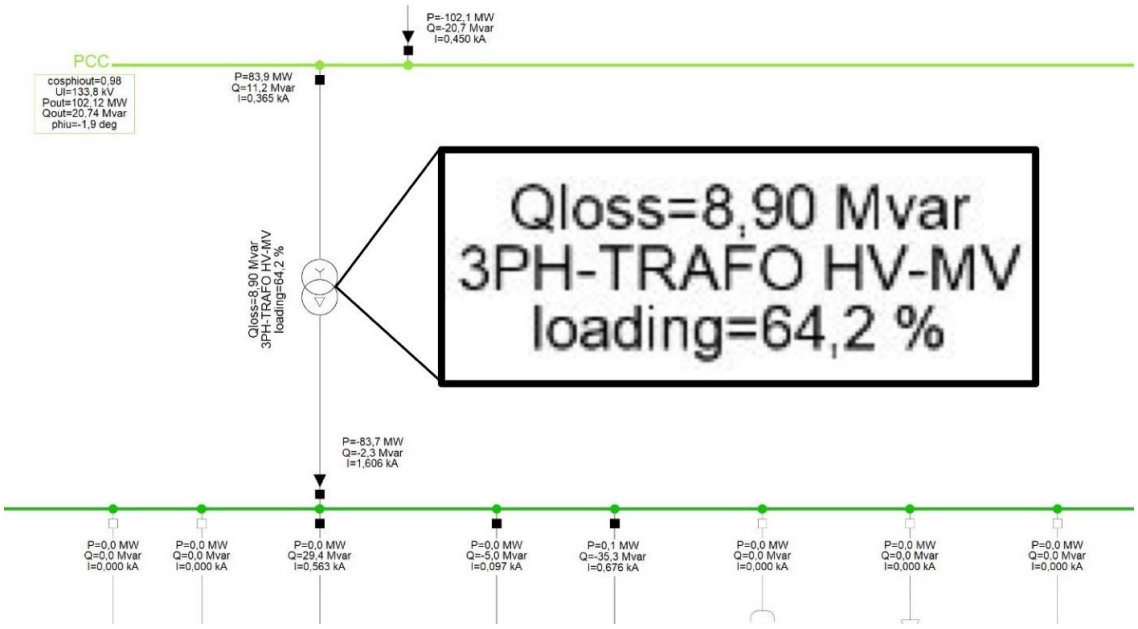


Figure 7-5 2nd scenario, losses on the transformer with STATCOM ON

Scenario 3:

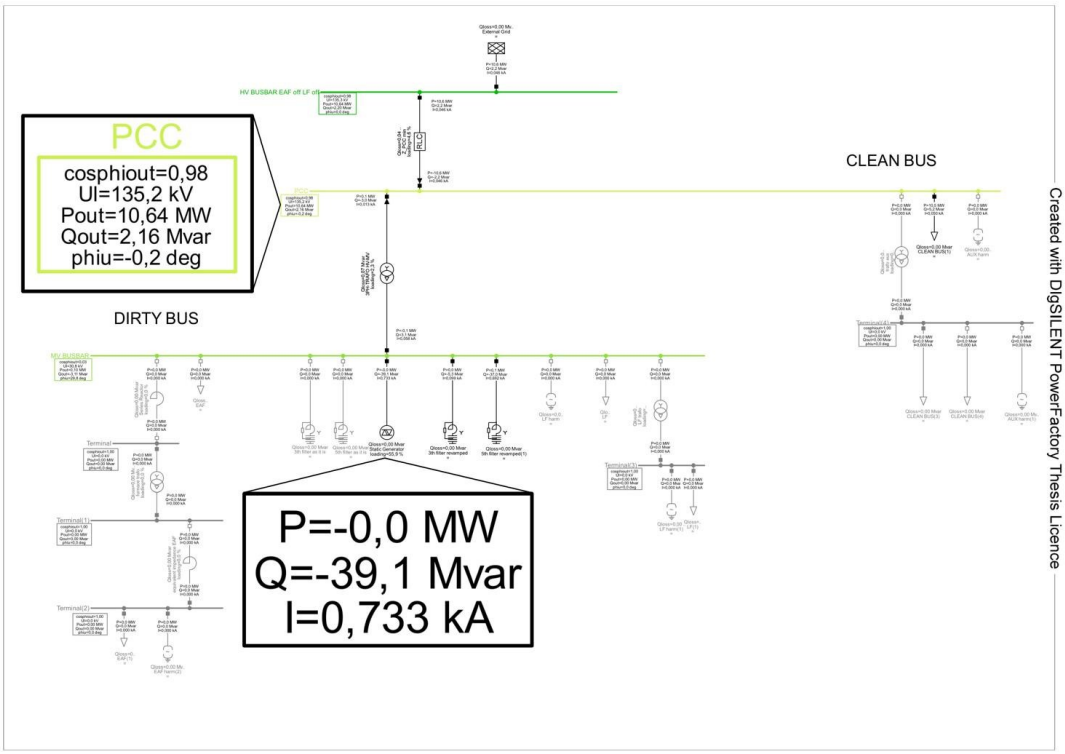


Figure 7-6 3rd scenario Q of the STATCOM for PF correction

With the third period, no active loads are connected on the medium busbar. This establishes the worst case scenario for the inductive behaviour of the STATCOM. Furthermore, with the assumption of no reactive power flowing through the transformer and without any other contribution derived from the active current, the estimated transformer losses are null:

$$Q_{loss} = 0\ Mvar$$

It can be observed that, also in the software, the losses are nearly zero.

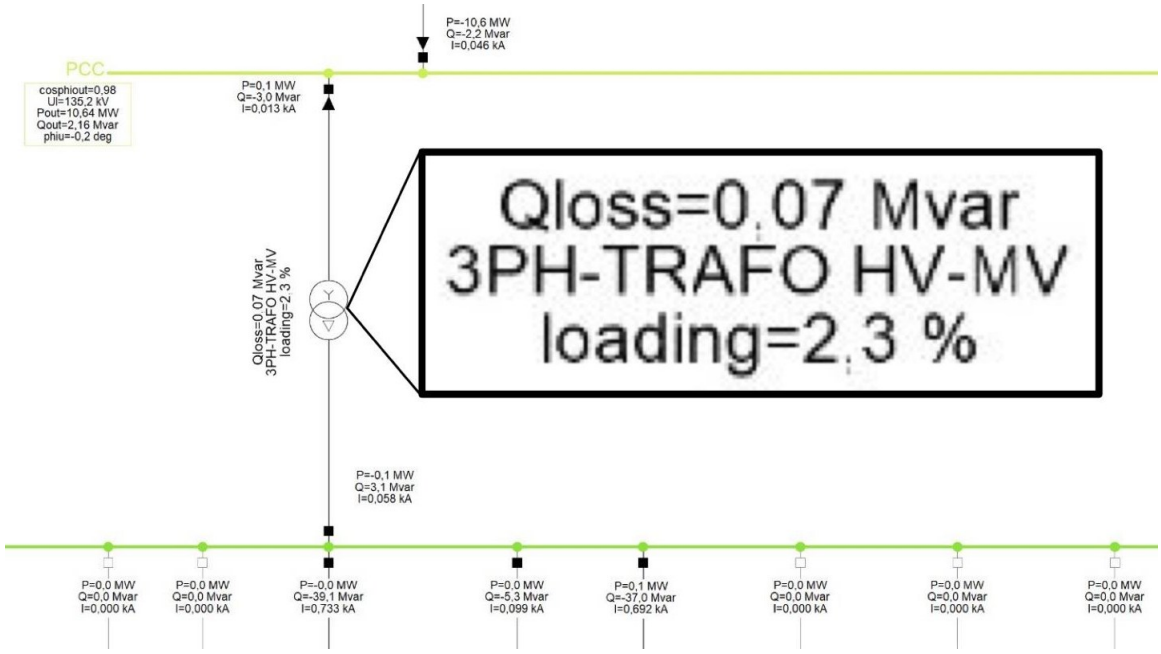


Figure 7-7 3rd scenario, losses on the transformer with STATCOM ON

As mentioned before, also the worst-case scenario for the capacitive reactive power compensation must be considered. This scenario is obtained by connecting both the furnaces on the SLD together with the clean bus in its worst operating condition.

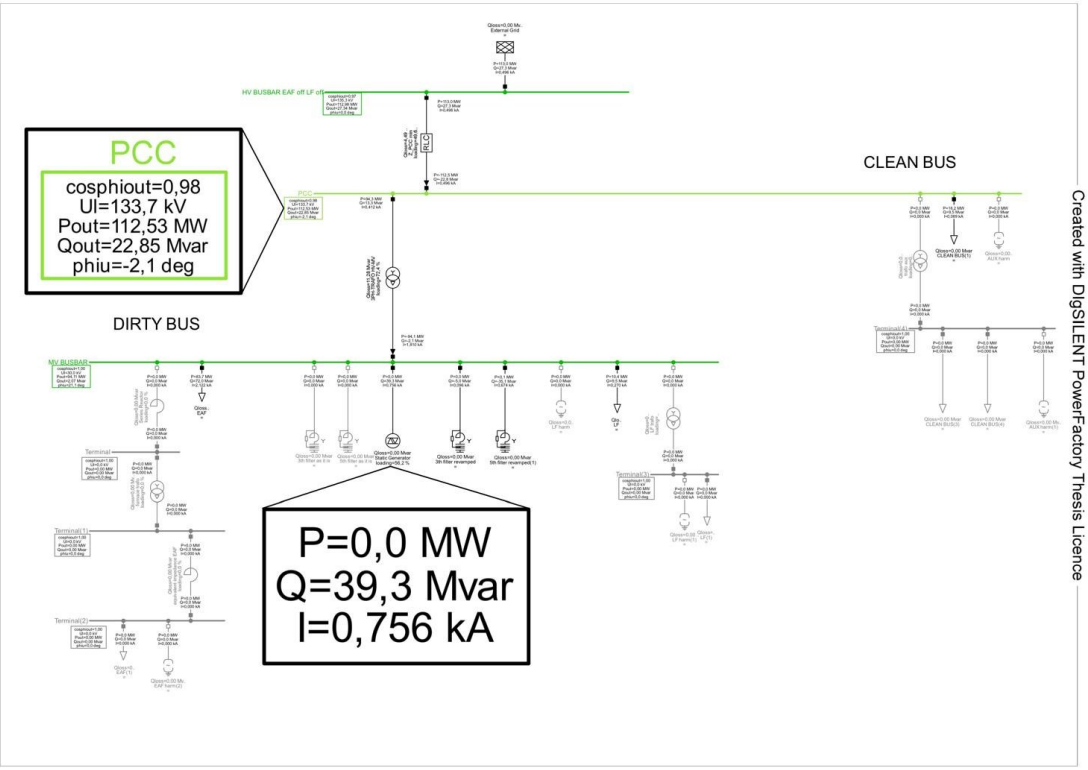


Figure 7-8 scenario ALL ON, Q of the STATCOM for PF correction

The results obtained suggest a STATCOM able to inject 39.3 $Mvar$ of capacitive reactive power, while its analytical counterpart was 42.29 $Mvar$. Also in this case, the capability curve of the STATCOM is symmetrical, ranging between $\pm\sim 39\ Mvar$.

To estimate the transformer losses in this situation, a way is summing up the contribution to the active current of both the electric arc furnace and the ladle furnace:

$I_{active} = I_{active_{EAF}} + I_{active_{LF}} = 1653.44 + 181.19 = 1834.63\ A,$

$I_{reactive} = 0\ A,$

$I_{total} = 1834.63\ A,$

Leading to: $Q_{loss} = 11.25\ Mvar$

In particular in this case, the losses observable on DIgSILENT are really similar to the estimated one:

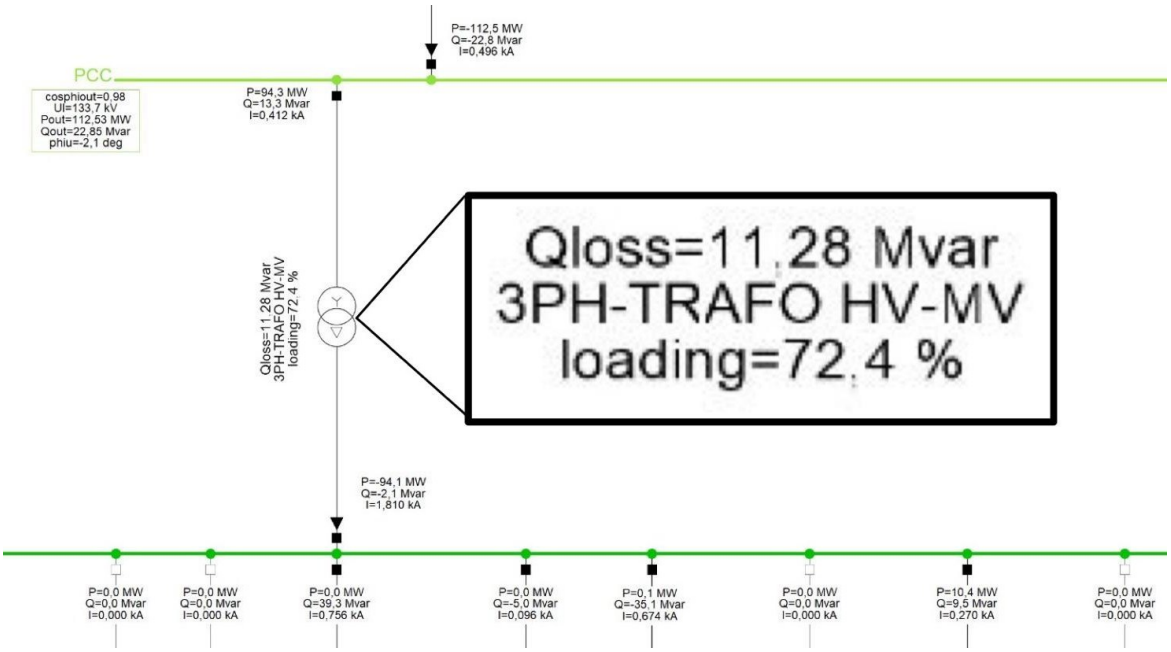


Figure 7-9 7 scenario ALL ON, losses on the transformer with STATCOM ON

In conclusion, considering only the compensating role of the STATCOM, the data suggest a size of the reactive power compensating system (RPCS) of:

$$\sim -42\ Mvar \leq Q_{statcom} \leq \sim 42\ Mvar$$

Considering the analytical calculation, or a RPCS of:

$$\sim -39\ Mvar \leq Q_{statcom} \leq \sim 39\ Mvar$$

if the software solution is adopted.

The two range of values obtained are extremely close. Considering that, as a standard procedure, a safety margin is always applied to the size of the proposed converter, it is not wrong to say that the two solutions converge to the same value, validating the analytical calculations with the software solutions.

However, the size of the STATCOM proposed is only adequate to properly compensate the power factor. Later in this chapter, the STATCOM must be oversized in order to properly mitigate the flicker effect.

7.3. HARMONIC ANALYSIS

The problem highlighted in the previous chapter about the harmonic analysis was not related to the THD. Perhaps, the total harmonic distortion factor was far below the threshold imposed by the standard. However, considering every single harmonic, the 8^{th} order was above its limit. This single issue alone does not justify a complete replacement of the existing filter system. However, considering their wear and the fact that their replacement had already been planned, it was decided to proceed with the revamping of the filters so that each individual harmonic would fall within the limits imposed by the standard.

The decision fall on two new filters still tuned on the 3^{rd} and 5^{th} harmonic order. In order to not drastically change the power flow of the system, the total reactive power rating of the filters system of $40\ Mvar$ was maintained. The differences with the previous ones are on the topology of the filters, their parameters and on the distribution of the power rating.

Filter tuned on the third harmonic:

The proposed filter is a single tuned filter. This topology is designed to properly attenuate a single dominant harmonic, the circuital structure is obtained with a series of an inductance and a capacitance, tuned to the harmonic order that the filter is intended to suppress.

With the following parameters:

- Resonant frequency: $150\ Hz$
- Rated voltage: $30\ kV$
- Rated reactive power: $5\ Mvar$
- Quality factor: 100

In DIgSILENT:

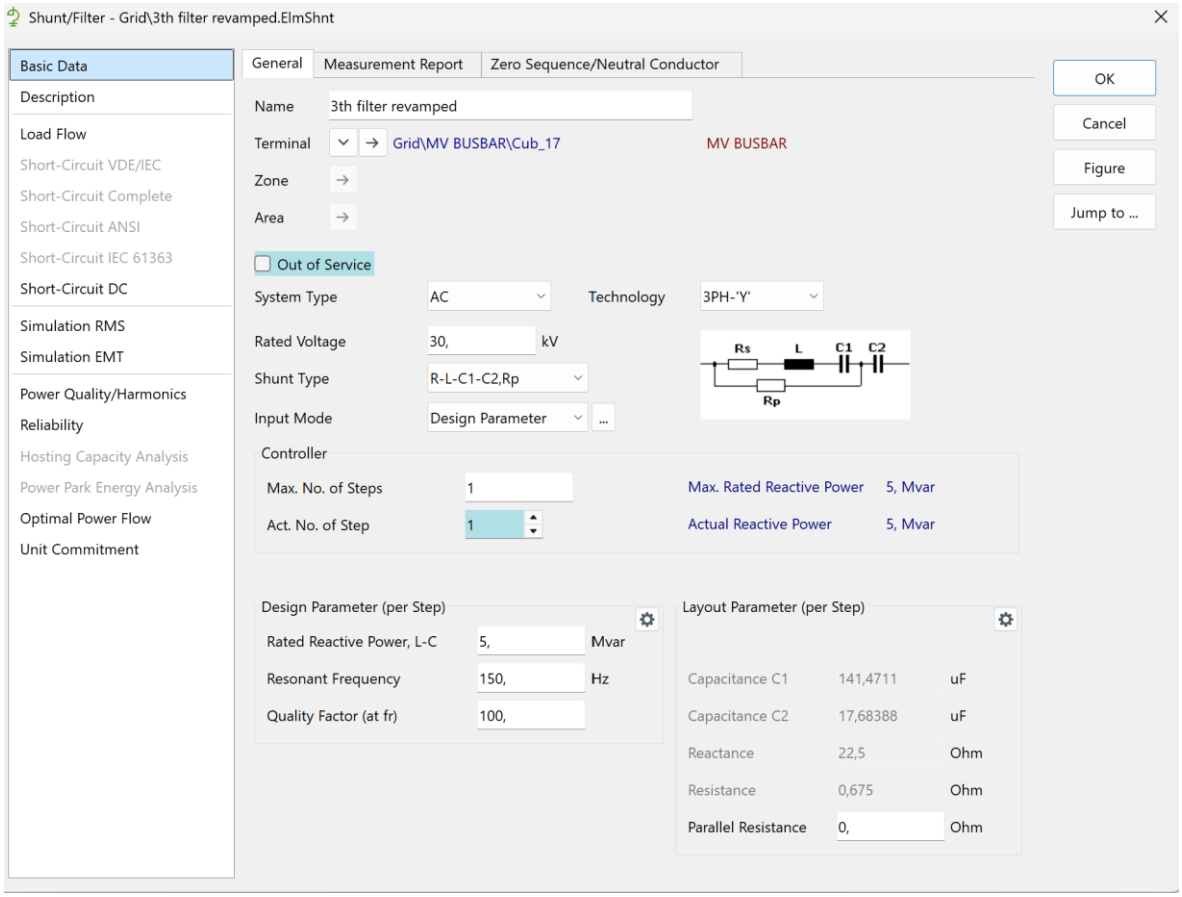


Figure 7-10 third harmonic revamped filter tab on the sofwae

where the parallel resistance (or damping resistance) is zero because it is a single-tuned LC.

Filter tuned on the fifth harmonic:

In this case, the choice still falls on a C-type filter. The C-type, in fact, introduces a damping factor, strongly recommended for increasing the stability of the system, nevertheless, it also limits the currents of the fundamental frequency on the inductive branch.

The selected parameters are:

- Resonant frequency: 250 Hz
- Rated voltage: 30 kV
- Rated reactive power: 35 $Mvar$
- Quality factor: 100
- Damping resistance: $R_d = 5\ \Omega$

In DIgSILENT:

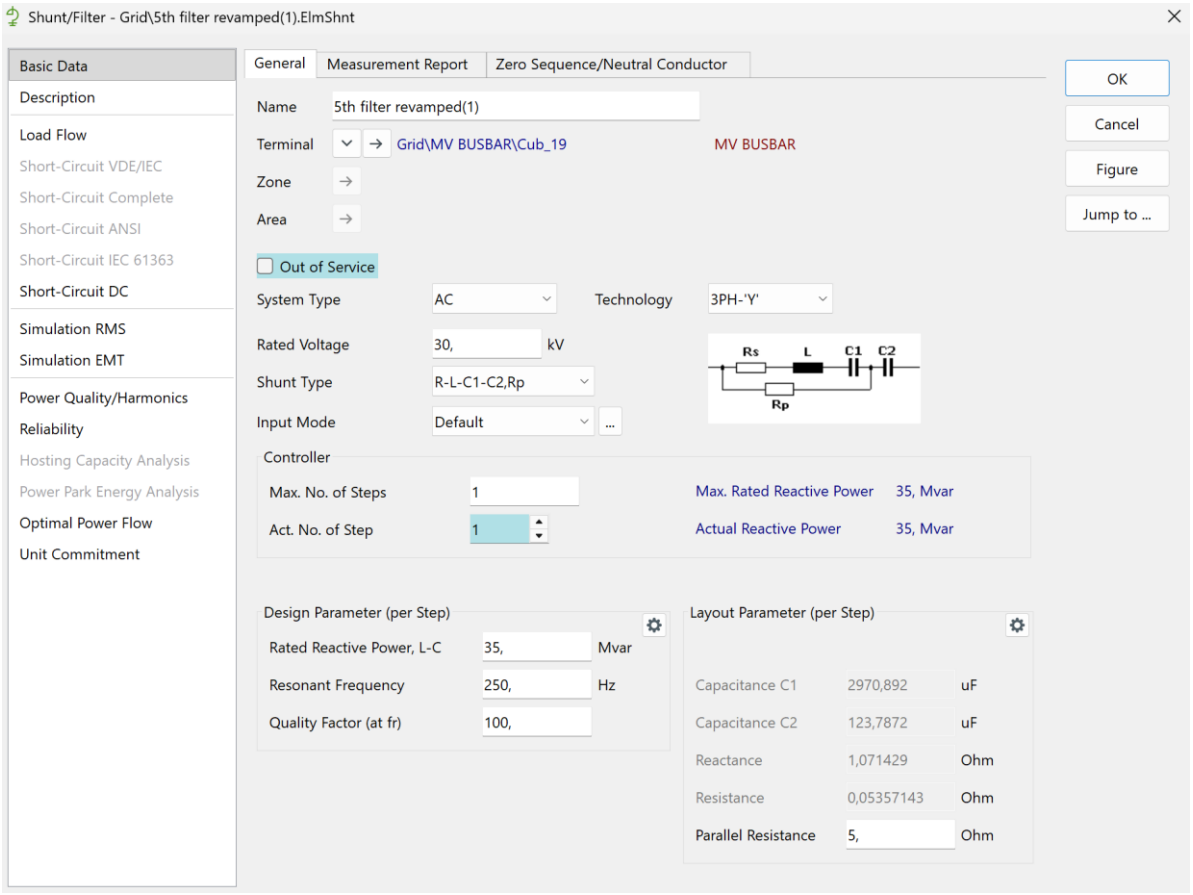


Figure 7-11 fifth harmonic revamped filter tab on the software

As observable, the total reactive power of the filters system is equal to the previous configuration of 40 $Mvar$.

The harmonic content provided by the loads is the same as in chapter 5 and it is represented by a current generator injecting each harmonic current for every loads.

With the new filters, the THD obtained at PCC is similar to the "as-it-is" situation, slightly higher. In fact, it is:

$$THD = 1{,}7\%$$

As observable in the SLD below:

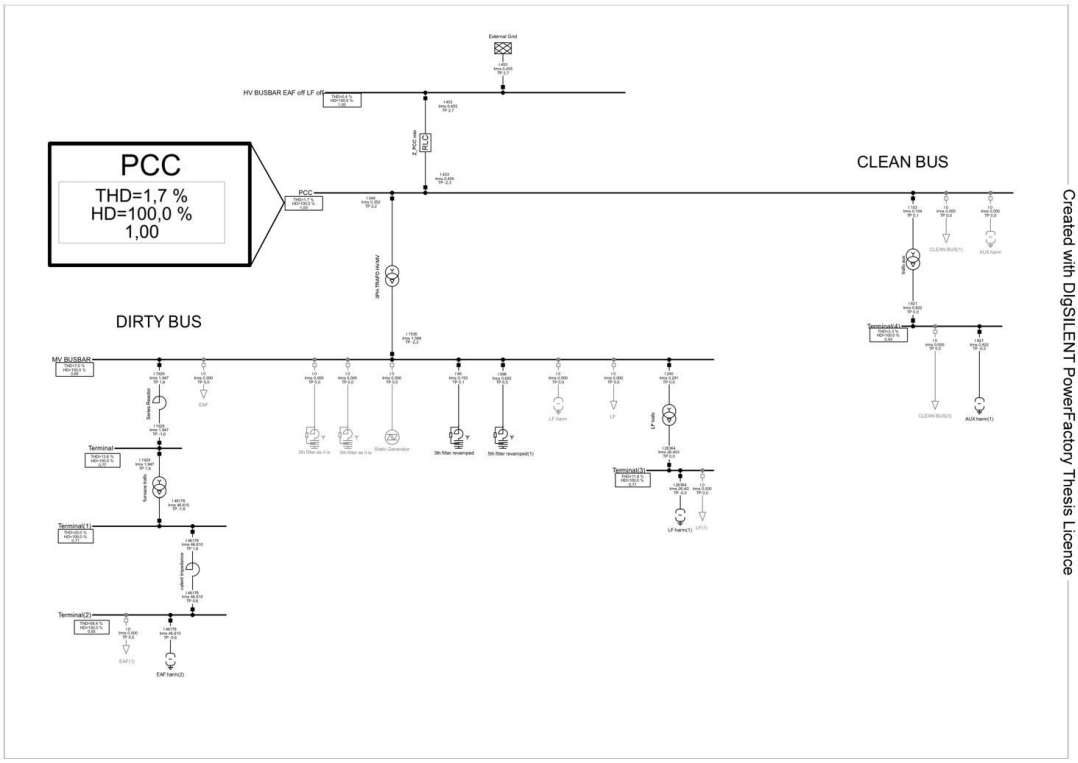


Figure 7-12 THD at PCC in the SLD with the revamped filters

It is obvious that the THD is still compliant with the IEC 61000-3-6. Furthermore, it is far below the imposed limit.

Considering the limits of every single harmonic, the new scenario is:

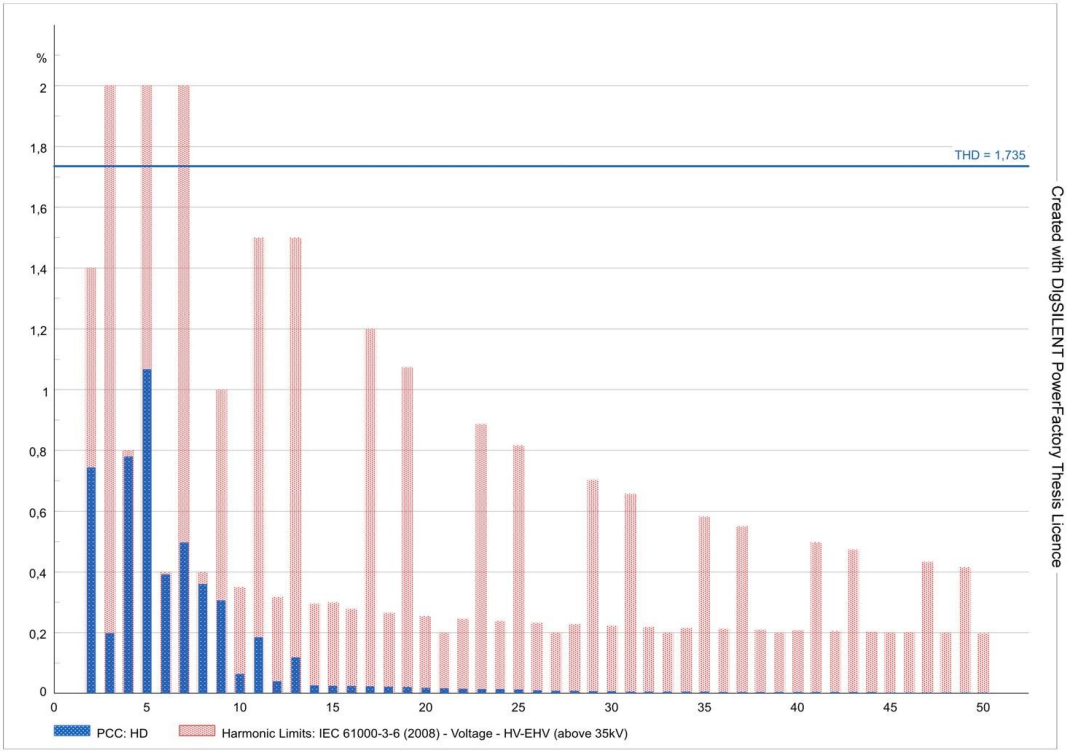


Figure 7-13 percentage of the harmonics components vs standard for every order

It can be noted that, with the selection of these filters, every single harmonic is within its range. With the proposed revamping the customer is 100% compliant with the standard.

Another aspect that must necessarily be verified is the acceptability of the network impedance over the entire frequency range. The presence of the filters, in fact, introduce impedance peaks that must be kept within acceptable limits when compared to the network impedance at the same frequency in the absence of filtering.

The resulting network impedances over the whole 50^{th} order harmonic spectra are reported in the figure below.

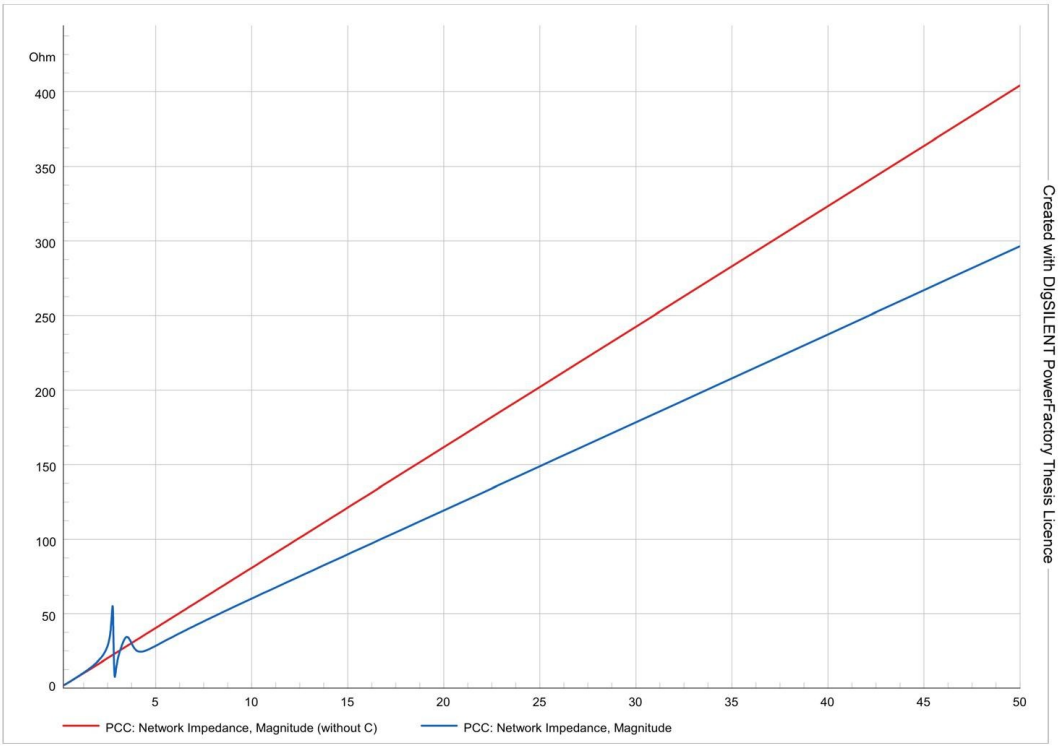


Figure 7-14 network impedance curve over frequency obtained with a sweep analysis

The network impedance, in fact, describes the response of the system to the currents flowing through it. Its behaviour is determined by resistive, inductive and capacitive components present in the network. A higher impedance value at a given frequency indicate that the system is more sensitive to voltage variations when a current of that harmonic order flows through it.

In this case, the impedance peaks have the following values (figure 7-15):

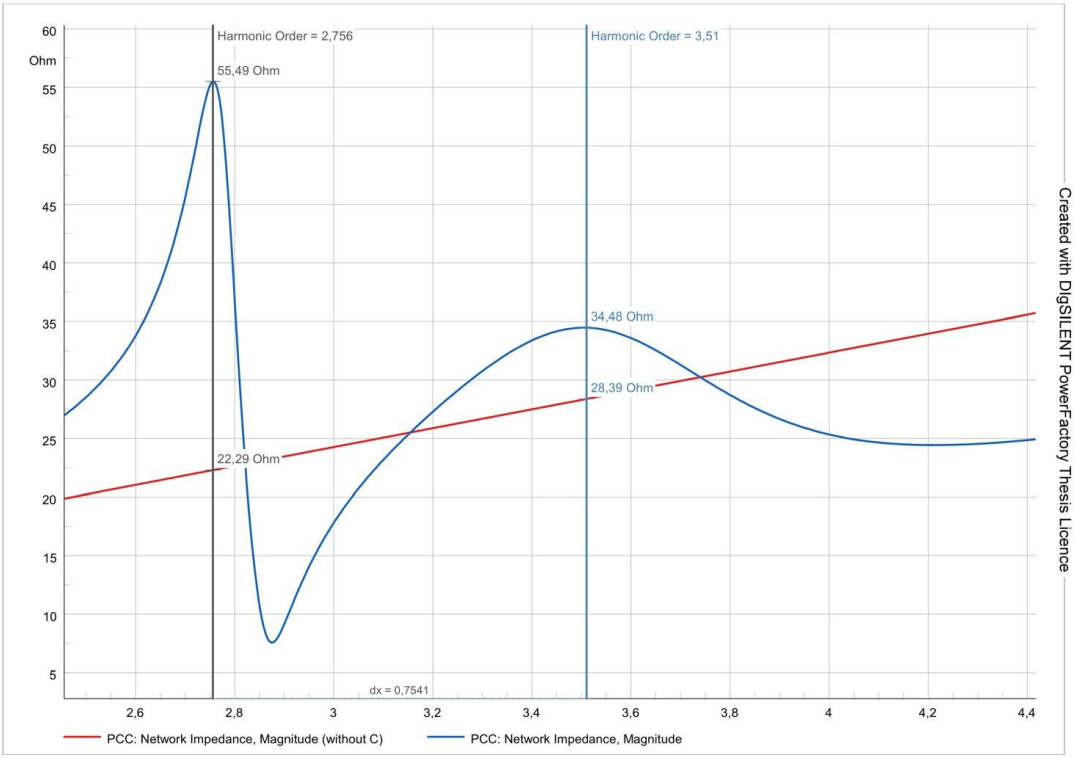


Figure 7-15 details of the peaks of the network impedance

Their positions are, respectively, at $H = 2.756$ and $H = 3.51$; where H represent the harmonic order. Considering an acceptable peak when it differs from its value in the absence of filters by no more than a factor of 10, it is possible to state that the obtained value fully satisfies this requirement. The factor-of-ten criterion is adopted here as a project-specific screening rule for identifying potentially critical parallel-resonance amplification. It is not presented as a limit prescribed by IEC 61000-3-6; therefore, the final filter design should also be checked against the applicable utility requirements and the expected range of network operating conditions.

Peak at $H = 2.756$:

$$z_{no\ filters} = 22.29\ \Omega$$

$$z_{with\ filters} = 55.49\ \Omega$$

$$\frac{z_{with\ filters}}{z_{no\ filters}} = 2.49 < 10$$

Peak at $H = 3.51$:

$$z_{no\ filters} = 28.39\ \Omega$$

$$z_{with\ filters} = 34.48\ \Omega$$

$$\frac{z_{with\ filters}}{z_{no\ filters}} = 1.21 < 10$$

7.4.FLICKER ANALYSIS

Because only line-to-line voltages were available, the corresponding phase-to-neutral voltages were first reconstructed by assuming a three-wire system with zero zero-sequence voltage. The reconstructed phase-voltage vector was then transformed into zero-, positive-, and negative-sequence components using the Fortescue transformation matrix.

$$T = \frac{1}{3} \cdot \begin{bmatrix} 1 & 1 & 1 \\ 1 & a^2 & a \\ 1 & a & a^2 \end{bmatrix} \tag{7.3}$$

The phase-to-ground voltages V_A, V_B, V_C are transformed into:

$$\begin{bmatrix} V_0 \\ V_D \\ V_I \end{bmatrix} = \frac{1}{3} \cdot \begin{bmatrix} 1 & 1 & 1 \\ 1 & a^2 & a \\ 1 & a & a^2 \end{bmatrix} \cdot \begin{bmatrix} V_A \\ V_B \\ V_C \end{bmatrix} \tag{7.4}$$

The direct sequence is what really interests the flicker analysis. A perfect situation is represented by a positive component vector with all its components equal to the nominal value of the medium voltage busbar, in this case $V_n = \frac{30}{\sqrt{3}}\ kV$. In order to represent the imbalance, at every component of the direct sequence, represented in its module-phase representation, the nominal voltage value V_n has been subtracted. In this way, a vector representing the voltage imbalance is obtained:

$$\Delta V = |V_D - V_n| \angle V_D \tag{7.5}$$

The STATCOM, for every period, must be able to inject the current value that nullifies this imbalance. A block diagram of the control can be schematized as it follows:

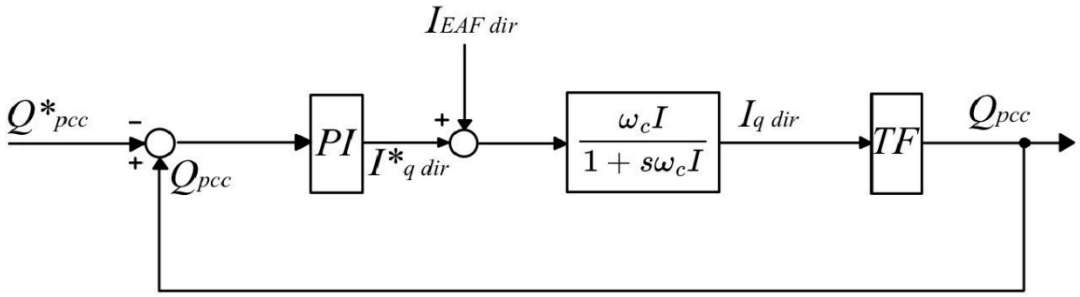


Figure 7-16 block diagram of STATCOM control

The outer, slower closed loop generates the reference for the faster inner current-control loop. The outer loop regulates the power factor at the PCC, whereas the inner loop tracks the compensating-current reference required to counteract the rapid current variations produced by the EAF.

The current that the STATCOM need to inject is achievable by means of its decoupling reactor:

$$I_{STATCOM} = \frac{\Delta V}{X_{reactor}} \tag{7.6}$$

The reactive power that the STATCOM must inject is equal to:

$$Q = 3 \cdot Imm(V \cdot I^*) \tag{7.7}$$

Where:

- Imm indicate the operator that give as output the imaginary part of the argument
- I^* is the conjugate of the current vector

A vector where the components represent the instantaneous values of reactive power is obtained.

In the ideal scenario, the STATCOM is sized to fully cover the voltage fluctuations, this leads to obtaining the following value:

$$Q_{STATCOM} = \max(Q) = 446.08\ Mvar$$

In the reality, a converter that always fully guarantee no voltage imbalance is unfeasible. There are, in fact, two limitations:

1) The power is too high; there are not solutions economically sustainable for a converter of this size.

2) The variations in the voltages are too fast, even if the converter could inject such a high power, it cannot instantly react to the current without dead time.

The real bottleneck in this case is given by the saturation current. In fact, in the cascade H-bridge topology, the current flowing in every power module, equal in magnitude, cannot overcome the insulating and safety limits. In this case, considering the power modules installed in the SILCOVAR-H, the current limit is:

$$I_{MAX} = 1260\ A$$

causing the STATCOM to inject a maximum reactive power of the following value:

$$Q_{STATCOM_{MAX}} = 3 \cdot V_{MV} \cdot I_{MAX} = 113.4\ Mvar$$

Controlling the STATCOM as suggest in the previous block diagram, it is clearly observable that the converter is balancing the direct component of the furnace current (figure 7-17):

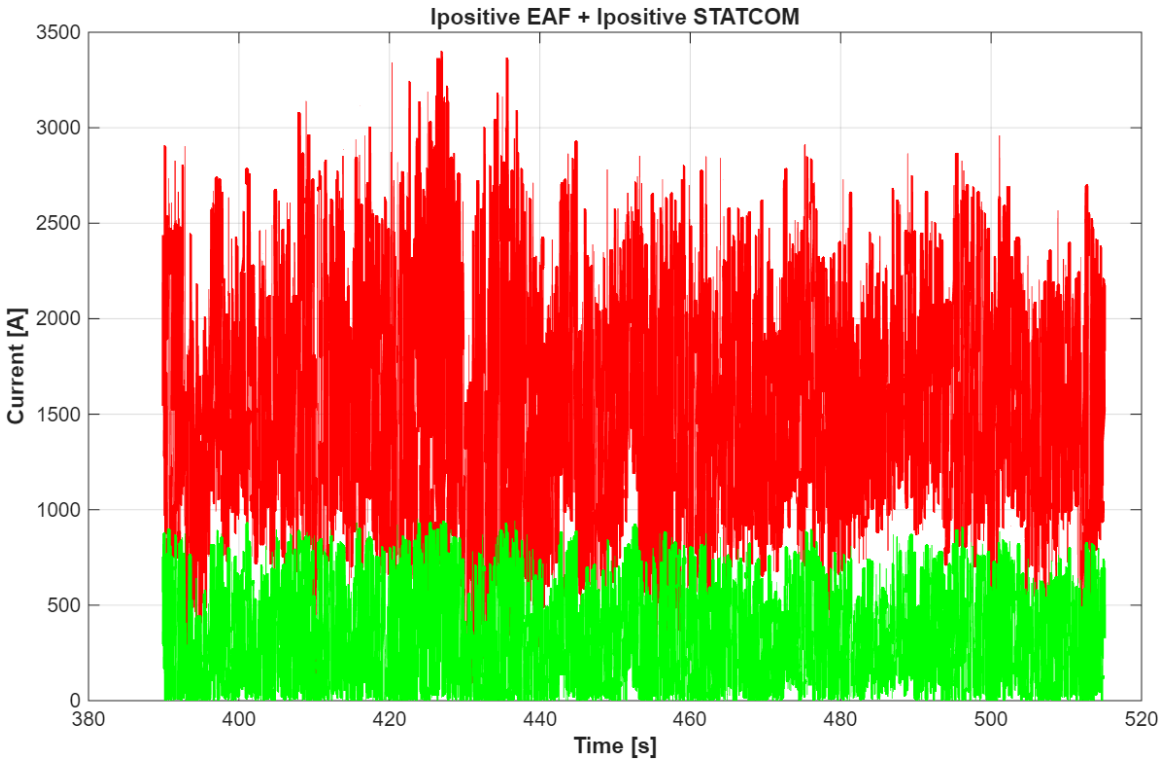


Figure 7-17 I eaf VS I STATCOM

An anticipation of the correct functioning of the STATCOM can be appreciated by observing the graphs of the instantaneous flicker severity on every phase. This indicator, in fact, is strictly related to the P_{st} and it contains a value for every sampling instant:

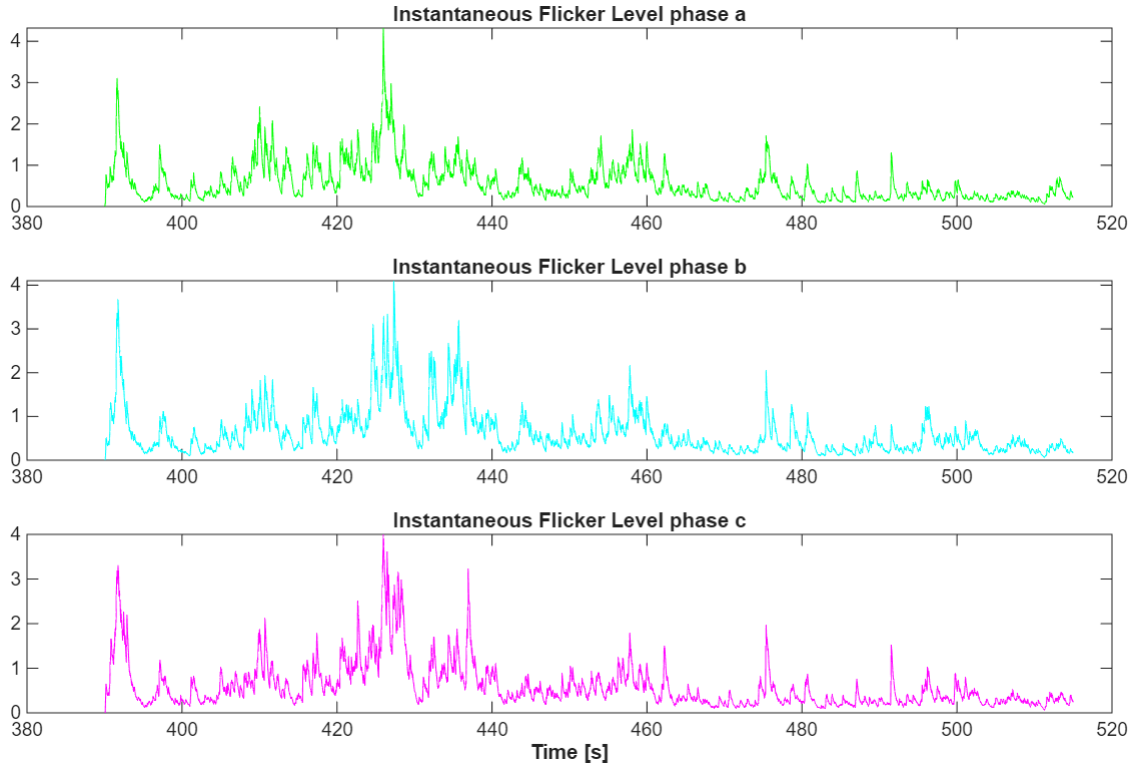


Figure 7-18 IFS of each phase

Only observing the graphs, it can be easily deduced that the flicker effect must be severely reduced. In the as-it-is situation the peaks of the IFS were in the range of $100 - 120$ while, with the proposed STATCOM, the simulation suggests an average reduction of 23 times.

Finally, the short-term flicker index on each phase confirms the effectiveness of the operation of the converter. The simulated values of P_{st} on every phase at PCC are:

- Phase a: $P_{st_a} = 1.01$
- Phase b: $P_{st_b} = 1.00$
- Phase c: $P_{st_c} = 0.91$

Resulting in an average value of:

$$P_{st} = 0.973$$

Achieving a Flicker Reduction (FR) factor of:

$$FR = \frac{P_{st_{EX\ ANTE}}}{P_{st_{EX\ POST}}} = \frac{4.033}{0.973} = 4.144 \tag{7.8}$$

Concluding, the size of the proposed STATCOM coincide with the maximum allowable size for a converter connected at $30\ kV$ and equipped with power modules allowing a maximum current of $1260\ A$.

STATCOM size: $113\ Mvar$

A flicker reduction factor (FR) in the range of 4 units is the standard value for a solution of this type. Higher FR requires an oversized converter, falling into a not cost-effective solution.

8. CONCLUSION

This thesis has examined the electrical behaviour, power quality performance and regulatory compliance of an Electric Arc Furnace (EAF) installation, with a particular focus on the dynamic disturbances generated during the steelmaking process. Through a combination of field measurements, analytical calculations and DIgSILENT simulations, the study has assessed the "as-it-is" situation of the plant and evaluated the expected improvements achievable through the integration of a Reactive Power Compensation System (RPCS): specifically, a STATCOM solution.

The analysis confirm that the EAF represents one of the most challenging industrial loads from the point of view of the network stability (voltage quality, harmonic distortion, flicker effect). The results obtained highlight the critical need for fast and dynamic compensation systems capable of mitigating the disturbances produced during the meltdown phase of the furnace and ensuring compliance with the adopted grid standards.

8.1. AS-IT-IS SITUATION

The Power Factor measured at the PCC show that the installation is significantly affected by the furnace operating cycle. In the worst-case scenario, PF drop down to 0.74 considering the inductive behaviour, while when the system is injecting reactive power at PCC the power factor is 0.26. These values fall below the limits prescribed by the standard "DELIBERAZIONE 20 DICEMBRE 2022 712/2022/R/EEL", resulting in increased reactive power circulation and potential economic penalties.

The Harmonic analysis reveals an already compliance of the THD at PCC, thanks to the installed filters, with a THD of 1.6%. However, specific harmonic order (the 8^{th}) was not below the standard adopted "IEC/TR 61000-3-6" where all the harmonic orders until the 50^{th} are regulated, confirming the inadequacy of the existing filtering system.

Considering the flicker effect, the as-it-is situation present a severe voltage fluctuation during the whole period, especially in the meltdown phase. The short-term flicker index in the worst $125\ s$ result in $P_{st} = 4.033$. These values surpass the compatibility limits dictated in the standard "IEC/TR 61000-3-7"

8.2.STANDARD LIMITS

The considered standard suggests the following limits in order to be compliant at the PCC:

- "DELIBERAZIONE 20 DICEMBRE 2022 712/2022/R/EEL" for power factor limits:
  $PF_{max} = 0.95$
- "IEC/TR 61000-3-6" for harmonics content limits: $THD_{HV-EHV} = 3\%$ and specific limits for every harmonic order.
- "IEC/TR 61000-3-7" for flicker effect: the EAF falls in the stage 3 (acceptance of higher emission level) and in most of the cases as the considered one the short-term flicker index must be lower than $P_{st} < 1.0$

The deviations from those limits expose the plant to potential penalties under the country regulatory entities, compromising the upstream HV network. The economic impact of non-compliance, including increased losses, reduced transformer efficiency and potential contractual energy, reinforce the need for corrective actions.

8.3.REVAMPED SITUATION

By analytical calculations, confirmed via software, the following STATCOM size along with these filters must be installed:

For the power factor correction, a STATCOM able to reach the following values is mandatory:

$$\sim -39\ Mvar \leq Q_{statcom} \leq \sim 39\ Mvar$$

Later, correcting the flicker effect, this size has been greatly increased.

For the correction of the not compliant harmonics, a revamped set of filters has been proposed. In particular, maintaining the constraint of the same reactive power of $40\ Mvar$, the two proposed filters are:

1. 3rd harmonic filter, single tuned of $5\ Mvar$.
2. 5th harmonic filter, C-type of $35\ Mvar$, with a damping resistance of $R_d = 5\ \Omega$.

Finally, considering the flicker effect, it results that only the maximum possible installed power at $30\,kV$ can mitigate the P_{st} under the prescribed threshold. Oversizing the STATOCOM at the size of:

$$-113\ Mvar \leq Q_{statcom} \leq 113\ Mvar$$

this RPCS assure the totally compliance with the considered standard. Furthermore, from the point of view of the electrical network side this benefit has been achieved:

- Reduction of the regulatory penalties
- Lower maintenance costs for transformers and filters
- Increased furnace availability

Instead, if the Electric Arc Furnace is considered, the integration of the STATCOM is expected to produce several operational benefits:

- Improved arc stability, reducing arc extinction events;
- Lower electrodes consumption;
- Reduced furnace wear due to stabilized current and voltage profile;
- Enhanced steel quality thanks to reduced voltage dips and cleaner power supply;
- Increased process continuity during meltdown and tapping phases.

In conclusion, this thesis aims to demonstrate that modern steelmaking plants require advanced compensation systems to ensure network stability, regulatory compliance and high production efficiency. The analysis confirms that a RPCS based on a STATCOM represents a robust and effective solution for mitigating the disturbances generated by EAF operation. By stabilizing voltage, improving power factor, lowering harmonic distortion and reducing flicker effect, the STATCOM significantly enhances both electrical performance and industrial productivity.

As industrial processes continue to evolve toward higher power density and greater electrical complexity, advanced power electronics solutions will remain a cornerstone for ensuring robust power quality.

9. REFERENCES

[1] *Basic Oxygen Furnace VS Electric Arc Furnace Differences*,https://www.srfurnace.com/basic-oxygen-furnace-vs-electric-arc-furnace-differences.html

[2] IEA (2025), Breakthrough Agenda Report 2025, IEA, Paris https://www.iea.org/reports/breakthrough-agenda-report-2025, Licence: CC BY 4.0

[3] Karbowniczek, Miroslaw. (2021). Electric Arc Furnace Steelmaking. 10.1201/9781003130949.

[4] Mahdavi Tabatabaei, N., Jafari Aghbolaghi, A., Bizon, N., & Blaabjerg, F. (Eds.). (2017). *Reactive Power Control in AC Power Systems: Fundamentals and Current Issues*. Springer. https://doi.org/10.1007/978-3-319-51118-4

[5] Miller, T. J. E. (Ed.). (1982). *Reactive power control in electric systems*. Wiley.

[6] DELIBERAZIONE 20 DICEMBRE 2022 712/2022/R/EEL: DISPOSIZIONI IN MATERIA DI REGOLAZIONE TARIFFARIA DELL'ENERGIA REATTIVA SULLE RETI ELETTRICHE IN ALTISSIMA E ALTA TENSIONE

[7] IEC/TR 61000-3-6:2008" Electromagnetic compatibility (EMC) - Part 3-6: Limits - Assessment of emission limits for the connection of distorting installations to MV, HV and EHV power systems"

[8] IEC/TR 61000-3-7:2008" Electromagnetic compatibility (EMC) - Part 3-7: Limits - Assessment of emission limits for the connection of fluctuating installations to MV, HV and EHV power systems"

[9] Bin Wu, Mehdi Narimani, High-Power Converters and AC Drives, 2nd Edition, December 2016, ISBN: 978-1-119-15607-9, Wiley-IEEE Press

[10] Mohan, N. (2003). *Power electronics: converters, applications and design* (3rd ed.). Hoboken, NJ: John Wiley & Sons.

[11] ICNIRP GUIDELINES FOR LIMITING EXPOSURE TO TIME-VARYING ELECTRIC AND MAGNETIC FIELDS (1 Hz TO 100 kHz), HEALTH PHYSICS 99(6):818-836; 2010